



NUCLEAR WASTE  
MANAGEMENT  
ORGANIZATION

SOCIÉTÉ DE GESTION  
DES DÉCHETS  
NUCLÉAIRES

## Phase 2 Geoscientific Preliminary Assessment, Lineament Interpretation

**TOWNSHIP OF IGNACE, ONTARIO**



**APM-REP-06145-0003**

**FEBRUARY 2015**



*This report has been prepared under contract to the NWMO. The report has been reviewed by the NWMO, but the views and conclusions are those of the authors and do not necessarily represent those of the NWMO.*

*All copyright and intellectual property rights belong to the NWMO.*

*For more information, please contact:*

**Nuclear Waste Management Organization**

22 St. Clair Avenue East, Sixth Floor

Toronto, Ontario M4T 2S3 Canada

Tel 416.934.9814

Toll Free 1.866.249.6966

Email [contactus@nwmo.ca](mailto:contactus@nwmo.ca)

[www.nwmo.ca](http://www.nwmo.ca)

# **Phase 2 Geoscientific Preliminary Assessment, Lineament Interpretation, Township of Ignace, Ontario**

Report Prepared for  
**Nuclear Waste Management Organization**



Report Prepared by



SRK Consulting (Canada) Inc.  
SRK Project Number: 3CN020.003  
NWMO Report Number: APM-REP-06145-0003  
February, 2015

# **Phase 2 Geoscientific Preliminary Assessment, Lineament Interpretation, Township of Ignace, Ontario**

## **SRK Consulting (Canada) Inc.**

Suite 1300, 151 Yonge Street  
Toronto, Ontario  
M5C 2W7

E-mail: [toronto@srk.com](mailto:toronto@srk.com)

Website: [www.srk.com](http://www.srk.com)

Tel: +1 416 601 1445

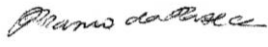
Fax: +1 416 601 9046

**SRK Project Number: 3CN020.003**

**NWMO Report Number: APM-REP-06145-0003**

**February 2015**

**Authored by:**



Anna Fonseca, MSc, PGeo  
Senior Consultant (Geology)

**Reviewed by:**



James Siddorn, PhD, PGeo  
Principal Consultant (Structural Geology)

---

## Executive Summary

This technical report documents the results of an updated surficial and geophysical lineament interpretation study conducted as part of the Phase 2 Geoscientific Preliminary Assessment, to further assess the suitability of the Ignace area to safely host a deep geological repository (Golder, 2015). This study followed the successful completion of a Phase 1 Geoscientific Desktop Preliminary Assessment (NWMO, 2013; Golder, 2013). The desktop study identified four large potentially suitable areas warranting further studies such as high-resolution surveys and geological mapping.

The purpose of the Phase 2 lineament interpretation was to provide an updated interpretation of the geological and structural characteristics of the bedrock units within the potentially suitable areas identified in Phase 1 desktop assessment. The assessment area considered for the lineament study includes the areas covered by the newly acquired Phase 2 airborne surveys (Golder, 2015). The interpretation of lineaments was conducted using the new high-resolution airborne magnetic and topographic data, as well as high-resolution satellite data.

The lineament interpretation followed a systematic workflow involving three steps. The first step included an independent lineament interpretation by two separate interpreters for each data set and assignment of certainty level (low certainty, medium certainty, or high certainty). The second step involved the integration of interpreted lineaments for each individual data set and first determination of reproducibility. The third and final step involved the integration of lineament interpretations for the surficial data sets (topography and aerial imagery) followed by integration of the combined surficial data set with the magnetic data set, with determination of coincidence in each integration step. Over the course of these three steps, a comprehensive list of attributes for each lineament was compiled. The four key lineament attributes and characteristics used in the assessment include certainty, length, density and orientation.

Geophysical lineaments were interpreted using the newly acquired high-resolution magnetic data (SGL 2015), which provides a significant improvement to the overall resolution and quality of magnetic data compared with the available data interpreted during the Phase 1 preliminary assessment. Lineaments interpreted using the magnetic data are typically less affected by the presence of overburden than surficial datasets, and more likely reflect potential structures at depth that may or may not have surficial expressions. In general, a lower density of geophysical lineaments is observed in the intrusive bodies such as the Revell, Indian Lake and Basket Lake batholiths than in the adjacent greenstone belts.

Surficial lineaments were interpreted using the high-resolution topographic data (DEM) from the airborne surveys, and high-resolution aerial imagery data with a cell resolution of 0.4 m. Surficial lineaments were interpreted as linear traces along topographic valleys, escarpments, and drainage patterns such as river streams and linear lakes. These linear traces may represent the expression of fractures on the ground surface. However, it is uncertain what proportion of surficial lineaments represent actual geological structures and if so, whether the structures extend to significant depth. The observed distribution and density of surficial lineaments is highly influenced by the presence of overburden cover and water bodies, which can mask the surface expressions of potential fractures. This is particularly evident in the northeastern part of the Ignace area, which is extensively covered by thick overburden deposits.

---

## Table of Contents

<b>Executive Summary .....</b>	<b>ii</b>
<b>Table of Contents .....</b>	<b>iii</b>
<b>List of Tables .....</b>	<b>iv</b>
<b>List of Figures.....</b>	<b>iv</b>
<b>1 Introduction .....</b>	<b>7</b>
1.1 Scope of Work and Work Program.....	7
1.2 Assessment Area.....	8
1.3 Qualifications of SRK and SRK Team.....	8
<b>2 Summary of Geology .....</b>	<b>10</b>
2.1 Geological Setting.....	10
2.2 Bedrock Geology .....	10
2.2.1 Intrusive Rocks .....	10
2.2.2 Supracrustal Rocks.....	12
2.2.3 Mafic Dykes .....	13
2.3 Structural History and Mapped Structures.....	13
2.4 Metamorphism.....	15
2.5 Quaternary Geology .....	15
<b>3 Methodology .....</b>	<b>17</b>
3.1 Source Data Description .....	17
3.1.1 High-resolution Magnetic Data .....	17
3.1.2 Digital Elevation Model .....	18
3.1.3 High-resolution Aerial Imagery .....	18
3.2 Lineament Interpretation Workflow.....	19
3.2.1 Step 1: Lineament Interpretation and Certainty Level .....	20
3.2.2 Step 2: Lineament Reproducibility Assessment 1 (RA_1).....	22
3.2.3 Step 3: Coincidence Assessment (RA_2).....	24
3.2.4 Lineament Length .....	25
3.2.5 Lineament Trends.....	26
3.2.6 Lineament Density .....	26
<b>4 Lineament Interpretation Results.....</b>	<b>27</b>
4.1 Geophysical Lineaments.....	27
4.2 Surficial Lineaments.....	28
4.2.1 DEM Lineaments .....	28
4.2.2 Digital Aerial Imagery Lineaments.....	29
4.3 Integrated Surficial Lineaments (RA_2).....	30
4.4 Integrated Final Lineaments (RA_2) .....	30
4.5 Description of Lineaments by Geological Units .....	31
4.5.1 Revell Batholith .....	31
4.5.2 Indian Lake Batholith .....	32
4.5.3 Basket Lake Batholith .....	32
4.5.4 Gneissic Rocks .....	32
<b>5 Discussion .....</b>	<b>34</b>
5.1 Lineament Reproducibility (RA_1) and Coincidence (RA_2) .....	34
5.2 Lineament Trends.....	35

---

5.2.1	Relationship between Lineament sets and Regional Stress Field .....	35
5.3	Lineament Length .....	36
5.4	Density .....	37
5.4.1	Lineament Density .....	37
5.4.2	Intersection Density .....	38
5.5	Lineament Truncation and Relative Age Relationships .....	39
5.5.1	Mapped Fault, Dyke and Lineament Relationships .....	40
<b>6</b>	<b>Summary of Results .....</b>	<b>42</b>
<b>7</b>	<b>References .....</b>	<b>44</b>
<b>8</b>	<b>APPENDIX .....</b>	<b>49</b>

## List of Tables

Table 1: Bounding Coordinates of the Ignace Area, Ontario (UTM NAD83 Zone 15)

Table 2: Summary of the Geological and Structural History of the Ignace Area

Table 3: FRI Digital Aerial Imagery Band Ranges and Resolution

Table 4: Summary of Attribute Fields Populated for the Lineament Interpretation

## List of Figures

Figure 1: Location and Overview of the Ignace Area

Figure 2: Bedrock Geology of the Ignace Area

Figure 3: Terrain Features of the Ignace Area

Figure 4: Pole Reduced Magnetic Data (First Vertical Derivative) of the Ignace Area

Figure 5: Digital Elevation Data of the Ignace Area

Figure 6: Aerial Imagery Data of the Ignace Area

Figure 7: Ductile Features of the Ignace Area

Figure 7a: Ductile Features of the Ignace Area - Block A

Figure 7b: Ductile Features of the Ignace Area - Block B

Figure 8: Interpreted Lineaments (RA\_1) from Pole Reduced Magnetic Data (1VD) of the Ignace Area

Figure 8a: Interpreted Lineaments from Pole Reduced Magnetic Data of the Ignace Area - Block A

Figure 8b: Interpreted Lineaments (RA\_1) from Pole Reduced Magnetic Data (1VD) of the Ignace Area - Block B

Figure 9: Interpreted Lineaments from Digital Elevation Data of the Ignace Area

Figure 9a: Interpreted Lineaments from Digital Elevation Data of the Ignace Area - Block A

Figure 9a: Interpreted Lineaments from Digital Elevation Data of the Ignace Area - Block B

Figure 10: Interpreted Lineaments from Aerial Imagery Data of the Ignace Area

Figure 10a: Interpreted Lineaments from Aerial Imagery Data of the Ignace Area - Block A

Figure 10b: Interpreted Lineaments from Aerial Imagery Data of the Ignace Area - Block B

Figure 11: Interpreted Lineaments from Surficial Data of the Ignace Area

Figure 11a: Interpreted Lineaments from Surficial Data of the Ignace Area - Block A

Figure 11b: Interpreted Lineaments from Surficial Data of the Ignace Area - Block B

Figure 12: Interpreted Lineaments from Pole Reduced Magnetic Data of the Ignace Area

Figure 12a: Interpreted Lineaments from Pole Reduced Magnetic Data of the Ignace Area - Block A

Figure 12b: Interpreted Lineaments from Pole Reduced Magnetic Data of the Ignace Area - Block B

Figure 13: Final Integrated Interpreted Lineaments (RA\_2) of the Ignace Area

Figure 13a: Final Integrated Interpreted Lineaments (RA\_2) of the Ignace Area - Block A

Figure 13b: Final Integrated Interpreted Lineaments (RA\_2) of the Ignace Area - Block B

Figure 14: Geophysical Lineaments by Length for the Ignace Area - Block A

Figure 15: Geophysical Lineaments by Length for the Ignace Area - Block B

Figure 16: Surficial Lineaments by Length for the Ignace Area - Block A

Figure 17: Surficial Lineaments by Length for the Ignace Area - Block B

Figure 18: Final Integrated Lineaments by Length for the Ignace Area - Block A

Figure 19: Final Integrated Lineaments by Length for the Ignace Area - Block B

Figure 20: Geophysical Lineament Density for the Ignace Area - Block A

Figure 21: Geophysical Lineament Density for the Ignace Area - Block B

Figure 22: Surficial Lineament Density for the Ignace Area - Block A

Figure 23: Surficial Lineament Density for the Ignace Area - Block B

Figure 24: Final Integrated Lineament Density for the Ignace Area - Block A

Figure 25: Final Integrated Lineament Density for the Ignace Area - Block B

Figure 26: Geophysical Lineament Intersection Density for Ignace Area - Block A

Figure 27: Geophysical Lineament Intersection Density for Ignace Area - Block B

Figure 28: Surficial Lineament Intersection Density for Ignace Area - Block A

Figure 29: Surficial Lineament Intersection Density for Ignace Area - Block B

Figure 30: Final Integrated Lineament Intersection Density for Ignace Area - Block A

Figure 31: Final Integrated Lineament Intersection Density for Ignace Area - Block B

Figure 32: Relative Age Relationships of Interpreted Lineaments of the Ignace Area

## Copyright

Both parties retain all rights to methodology, knowledge, and data brought to the work and used therein. No rights to proprietary interests existing prior to the start of the work are passed hereunder other than rights to use same as provided for below. All title and beneficial ownership interests to all intellectual property, including copyright, of any form, including, without limitation, discoveries (patented or otherwise), software, data (hard copies and machine readable) or processes, conceived, designed, written, produced, developed or reduced to practice in the course of the work, shall vest in and remain with NWMO. For greater certainty, all rights, title and interest in the work or deliverables will be owned by NWMO and all intellectual property created, developed or reduced to practice in the course of creating a deliverable or performing the work will be exclusively owned by NWMO.



# 1 Introduction

This technical report documents the results of an updated surficial and geophysical lineament interpretation study conducted as part of the Phase 2 Geoscientific Preliminary Assessment, to further assess the suitability of the Ignace area to safely host a deep geological repository (Golder, 2015). This study followed the successful completion of a Phase 1 Geoscientific Desktop Preliminary Assessment (NWMO, 2013; Golder, 2013). The desktop study identified a number of large potentially suitable areas warranting further studies such as high-resolution surveys and geological mapping. The purpose of the Phase 2 lineament interpretation was to provide an updated interpretation of the geological and structural characteristics of the potentially suitable bedrock units located within the survey areas using the newly acquired high-resolution airborne magnetic and topographic data (DEM), as well as purchased high-resolution aerial imagery data.

The purpose of the Phase 2 lineament interpretation was to provide an updated interpretation of the geological and structural characteristics of the bedrock units within the potentially suitable areas identified in Phase 1 desktop assessment. The assessment area considered for the lineament study includes the areas covered by the newly acquired Phase 2 airborne surveys (Golder, 2015).

The interpretation of geophysical and surficial lineaments was conducted using newly acquired high-resolution airborne magnetic surveys (SGL, 2015). The interpretation of surficial lineaments was conducted using newly acquired topographic data (SGL, 2015) and high-resolution satellite imagery of the area (MNR, 2010).

## 1.1 Scope of Work and Work Program

The scope of work includes the completion of a structural lineament interpretation of remote sensing and geophysical data of the Ignace area in northwestern Ontario (Figure 1). The lineament study involved the interpretation of remotely-sensed data sets, including surficial (aerial imagery, digital elevation) and geophysical (magnetic) data sets (SGL, 2015) of the Ignace area. The investigation interpreted the implication of lineament location and orientation as potential bedrock structural features (e.g., individual fractures or fracture zones) and evaluated their relative timing relationships within the context of the local and regional geological setting. For the purpose of this report, a lineament was defined as, ‘an extensive linear or arcuate geophysical or topographic feature’. The approach undertaken in this lineament investigation is based on the following:

- Lineaments were interpreted using newly acquired high-resolution magnetic and digital elevation data (SGL, 2015), and purchased high-resolution digital aerial imagery (Forest Resource Inventory (MNR, 2010));
- Lineament interpretations for each data set were made by two specialist interpreters for each using a standardized workflow;
- Lineaments were interpreted as being brittle, dyke or ductile features by each interpreter;
- Lineaments were analyzed based on an evaluation of the quality and limitations of the available data sets;
- Lineaments were evaluated using: age relationships; reproducibility tests, particularly the coincidence of lineaments extracted by different interpreters; coincidence of lineaments extracted from different data sets; and comparison to literature; and

- Classification was applied to indicate the significance of lineaments based on certainty, length and reproducibility.

These elements address the issues of subjectivity and reproducibility normally associated with lineament investigations and their incorporation into the methodology increases the confidence in the resulting lineament interpretation.

## 1.2 Assessment Area

The Ignace Phase 2 assessment area used for the lineament assessment and interpretation covers two subareas (Block (A) and Block (B); Figure 1) totalling approximately 1,809 square kilometres (km<sup>2</sup>) in area, and was provided by NWMO as a shape file. The approximate coordinates defining the boundaries of the assessment areas are listed in Table 1 (UTM NAD83, Zone 15N).

The square-shaped Block (A) comprises 339 km<sup>2</sup> and lies northwest of Block (B), which is irregularly shaped and covers 1,409 km<sup>2</sup>.

**Table 1: Bounding Coordinates of the Phase 2 Assessment Areas in the Ignace area, Ontario (UTM NAD83 Zone 15N)**

X UTM	Y UTM	Block
608,800	5,497,600	A
627,000	5,497,600	A
627,000	5,478,950	A
608,800	5,478,950	A
548,511	5,482,367	B
548,511	5,491,394	B
559,343	5,498,074	B
569,363	5,515,677	B
591,000	5,502,227	B
591,000	5,468,900	B
567,600	5,468,900	B
557,000	5,468,900	B

## 1.3 Qualifications of SRK and SRK Team

The SRK Group comprises of more than 1,400 professionals, offering expertise in a wide range of resource engineering disciplines. The independence of the SRK Group is ensured by the fact that it holds no equity in any project it investigates and that its ownership rests solely with its staff. These facts permit SRK to provide its clients with conflict-free and objective recommendations on crucial issues. SRK has a proven track record in undertaking independent assessments of mineral resources and mineral reserves, project evaluations and audits, technical reports and independent feasibility evaluations to bankable standards on behalf of exploration and mining companies, and financial institutions worldwide. Through its work with a large number of major international mining companies, the SRK Group has established a reputation for providing valuable consultancy services to the global mining industry.

The lineament interpretation and the compilation of this report were completed by Ms. Anna Fonseca, PGeo and Dr. Iris Lenauer. Dr. James P. Siddorn, PGeo served as a technical advisor and reviewed lineament interpretations and drafts of this report prior to their delivery to the NWMO as per SRK internal quality management procedures.

Following is a brief description of the qualifications of the project team members.

**Ms. Anna Fonseca, MSc, PGeo** is a Principal Consultant (Geology) and has more than 20 years of international experience in geological mapping at various scales. She recently conducted structural lineament interpretations of remote sensing data sets for the Rice Lake Greenstone Belt and the Eastmain Greenstone Belt in the Superior Province and of the Yaramoko area in Burkina Faso. In this study, Ms. Fonseca was the lead interpreter and the report author.

**Dr. Iris Lenauer** is a Consultant (Structural Geology) and specializes in regional mapping, structural analysis in various tectonic settings, and brittle fault analysis. She recently completed a regional structural lineament interpretation of the Red Lake Greenstone Belt in the Superior Province, and of the Palmarejo area in Mexico. In this study, Dr. Lenauer was the second interpreter.

**Dr. James Siddorn, PGeo** is a Practice Leader (Structural Geology) and specialist in applied structural interpretation of geophysical data sets combined with the structural analysis of ore deposits. Dr. Siddorn has conducted numerous detailed interpretations of magnetic and electromagnetic data sets for gold and diamond exploration, and rock mechanics/hydrogeological engineering studies. He completed a Phase 1 structural lineament interpretation of the Ignace study area for the NWMO. He oversaw the Phase 1 structural lineament interpretations for Schreiber and Ear Falls in 2012 and for White River and Manitouwadge in 2013 for NWMO. In this study, Dr. Siddorn was the senior reviewer.

**Mr. Jason Adam** is an Associate Consultant (GIS) who has a broad experience in GIS. Mr. Adam provided GIS support for the study, mainly for the preparation of figures, under the direction of Ms. Fonseca.

---

## 2 Summary of Geology

Details of the geology of the Ignace area were described in the Phase 1 Geoscientific Desktop Preliminary Assessment (Golder, 2013). A brief description of the geological setting, bedrock geology, structural history and mapped structures, metamorphism and Quaternary geology is provided in the following subsections, with a focus on the areas identified during Phase 1 as being potentially suitable (Revell, Basket Lake and Indian Lake batholiths), their surrounding bedrock units and important structural features.

### 2.1 Geological Setting

The Ignace area is located in the central portion of the Archean Wabigoon Subprovince of the Superior Province. The Wabigoon Subprovince is approximately 900 km long and 150 km wide and is bounded by the Winnipeg River Subprovince to the northwest, the English River Subprovince to the northeast, and the Quetico Subprovince to the south (Blackburn et al., 1991). The Wabigoon Subprovince is further subdivided into three lithotectonic terranes: the granitoid Marmion terrane, the predominantly volcanic Western Wabigoon terrane, and the plutonic Winnipeg River terrane. The Ignace area includes portions of all three terranes. The boundaries between lithotectonic terranes are not sharply defined due to the emplacement of younger plutonic rocks at places along the inferred terrane boundaries (Stone, 2010a).

### 2.2 Bedrock Geology

The geology of the Ignace area is dominated by large granitic intrusions and associated tonalitic units, including the Indian Lake, Revell, and Basket Lake batholiths, where the four general potentially suitable areas were identified in Phase 1 Geoscientific Desktop Preliminary Assessment (Figure 2; Golder, 2013). These intrusions were emplaced into the older Raleigh Lake and Bending Lake greenstone belts. These bedrock units exhibit evidence of both ductile and brittle deformation and are transected by at least two suites of undeformed diabase dykes. A description of these three granitic batholiths, associated tonalitic units, and surrounding greenstone belts and dykes is provided in the following subsections.

#### 2.2.1 Intrusive Rocks

##### Revell Batholith

The Revell batholith is the oldest granitoid intrusion in the Ignace area, and is found in the southwestern portion of the Ignace Block (B) (Figure 2). It is roughly rectangular in shape, trends northwest, is approximately 40 km in length, and it covers an area of approximately 455 km<sup>2</sup>. Szewczyk and West (1976) interpreted this batholith to be a sheet-like intrusion approximately 1.6 km thick.

Three different intrusive phases are currently recognized in the Revell batholith (Stone et al., 2011a and b). The oldest phase corresponds to an approximately 2.734 Ga, medium-grained, foliated, mesocratic biotite tonalite (Stone et al., 2010) exposed primarily along the western margin of the batholith and in its southern portion. A younger 2.732 Ga phase (Stone et al., 2010) consisting of coarse-grained mesocratic gneissic hornblende tonalite is also found along the western margin of the

batholith. The youngest phase, approximately 2.694 Ga (Buse et al., 2010), consists of mesocratic to leucocratic feldspar megacrystic biotite granodiorite to granite; this phase extends over most of the remaining surface extent of the batholith. A distinctive oval-shaped, K-feldspar megacrystic lithofacies of this younger phase that is approximately 47 km<sup>2</sup> in areal extent is identified on the central-east portion of the batholith based on previous mapping and interpretation of existing geophysical data (Stone et al., 2011a, 2011b; Stone et al., 2007; PGW, 2013; SGL, 2015).

## **Basket Lake Batholith**

The Basket Lake batholith is exposed in the northern part of the Ignace Block (B). The batholith is approximately 10 to 15 km in width and 35 km in length, with almost half of this batholith extending beyond Block (B) to the northwest (Figure 2). Szewczyk and West (1976) estimated the thickness of the northern part of the Basket Lake batholith to be at least 8 km and thinning progressively to 0.5 km to the southeast, forming a tongue-like extension of the main batholith body.

Detailed mapping of the eastern portion of the Basket Lake batholith describes the lithology as hornblende-biotite quartz-diorite to tonalite (Sage et al., 1974). The western-northwestern portion of the batholith consists mainly of leucocratic biotite-rich granodiorite, which varies to granite with subordinate tonalite, quartz monzonite, quartz diorite and a mixed hybrid zone locally developed near the contact with the Bending Lake and Raleigh Lake greenstone belts (Berger, 1988). The contact zone contains white tonalite dykes which cross-cut the granite and granodiorite facies of the intrusion, as well as the adjacent metavolcanics. These dykes are interpreted to be a late phase of the Basket Lake batholith (Berger, 1988).

Bedrock of the Basket Lake batholith is commonly foliated, with foliation being weak and mostly defined by alignment of biotite and a fine- to medium-grained character. This suggests that this batholith experienced some degree of ductile deformation (Szewczyk and West, 1976), and that it pre-dates the intrusion of the Indian Lake batholith, as well as the youngest phase of the Revell batholith.

A small swarm of Wabigoon dykes cut across the southern margin of the batholith while two mapped Kenora-Fort Frances dykes occur immediately to the southeast (Figure 2).

## **Indian Lake Batholith**

The approximately 2.671 Ga Indian Lake batholith (Tomlinson et al., 2004) covers a total surface area of about 1,366 km<sup>2</sup>, with 563 km<sup>2</sup> within Blocks (A) and (B) (Figure 2). This batholith has previously been estimated to be a sheet-like intrusion up to 2 km thick (Szewczyk and West, 1976; Everitt, 1999).

The Indian Lake batholith is composed of light grey-white to pale pink biotite granite, typically medium- to coarse-grained, inequigranular, leucocratic, and is massive to weakly foliated. It usually contains a small percentage of biotite (3-5%) and subequal proportions of quartz, plagioclase and potassium feldspar (Stone et al., 1998). Non-tectonic foliation present in the batholith is defined by the alignment of igneous minerals that delineate concentric patterns in the granite (Stone et al., 1998).

An enclave of biotite-hornblende tonalite to granite, approximately 35 km<sup>2</sup> in area is mapped within the Indian Lake batholith (Figure 2), extending from the southern portion of the Township of Ignace southward beyond its boundaries (OGS, 2011). This enclave is generally coarse, granular and

mesocratic and, when hornblende granite is present, it is characterized by large potassium feldspar megacrystals that are 1 to 5 cm in size (Stone et al., 1998). It is not known whether this tonalitic body is a separate intrusive body, the product of different phases of magmatic injection, or compositional zoning.

## **Tonalitic Units**

The region in the northeastern part of Block (B), surrounding the Basket Lake and Indian Lake batholiths has been mapped as compositionally heterogeneous tonalitic gneiss and biotite tonalite (Figure 2).

The Biotite Tonalite Suite is typically white to grey, medium grained, and variably massive to foliated. Weakly gneissic biotite tonalite to granodiorite is the principal type of rock within this suite. The Biotite Tonalite Suite grades into the Tonalite Gneiss Suite largely through progressive development of a gneissic texture. Intrusions of the Biotite Tonalite Suite show considerable variation in age, ranging from approximately 2.994 to 2.688 Ga (Stone, 2010a).

The Tonalite Gneiss Suite comprises older gneissic, foliated, migmatized tonalite-granodiorite, intruded by younger granitoid batholiths. The Tonalite Gneiss Suite is layered with individual gneissic layers varying compositionally from leucocratic tonalite and granodiorite through mesocratic tonalite and granodiorite to diorite and amphibolite. They range substantially in age from approximately 3.009 to 2.673 Ga, similar to the variation in age shown by the Biotite Tonalite Suite (Stone, 2010a). The gneiss commonly shows strongly foliated to mylonitic textures and belts of gneiss are spatially associated with zones of high ductile strain such as the margins of large batholiths (Stone, 2010a). Locally, the tonalitic gneiss is gradational in composition to amphibolitic gneiss of volcanic or migmatized sedimentary rock origin, whereas the more felsic phases are gradational to biotite tonalite (Stone, 2010a).

### **2.2.2 Supracrustal Rocks**

The Raleigh Lake and Bending Lake greenstone belts surround the Revell batholith and the area adjacent to the Indian Lake and Basket Lake batholiths (Figure 2). These greenstone belts are composed of alternating units of mafic pillowed metavolcanic rocks and intermediate fragmental metavolcanic rocks, both metamorphosed to amphibolite facies.

The northwest-trending Raleigh Lake greenstone belt occurs north of the Revell batholith and extends over a length of 50 km. The Raleigh Lake greenstone belt is dominated by mafic metavolcanic rocks, and contains approximately 30% intermediate to felsic fragmental metavolcanic rocks (Stone, 2010a). The greenstone belt is intruded by oval, smaller felsic to intermediate plutons such as the Raleigh Lake intrusions, which consist of three epizonal granitic stocks hosted in the metavolcanic rocks of the Raleigh Lake greenstone belt (Figure 2). These small bodies are compositionally similar to the larger granodioritic to granitic batholiths that dominate the Ignace area.

The northwest-trending Bending Lake Greenstone Belt occurs southwest of the Revell batholith. It is composed of mafic metavolcanic rocks, with subordinate gabbro, intermediate metavolcanic rocks, and clastic metasedimentary rocks (wacke and argillite; Stone, 2010b).

### 2.2.3 Mafic Dykes

Mafic dykes in the Ignace area include the Kenora-Fort Frances and Wabigoon swarms, emplaced between approximately 2.20 and 1.96 Ga (Osmani, 1991). The Wabigoon dyke swarm constitutes the most prominent dyke generation and extends in a northwest orientation for at least 70 km from Ignace to Lac des Mille Lacs without offsets along any terrane boundaries. Within the Ignace area, the Wabigoon dykes are typically 100 to 200 m in width. Fahrig and West (1986) obtained a K/Ar age of approximately 1.9 Ga for the Wabigoon dykes.

The Kenora-Fort Frances dyke swarm contains hundreds of northwest-trending dykes up to 100 km long and 120 m wide, covering an area of approximately 90,000 km<sup>2</sup> (Osmani, 1991). The Kenora-Fort Frances dykes form clusters in the Melgund Lake area to the northwest of the Revell batholith, and in the Mameigwess Lake area between the Basket and Indian Lake batholiths. The Kenora-Fort Frances dykes are composed of variable amounts of plagioclase, pyroxene, quartz, hornblende, as well as varying degrees of alteration minerals. Southwick and Halls (1987) reported a Rb-Sr age of approximately 2.120 Ga for these dykes.

## 2.3 Structural History and Mapped Structures

Information on the structural history of the Ignace area and surrounding region is limited. This summary was written using information available for the Wabigoon Subprovince and is largely based on Bethune et al. (2006), Percival et al. (2004), Sanborn-Barrie and Skulski (2006), and Stone (2010a). Five episodes of penetrative strain (D<sub>1</sub> to D<sub>5</sub>) affected the central Wabigoon Subprovince (Percival et al. 2004). Gneissic tonalitic rocks (Tonalite Gneiss Suite) commonly display D<sub>1</sub> and D<sub>2</sub> fabrics, overprinted by pervasive, regional D<sub>3</sub> to D<sub>5</sub> fabrics or structures. Table 2 provides a tabulated summary of the structural history of the Ignace area.

S<sub>1</sub> gneissic foliation is folded into tight to isoclinal F<sub>2</sub> folds. The geometric and kinematic character of the D<sub>1</sub> and D<sub>2</sub> deformation is cryptic as a result of structural (D<sub>3</sub>-D<sub>5</sub>) and magmatic overprinting (Percival et al. 2004). D<sub>1</sub> and D<sub>2</sub> deformation fabrics are confined to gneissic rocks in the central Wabigoon Subprovince. The best constraints on the age of the D<sub>1</sub>-D<sub>2</sub> deformations are 2.725 to 2.713 Ga (Percival et al. 2004).

Two episodes of penetrative strain (D<sub>3</sub> and D<sub>4</sub> of Percival et al. 2004; D<sub>1</sub>, D<sub>2</sub> of Sanborn-Barrie and Skulski, 2006), hereby termed D<sub>3</sub> and D<sub>4</sub>, affected the supracrustal rocks of the central Wabigoon Subprovince. D<sub>3</sub> and D<sub>4</sub> deformation events are interpreted to have occurred prior to 2.698 Ga (Percival et al. 2004). D<sub>3</sub> resulted in the development of F<sub>3</sub> northwest-trending folds and an associated S<sub>3</sub> axial planar cleavage. These are well exposed in the nearby Savant-Sturgeon Lake Greenstone Belt to the northeast of the Ignace area; where they have been correlated with a northwest-striking foliation (locally known as F<sub>1</sub> and S<sub>1</sub>) within the Lewis Lake biotite-tonalite (2.735 to 2.730 Ga; Sanborn-Barrie and Skulski, 2006). In the Raleigh Lake and Bending Lake greenstone belts, within the Ignace area, D<sub>3</sub> structures dominate as shown in the strong north-west grain observed in the supracrustal rocks. D<sub>4</sub> east- to northeast-striking structures locally overprint the northwest-striking S<sub>3</sub> foliation. S<sub>4</sub> foliation occurs as a moderately- to strongly-developed schistosity characterized by a uniformly steep dip. The S<sub>4</sub> foliation is commonly axial planar to 050-070° trending, steeply plunging F<sub>4</sub> folds (locally known as F<sub>2</sub>; Sanborn-Barrie and Skulski, 2006).

Percival et al. (2004) attributed sinistral shear zone development in plutonic and gneissic rocks to a D<sub>5</sub> deformation event in the central Wabigoon Subprovince, bracketed between approximately 2.690 Ga (Davis, 1989) and 2.678 Ga (Brown, 2002). These shear zones are associated with significant

sinistral strike-slip displacement along the Miniss River fault zone and dextral strike-slip motion along the Sydney-Lake St. Joseph fault zone 150 km north of the Ignace area (Bethune et al., 2006). Regional differential uplift associated with movement along these shear zone systems continued until approximately 2.4 Ga (Hanes and Archibald, 1998) indicating a protracted D<sub>5</sub> fault history.

### Mapped Structures and Named Faults

There are two mapped faults within the Ignace area. One, the Washeibemaga fault, trends east and is located to the west of the Revell batholith. An unnamed fault is located in the northwestern corner of the Ignace area and trends northeast close to Minnitaki Lake. There are no mapped faults within the two Ignace Phase 2 assessment areas (Figure 2).

The northeast-trending Finlayson-Marmion fault is located approximately 30 km south of Ignace Block (A), and extends northeast from Steep Rock Lake where it intersects, and is thought to represent a splay of the east-west trending Quetico Fault. The Finlayson-Marmion fault crosscuts the Indian Lake batholith and is interpreted to represent a D<sub>5</sub> shear zone. This fault caused the mylonitization and brittle deformation of the granitoid rocks within the Indian Lake batholith (Schwerdtner et al., 1979; Stone, 2010a). To the south, close to the Quetico fault, the Finlayson-Marmion fault broadens to a complex braided zone of fault segments, some of which are auriferous (Stone, 2010a). The latest known movement along the associated Quetico fault, and therefore potentially the D<sub>5</sub> Finlayson-Marmion fault, occurred at approximately 1.947 Ga with the development of pseudotachylite (Peterman and Day, 1989). Immediately to the southeast of the Ignace area, a Wabigoon dyke (1.9 Ga; Buchan and Ernst, 2004) crosscuts the Finlayson-Marmion fault, which indicates that only limited movement could have occurred along the Finlayson-Marmion fault since the intrusion of the Wabigoon dyke swarm.

**Table 2: Summary of the Geological and Structural History of the Ignace Area**

Time Period (Ga)	Geological Event
ca. 3.0	Assemblage of the oldest rocks in the Ignace area comprising the Marmion terrane – essentially a micro-continent comprising tonalite basement rocks dominated by the Marmion batholith which occurs immediately south of the Ignace area.
ca. 3.0 to 2.74	Progressive growth of the Marmion terrane through the additions of magmatic and crustal material in continental arcs and through accretion of allochthonous crustal fragments. This growth included the emplacement of the Phyllis Lake gneisses and tonalites approximately 2.955 to 2.989 Ga ago and amalgamation of the Winnipeg River and Marmion terranes by approximately 2.93 to 2.87 Ga (Tomlinson et al. 2004; Percival and Easton, 2007).
ca. 2.745 to 2.711	A major period of volcanism, derived from subduction, occurred in the Winnipeg River-Marmion terrane (Blackburn et al., 1991). The result of this volcanic period is the Raleigh Lake and Bending Lake greenstone belts (Stone, 2010a). Sedimentation within the greenstone belts was largely synvolcanic, although sediment deposition in the Bending Lake area may have continued past the volcanic period (Stone, 2009b; Stone, 2010b). Synvolcanic to post-volcanic plutonism in the Ignace area included minor mafic intrusions (possibly flow centres) of gabbroic composition and the intrusion of tonalitic phases of the Revell batholith, approximately 2.737 to 2.732 Ga ago (Larbi et al., 1998; Buse et al., 2010). D1-D2 (Percival, 2004) ca. 2.71 Collision of the Winnipeg River-Marmion terrane and a northern superterrane (Uchian Orogeny) (Corfu et al., 1995).
ca. 2.70 to 2.67	Collision of the volcanic island arc (Western Wabigoon terrane) against the superterrane (Central Superior Orogeny) (Percival et al., 2006; Stone, 2010a). The central Superior Orogeny was accompanied by widespread regional plutonism. In the Ignace area, this resulted in emplacement of intrusive rocks including the major batholiths of interest. Specific dates include: Ca. 2.694 Ga: Crystallization age of the youngest phase of the Revell batholith; Ca. 2.685 Ga: Crystallization age of the White Otter Lake batholith; Ca. 2.685 Ga: Crystallization age of the White Otter Lake batholith; Ca. 2.685 Ga: Crystallization age of the White Otter Lake batholith; Ca. 2.671 Ga: Crystallization age of the Indian Lake batholith; and Ca. 2.697 to 2.684 Ga: an interval of sanukitoid magmatism (Stone, 2010a), which is expressed in the Ignace area by the emplacement of small plutons, such as the Islet pluton (Stone, 2009a) D3 and D4 (Percival, 2004).
ca. 2.6 to 2.4	Regional faulting and brittle fracturing (Kamineni et al., 1990).
ca. 2.12	Emplacement of the northwest trending Kenora-Fort Frances dyke swarm (Southwick and Halls,



	1987).
ca. 1.947	Brittle reactivation of regional-scale faults (Peterman and Day, 1989).
ca. 1.900	Emplacement of the west-northwest trending Wabigoon dyke swarm (Fahrig and West, 1986; Osmani, 1991).
ca. 1.13 to 1.14	Emplacement of the northwest trending dykes of Eye–Dashwa swarm (Kamineneni and Stone, 1983).
Post-1.14	A complex interval of erosion, brittle fracture, repeated cycles of burial and exhumation, and glaciations, particularly from the latest Miocene to the present.

## 2.4 Metamorphism

Metamorphism in the Central Wabigoon region occurred in late Neoarchean time, from approximately 2.722 to 2.657 Ga (Stone, 2010a) and peaked at approximately 2.701 Ga (Easton, 2000). The regional metamorphism may be related to the collision of the Western Wabigoon terrane with the Winnipeg River-Marmion terrane at approximately 2.7 Ga (Percival et al., 2006).

Metamorphism in the Central Wabigoon region is generally restricted to greenschist facies, and increases locally to middle amphibolite facies in parts of the greenstone belts (Sage et al., 1974; Blackburn et al., 1991; Easton, 2000; Sanborn-Barrie and Skulski, 2006). Very high grade (i.e., granulite facies) and very low grade (e.g., zeolite facies) metamorphism is largely absent in the Central Wabigoon region (Stone, 2010b).

A low to medium metamorphic grade overprint is present in the Ignace area, mainly within the Raleigh Lake and Bending Lake greenstone belts and within marginal zones of the Revell batholith. High metamorphic grade and migmatization occurs locally in the Ignace area in tonalite adjacent to plutons and greenstone belts. Medium metamorphic grade is widespread in the Raleigh Lake greenstone belt, where greenschist facies metamorphism grades into amphibolite facies. Numerous amphibolite and garnetiferous layers and clasts are found in rocks in the Raleigh Lake greenstone belt (Blackburn and Hinz, 1996).

In the Bending Lake greenstone belt, mineral assemblages are indicative of low to medium metamorphic grade. In general, rocks at the margins and in narrow extensions of the greenstone belt exhibit higher metamorphic grade than rocks in the core of the belt, implying a degree of contact metamorphism adjacent to the surrounding intrusive bodies (Stone, 2010a).

## 2.5 Quaternary Geology

Information on Quaternary geology in the Ignace area is described in detail in the Phase 1 terrain analysis for the Ignace area (JDMA, 2013) and has been summarized here.

The Quaternary deposits in the Ignace area accumulated during and after the last glacial maximum, known as the Late Wisconsinan Glaciation, with a significant amount of the material deposited during the progressive retreat of the Laurentide Ice Sheet. Advancement of the Laurentide Ice Sheet from the northeast across the area deposited a veneer of till throughout the areas mapped as bedrock terrain on Figure 3, with thicker accumulations of till mapped as morainal terrain. During the retreat of the Laurentide Ice Sheet, significant deposition of glaciofluvial outwash and glaciolacustrine plains occurred, with two major end moraines (Lac Seul and Hartman moraines) extending through the Ignace area recording the progressive retreat of the ice sheet.

The Hartman moraine is a significant Quaternary landform in the Ignace area that divides the area into distinct zones based on the thickness of Quaternary deposits. Thicker till, glaciofluvial outwash,

and deep-water glaciolacustrine deposits occur north of this moraine, whereas surficial deposits are generally thinner to the south (Figure 3). Areas mapped as bedrock terrain to the north of the Hartman moraine represent a spattering of islands within a proglacial lake known as Glacial Lake Agassiz that subsequently contracted into a set of large modern lakes.

Information on the thickness of Quaternary deposits within the Ignace area is described in detail in JDMA (2013). Measured thicknesses are limited to a small number of water well records for rural residential properties, typically along the TransCanada highway, and to diamond drill holes concentrated in the greenstone belts. Recorded depths to bedrock in the Ignace area range from 0 to 80 m, with an average depth of about 7 to 10 m. The thickness of the Quaternary deposits southwest of the highway in the periphery of the Township of Ignace is typically less than 5 m. The thickest overburden is inferred to occur along the axes of the Hartman and Lac Seul moraines.

## 3 Methodology

The structural interpretation of the Ignace area was based on high-resolution remote sensing data sets, including a high-resolution magnetic survey contracted by the NWMO to Sander Geophysics Limited (SGL, 2015), topographic data collected during the airborne magnetic survey, and Ontario Ministry of Natural Resources Forest Resources Inventory (FRI) digital aerial imagery (MNR, 2010).

### 3.1 Source Data Description

All data were assessed for quality, processed, and reviewed before use in the lineament interpretation. The geophysical data were used to evaluate deeper bedrock structures and proved invaluable to identifying potential bedrock structures beneath areas of surficial cover and aiding in establishing the age relationships among the different lineament sets. Topography (DEM) and digital aerial imagery data sets were used to identify surficial lineaments expressed in the topography, drainage, and vegetation. Throughout this study, the best resolution data available was used for the lineament interpretation.

#### 3.1.1 High-resolution Magnetic Data

Sander Geophysics Limited (SGL) completed a fixed-wing high-resolution airborne magnetic survey in the Ignace area between April 3 and May 5, 2014 (SGL, 2015). The survey area included the two blocks (Blocks (A) and (B)) located to the east and west of the Township of Ignace (Figure 4).

The airborne survey in the Ignace area included a total of 23,997 km of flight lines covering a surface area of approximately 100 km<sup>2</sup>. Flight operations were conducted out of the Dryden Regional Airport, in Dryden, Ontario using a Cessna Grand Caravan. Data were acquired along traverse lines flown in a north-south direction spaced at 100 m, and control lines flown east-west spaced at 500 m. The survey was flown at a target altitude of 80 metres above ground level, with an average ground speed of 100 knots (185.2 km/h). Magnetic data were acquired using a magnetometer sensor mounted in a fibreglass stinger extending from the tail of the aircraft. The survey acquisition parameters are listed below:

- Traverse line spacing of 100 m
- Traverse line azimuth of 000 - 180°
- Control line spacing of 500 m
- Control line azimuth of 270 – 090°
- Grid cell size of 25 m
- Targeted sensor height of 80 m
- Acquisition date of April 3 to May 5, 2014

Acquired data was processed by the Sander Geophysics Limited (SGL, 2015) and provided to SRK as GRD files. The following products of the high-resolution airborne magnetic survey were available for this structural lineament interpretation:

- Total magnetic intensity
- First vertical derivative of the total magnetic intensity
- Second vertical derivative of the total magnetic intensity

- Reduction to the pole of the total magnetic intensity
- First vertical derivative of the reduction to the pole of the total magnetic intensity
- Second vertical derivative of the reduction to the pole of the total magnetic intensity
- Tilt derivative of the reduction to the pole of the total magnetic intensity
- Analytic signal of the total magnetic intensity
- Total horizontal derivative of total magnetic intensity
- Total horizontal derivative of reduction to the pole of the total magnetic intensity
- Total magnetic intensity with high-pass Butterworth filter applied
- Total magnetic intensity with low-pass Butterworth filter applied
- Reduction to pole of total magnetic intensity with high-pass Butterworth filter applied
- Reduction to pole of total magnetic intensity with low-pass Butterworth filter applied

The first and second vertical derivatives, and tilt derivative grids were converted to ERS images that had data ranges, shading, and colour ranges enhanced in in ERMapper to outline the structures present. A series of compressed raster images was created in ERMapper for use in ArcGIS.

### 3.1.2 Digital Elevation Model

Topographic data was collected during the magnetic survey conducted by Sander Geophysics Limited (SGL, 2015). The survey acquisition parameters are identical to those described for the high-resolution magnetic data in Section 3.1.1.

Topographic data was processed by Sander Geophysics Limited and provided to SRK as GRD files. The data grid was then converted to an ERS image, and the data ranges, shading (including hill shade and shaded relief), and colour ranges of the digital elevation model (DEM) were enhanced in ERMapper to highlight the structures present (Figure 5). Compressed raster images were created in ERMapper for use in ArcGIS.

### 3.1.3 High-resolution Aerial Imagery

High resolution aerial imagery was obtained from the Ontario Ministry of Natural Resources Forest Resources Inventory (FRI) (MNR, 2010).

Digital aerial imagery was collected using a Leica ADS40 Airborne Digital Sensor. The ADS40 sensor captures multispectral bands simultaneously at the same true resolution, and therefore produces a 4-band, truly co-registered and equal resolution imagery (not pan sharpened) from the data acquisition. The spectral ranges and spatial resolution of each band are listed in Table 3.

**Table 3: FRI Digital Aerial Imagery Band Ranges and Resolution**

<b>Band</b>	<b>Range (nm)</b>	<b>Resolution (m)</b>
Panchromatic	465 - 680	0.2
Blue	428 - 492	0.4
Green	533 - 587	0.4
Red	608 - 662	0.4

Prior to release to the public, the imagery tiles are run through a bidirectional reflectance distribution function (BRDF) process to remove atmospheric distortions associated with sun angles. Subsequently, blocks of orthorectified tile imagery were compiled and processed to be normalized

using the brightest and darkest values within the multi date acquisition. Each image consists of a mosaic of 5 by 5 km orthorectified tiles of 4-band data.

A natural colour composite of the FRI digital aerial imagery was created in ArcGIS and utilized for the lineament interpretations (Figure 6).

## 3.2 Lineament Interpretation Workflow

A structural lineament study of each of the two blocks was conducted to identify the location and orientation of potential individual fractures or fracture zones and to evaluate their relative timing relationships within the context of the local and regional geological setting.

Lineaments were interpreted using a workflow designed to address issues of subjectivity and reproducibility that are inherent to any lineament interpretation. The workflow follows a set of detailed guidelines using the high resolution airborne geophysical (magnetic), and high resolution surficial (DEM, Digital Aerial) data sets described above. The interpretation guidelines involved three steps:

- Step 1: Independent lineament interpretation by two individual interpreters for each data set and assignment of certainty level (1, 2, or 3 representing low, medium and high certainty).
- Step 2: Integration of lineament interpretations for each individual data set and first determination of reproducibility.
- Step 3: Integration of lineament interpretations for the surficial data sets (DEM and digital aerial imagery) followed by integration of the combined surficial data set with the magnetic data set, with determination of coincidence in each integration step.

Each identified lineament feature was classified in an attribute table in ArcGIS. The description of the attribute fields used is included in Table 4. Fields 1 to 9 are populated during Step 1. Fields 10 and 11 are populated during Step 2. Fields 12 to 20 are populated during Step 3.

The interpreted features were classified into three general categories based on a working knowledge of the structural history and bedrock geology of the Ignace area. These categories include ductile, brittle and dyke lineaments, described as follows:

- **Ductile lineaments:** Features which were interpreted as being associated with the internal fabric of the rock units (including sedimentary or volcanic layering, tectonic foliation or gneissosity, and magmatic foliation) were classified as ductile lineaments. This category also includes recognizable penetrative shear zone fabric. See Figure A1 for example.
  - **Brittle lineaments:** Features interpreted as fractures (joints or joint sets, faults or fault zones, and veins or vein sets) were classified as brittle lineaments. This category also includes brittle-ductile shear zones, and brittle partings interpreted to represent discontinuous re-activation parallel to the ductile fabric. Brittle lineaments are commonly characterized by continuous magnetic lows, offsets of magnetic highs and ductile lineaments (as described above), and breaks in topography and vegetation. At the desktop stage of the investigation, this category also includes features of unknown affinity. See Figure A2 for example.
  - **Dyke lineaments:** Features which were interpreted, on the basis of their distinct character, e.g., scale and composition of fracture in-fill, orientation, geophysical signature and topographic expression, were classified as dykes. Dykes were largely interpreted from the magnetic data set, and are commonly characterized by continuous linear magnetic highs.
-

The interpretation of dykes is often combined with pre-existing knowledge of the bedrock geology of the study area.

A detailed description of the three workflow steps, as well as the way each associated attribute field is populated for interpreted lineament is provided below.

### **3.2.1 Step 1: Lineament Interpretation and Certainty Level**

To accommodate the generation of the best possible, unbiased lineament interpretation, two individual interpreters followed an identical process for structural lineament analysis during Step 1. The first step of the lineament interpretation was to have each individual interpreter independently produce GIS lineament maps, and detailed attribute tables, for each of the three data sets. Step 1 of the structural lineament analysis is conducted up to a scale of 1:25,000 and follows a designated workflow.

The interpretation of magnetic data follows a two-step process. The first step involves the drawing of ductile features, interpreted as tectono-stratigraphic form lines using high-resolution first vertical derivative magnetic data (Figures 7, 7a, 7b). Additionally, the tilt angle grid was used for enhancement of areas of low magnetic contrast. The form lines trace the geometry of magnetic high lineaments and may represent the geometry of stratigraphy within metavolcanic and metasedimentary rocks or the internal fabric (foliation) within granitoid batholiths and gneissic rocks. Magnetic highs associated with dykes (i.e. linear crosscutting magnetic highs in orientations identified in the literature as dyke orientations) are not included in this process. This process highlights discontinuities between form lines, particularly in stratigraphic form lines (e.g., form lines intersecting) that represent structures (faults, folds), unconformities, or intrusive contacts. The process of drawing form lines is instrumental in highlighting lineaments in the magnetic data.

The second step involves drawing a structural base layer that represents all interpreted lineaments regardless of interpreted age, type (e.g., ductile, brittle or dyke), or kinematics. Evidence for interpreted lineaments can be derived from several sources in the magnetic data, including discontinuities between form lines, offset of magnetic units, or the presence of linear magnetic lows or highs. The first vertical derivative magnetic data is used mainly with the tilt angle grid to further enhance this interpretation.

The lineament interpretation of topographic data involved tracing linear or curvi-linear features along topographic valleys, slope walls and any other structurally related features that are visible in a colour mosaic constructed from the digital elevation model (DEM) derived from the high-resolution airborne geophysical survey data. Similarly, the lineament interpretation of aerial imagery involved tracing linear or curvi-linear features along visible shore lines, changes in colour intensity or texture (e.g., vegetation), linear rivers and streams, and along linear chains of features associated with lakes that are visible in FRI digital aerial imagery.

Lineaments from each of the data sets were assigned attributes by each interpreter to characterize what type of feature the lineament was drawn along, the interpreters certainty that the lineament represents a bedrock structure, and the general width of the topographic feature.

**Table 4: Attribute Table Fields Populated for the Lineament Interpretation**

ID	Attribute	Brief Description
1	Rev_ID	Reviewer initials
2	Feat_ID	Feature identifier
3	Data_typ	Data set used (MAG, DEM, FRI)
		Type of feature used to identify each lineament
		Aerial Imagery:
		A. Lineaments drawn along straight or curved lake shorelines
		B. Lineaments drawn along straight or curved changes in intensity or texture (i.e., vegetation)
		C. Lineaments drawn down centre of thin rivers or streams
		D. Lineaments drawn along a linear chain of lakes
		E. Other (if other, define in comments)
4	Feat_typ	Digital Elevation Model:
		A. Lineaments drawn along straight or curved topographic valleys
		B. Lineaments drawn along straight or curved slope walls
		C. Other (if other, define in comments)
		Airborne Geophysics (magnetic and electromagnetic data):
		A. Lineaments drawn along straight or curved magnetic high
		B. Lineaments drawn along straight or curved magnetic low
		C. Lineaments drawn along straight or curved steep gradient
		D. Other (if other, define in comments)
5	Name	Name of feature (if known)
6	Certain	Value describing the interpreters confidence in the feature being related to bedrock structure (1-low, 2-medium or 3-high)
7	Length*	Length of feature is the sum of individual lengths of mapped polylines and is expressed in kilometres
		Width of feature; this assessment is categorized into 5 bin classes:
8	Width**	A. < 100 m
		B. 100 – 250 m
		C. 250 – 500 m
		D. 500 – 1,000 m
		E. > 1,000 m
9	Azimuth	Lineament orientation expressed as degree rotation between 0 and 180 degrees
10	Buffer_RA_1	Buffer zone width for reproducibility assessment (in metres)
11	RA_1	Feature value (1 or 2) based on first reproducibility assessment
12	Buffer_RA_2	Buffer zone width for coincidence assessment (in metres)
13	RA_2	Feature value (1, 2 or 3) based on coincidence assessment
14	MAG	Feature identified in geophysical data set (Yes or No)
15	DEM	Feature identified in DEM data set (Yes or No)
16	SAT	Feature identified in aerial imagery data set (Yes or No)
17	F_Width	Final interpretation of the width of feature
18	Rel_age	Interpretation of relative age of feature, in accord with regional structural history
19	Comment	Comment field for additional relevant information on a feature
20	Object	Geological element identified, e.g., dyke, fault, joint, contact

\* The length of each interpreted feature is calculated based on the sum of all segment lengths that make up that lineament.

\*\* The width of each interpreted feature is determined by expert judgment and utilization of a GIS-based measurement tool. Width determination takes into account the nature of the feature as assigned in the Feature type (Feat\_typ) attribute.

Lineaments identified in the DEM and/or in the aerial imagery that were interpreted to be due to glacial transport were excluded from the lineament interpretation data set. The following criteria were utilized to decide whether a DEM or aerial imagery lineament should be excluded:

- The lineament coincides with a mapped ice-flow feature, moraine, or esker;
- The lineament is parallel to known eskers or moraines and is marked by narrow, curving ridges;
- The lineament is parallel to the local ice flow direction and is accompanied by drumlin-shaped hills in the topographic data set;
- The lineament in the aerial imagery is parallel to the local ice flow direction and coincides with a lineament from the topography interpreted that has been identified as glacial; and
- The lineament was considered to be representative of a magmatic foliation, and not of tectonic origin.

The Step 1 lineament analysis resulted in the generation of one interpretation for each data set (e.g., magnetic, DEM, aerial imagery) for each interpreter, resulting in a total of six individual GIS layer-based interpretations. Within these data sets, cross-cutting relationships between individual lineaments were assessed. Following this assessment, based on the expert judgement of each interpreter, lineament segments were merged, resulting in lineament lengths that correspond to the sum of all parts.

During Step 1, identified lineaments were attributed with fields one to nine as listed in Table 4.

### **3.2.2 Step 2: Lineament Reproducibility Assessment 1 (RA\_1)**

During Step 2, individual lineament interpretations produced by each interpreter were compared for each data set. This included a reproducibility assessment based on the coincidence, or lack thereof, of interpreted lineaments within a data set-specific buffer zone. The two individual lineament interpretations for each data set were then integrated and a single interpretation was generated for each data set (Figures 8 to 10). A discussion of the parameters used during this step follows.

#### **Buffer Size Selection**

Buffer sizes for lineaments in each data set were based on the magnetic grid resolution. It was determined using trial-and-error over a selected portion of the lineament interpretation that buffer sizes of five times the grid cell resolution provided a balanced result for assessing reproducibility.

A buffer of 125 m (either side of the lineament) was generated for the magnetic data. This value is equivalent to five times the data set grid cell resolution (25 m) of the high resolution magnetic data. Given that the DEM data was extracted from the same survey, the same buffer size was applied to the DEM data.

A 125-metre buffer was applied to the aerial imagery data in order to be consistent with the magnetic and DEM buffer size.

The buffer size widths were included in the attribute fields of each interpretation file (Table 4). The buffers were used as an initial guide to determine coincidence between lineaments, with the expert judgement of the interpreter ultimately determining which lineaments were coincident.



## Reproducibility Assessment

The generation of an integrated lineament interpretation for each data set, including the reproducibility assessment, followed a three-step process:

- Lineament buffers generated for the Step 1 interpretation were overlain on top of the buffers generated for the lead Step 1 interpretation for each data set. The lead interpretation Step 1 lineaments were then overlain on top of these buffers, and all lineaments that occurred within overlapping buffers were carried forward and copied into a new file for Step 2. These lineaments were attributed with a reproducibility value (RA\_1; Table 4) of two in the Step 2 attribute table.
- The remaining lineaments in the lead Step 1 interpretation were then manually analyzed by both interpreters on the basis of the available imagery for each data set. In some instances, this included adapting the shape and extent of individual lineaments to increase the accuracy of spatial location or length of the lineament, and carrying the adapted lineament forward into the Step 2 interpretation file. These lineaments were attributed a RA\_1 value of one in the Step 2 attribute table. Where it was determined by the two interpreters that these features were not representative of potential bedrock structure, they were removed from the data set.
- Finally, the lineament interpretation of the second Step 1 interpretation was overlain on top of the Step 2 integrated file, and all remaining lineaments in the second interpreter's Step 1 interpretation were then manually analyzed by both interpreters on the basis of the available imagery for each data set. In some instances, this included adapting the shape and extent of individual lineaments to increase the accuracy of spatial location or length of the lineament, and carrying the adapted lineament forward into the Step 2 interpretation file. These lineaments were attributed a RA\_1 value of one in the Step 2 attribute table. All remaining lineaments that were attributed a certainty value of one were removed, if it was determined by the two lineament interpreters that these features were not representative of potential lineaments.

As specified above, the decision on whether or not to adapt the shape and extent of an individual lineament and (or) whether the lineament was carried forward to the next step followed analysis of the specified lineament with the available imagery and a discussion between the two interpreters. The following guidelines were applied:

- If a lineament was drawn continuously by one interpreter but as individual, spaced or disconnected segments by the other interpreter, the lineament was carried forward to the Step 2 interpretation with a RA\_1 value of two.
- If more than two thirds of a lineament were identified by one interpreter compared to the other interpreter, the lineament was carried forward to the Step 2 interpretation with a RA\_1 value of two. If less than two thirds of a lineament were identified by one interpreter compared to the other interpreter, the longer lineament was cut, and each portion was attributed with RA\_1 values accordingly.

The resulting Step 2 interpretations for each data set (e.g., magnetics, topography, and aerial imagery) were then refined using expert judgement to avoid any structurally inconsistent relationships. This included adapting the lineaments within the limits of the assigned buffer zone to avoid any mutually crosscutting relationships, and updating the attribute fields.

### 3.2.3 Step 3: Coincidence Assessment (RA\_2)

During Step 3, the integrated lineament interpretations for each data set were amalgamated into one final interpretation. First, lineaments derived from the DEM and aerial imagery data were merged to produce an integrated surficial lineament data set. Subsequently, the geophysical lineaments were integrated with the integrated surficial lineaments to produce a final amalgamated interpretation. A discussion of the parameters used during this step follows below.

#### Surficial Integration

The FRI aerial imagery data have a resolution of 40 centimetres (cm) whilst the DEM data has a resolution of approximately 25 m. Furthermore, the orientation of minor and intermediate topographic features as identified in the DEM can be ambiguous due to the resolution of the data, while these features could be drawn with high confidence from the aerial imagery data. Therefore, lineaments derived from the aerial imagery data were used as the lead data set, and lineaments drawn from DEM data were used as the secondary data set.

A buffer of 125 m (five times the resolution of the DEM) was generated around the DEM lineaments and the aerial imagery lineaments were overlain on top of this buffer. Similar to the procedure in RA\_1, all lineaments that occurred within overlapping buffers were carried forward and copied into a new file. These lineaments were attributed with a RA\_2 coincidence value of two (RA\_2; Table 4). The remaining aerial imagery and DEM lineaments were then manually analyzed by both interpreters on the basis of the available imagery for each data set. In some instances, this included adapting the shape and extent of individual lineaments to increase the accuracy of spatial location or length of the lineament. These lineaments were attributed a RA\_2 value of one in the attribute table (RA\_2; Table 4).

#### Final Integration

The geophysical data supplies important information about structures in the subsurface. Therefore, for this step of the interpretation, the lineaments derived from geophysical data were given precedence over lineaments derived from surficial data, since the latter only provide information about the surface expression of structures.

On this premise, all lineaments derived from the magnetic data were included in the final interpretation. A buffer of 125 m (five times the resolution of the geophysical data and DEM) was generated around the integrated surficial lineaments, and the geophysical lineaments were overlain on top of this buffer. This buffer size was included as an attribute field for all interpreted lineaments (Buffer RA\_2; Table 4). As part of this comparison, coincident lines were identified and attributed. Next, non-coincident lineaments were evaluated against the magnetic data by both interpreters, and if required, were adapted and carried forward to the final Step 3 data set. This resulted in a combined interpretation with lineaments derived from the magnetic and surficial data sets.

The following rules were applied for determining coincidence between the data set-specific lineament maps:

- If any coincidence of lineaments occurred between two lineament data sets, the longest lineament was carried forward to the Step 3 interpretation and attributed as derived from two (or more) data sets, regardless of the length of overlap between the lineaments. This meant that if any part of a lineament derived from one data set was identified in another data set, it was considered that this lineament was reproduced.

- In the case that a lineament derived from topographic or aerial imagery data was longer than a coincident lineament derived from geophysical data, the former lineament was cut and the non-coincident portion was carried forward into the final Step 3 interpretation as a single entity. Both the lineament in the geophysical data and the non-coincident portion derived from another data set were then attributed accordingly in terms of coincidence.
- A lineament derived from topographic and (or) aerial imagery data that would fall within the buffer of a lineament derived from geophysical data would be attributed as coincident in the relevant data sets if the orientation of the lineaments did not deviate significantly.
- Short (less than 500 m) discontinuous topographic and aerial imagery data lineaments that are at low angles to geophysical data lineaments but extending outside the geophysical lineament buffer were considered to be coincident.
- Short (less than 500 m) topographic and aerial imagery data lineaments that are at high angles to geophysical data lineaments, largely overlapped with the buffer zone from the geophysical data lineament, and had no further continuity (i.e., singular elements), were not carried forward to the final interpretation. This was done on the basis that these short segments represent a subsidiary lineament that is related to a broader fault zone already included as a fault lineament in the final interpretation based on identification in the geophysical data.

During this process, each lineament was attributed with a text field highlighting in which data sets it was identified. The final coincidence value (RA\_2; Table 4) was then calculated as the sum of the number of data sets in which each lineament was identified (i.e., a value of 1 to 3).

The resulting lineament interpretation, representing the integration of all data sets, was then evaluated and modified (within the limits of relevant buffers) in order to develop a final lineament interpretation that is consistent with the known structural history of the Ignace area. This included defining the age relationships of the interpreted lineaments on the basis of crosscutting relationships between different generations of brittle lineaments and populating the relative age attribute field for each lineament (Rel\_Age; Table 4). This incorporated a working knowledge of the structural history of the Ignace area, combined with an understanding of the lineament characteristics in each lineament population (e.g., brittle versus ductile). The structural history of the area is described in Section 2.4, based on the existing literature.

The interpreted crosscutting and age relationships between different families of fault lineaments and within individual families of brittle lineaments were refined using the available data. Crosscutting relationships were evaluated based on the through-going nature and termination of brittle lineaments and evaluated against the regional structural history as described in Section 2.4.

### 3.2.4 Lineament Length

Lineament lengths were calculated using a simple geometrical calculation of the total length of the polyline in ArcGIS.

The length distribution of the various integrated data sets was analyzed through a comparison of summary statistics, frequency histograms, log-log plots and boxplots. Histograms and summary statistics were computed using Microsoft Excel's Data Analysis add-in. Histogram bins were computed using arbitrary 500 m bins.

There is no information available on the depth extent into the bedrock of the lineaments interpreted for the Ignace area. In the absence of available information, the interpreted length can be used as a proxy for the depth extent of the identified structures. However, this is highly dependent on the style

---

and structural history of a given fault. A preliminary assumption may be that the longer interpreted lineaments in the Ignace area may extend to greater depths than the shorter interpreted lineaments.

### 3.2.5 Lineament Trends

An analysis of lineament trends is an essential part of the structural lineament interpretation, as it allows the interpreter to identify different sets of structures and to relate those sets to the known structural history of the area. Lineament orientations were assessed for each data set within Block (A) and Block (B) to determine the dominant lineament trends, and potential conjugate sets.

Lineament orientations (azimuth) were calculated using ET EasyCalculate 10, an add-in extension to ArcGIS. This add-in provides a function (polyline\_GetAzimuth.cal) that calculates the azimuth of each polyline at a user-specified point and populates an assigned attribute field. SRK used the mid-point of each interpreted lineament to calculate the azimuth.

Rose diagrams are circular or semi-circular histograms that depict orientation (azimuthal) data and frequency for each data bin. The histogram peaks show the frequency of occurrence of lineament orientations within each bin. Rose diagrams were produced in Spheristat, with frequencies divided into 5° bins in order to avoid oversimplification of the lineament orientations. Lineament lengths are also used as a weight factor for computing rose diagrams that display the lineament trends.

### 3.2.6 Lineament Density

Analyses of lineament density were conducted for the Ignace area. The lineament density analysis was conducted using the ArcGIS Analysis and Spatial Analyst toolsets, and included creating lineament density plots, lineament intersection points, and conducting an intersection point density analysis for the magnetic, surficial, and final integrated lineament data sets.

Lineament line density of all interpreted lineaments in the Ignace area was determined by examining the statistical density of individual lineaments using ArcGIS Spatial Analyst. A grid cell size of 50 m and a search radius of 1.25 km (equivalent to half the size of the longest boundary of the minimum area size of a potential siting area) were used for this analysis. The spatial analysis used a circular search radius examining the lengths of polylines intersected within the circular search radius around each grid cell.

Lineament intersections were calculated using the ArcGIS Analysis Tools Intersect function. To improve visualization of the lineament intersection points, SRK gridded their density using the ArcGIS Spatial Analyst function. Spatial Analyst calculates point density conceptually by defining a neighbourhood around each raster cell centre, and the number of points that fall within the neighbourhood is totalled and divided by the area of the neighbourhood. A grid cell size of 50 m and a search radius of 1.25 km (equivalent to half the size of the longest boundary of the minimum area size of a potential siting area) were used.

## 4 Lineament Interpretation Results

The following sections describe the results of the lineament interpretation of the Ignace area based on analysis of the geophysical and surficial (DEM, aerial imagery) data sets. This includes discussion of the RA\_1 assessment of reproducibility. In addition, the RA\_2 results are discussed for the integration of the two surficial data sets and for the final integration of the geophysical data set with the surficial data sets.

### 4.1 Geophysical Lineaments

An interpretation of magnetic data allows for the distinction between ductile, dyke, and brittle lineaments. Ductile features traced from the magnetic data set are shown on Figure A1 and Figures 7, 7a and 7b and are interpreted as traces of the geometry of stratigraphy within the greenstone belts or the internal fabric (foliation) within plutonic and gneissic rocks. Discontinuities between ductile features highlight structures (potential fractures, and fold structures), unconformities, or intrusive contacts. Therefore, they constitute an essential data component that should be used along with the first vertical derivative of the magnetic data for interpreting brittle and dyke lineaments. Ductile features are included in this report to provide context to the lineament interpretation, but they were not included in the statistical analyses of the lineament data sets. Figure A1 shows an example of ductile lineaments interpreted in the Ignace area. Figure A2 shows brittle lineaments interpreted on the basis of geophysical, DEM, and digital aerial imagery.

Within the Ignace area, a total of 1,427 geophysical lineaments were interpreted. This data comprises lineaments that were identified and merged by the two interpreters based on interpretation from the geophysical data (Figure 8). The length of all geophysical lineaments ranges from 0.21 to 36.36 km, with a median of 2.11 km and a mean of 3.52 km. Of the total number of geophysical lineaments, 1,414 were characterized by discrete linear magnetic lows and interpreted as brittle lineaments and 13 were characterized by discrete linear magnetic highs and interpreted as dyke lineaments. It is worth noting that the dyke lineaments shown on Figure 8 have been traced as individual segments; which visually represent more than 13 dykes. However, a number of these dyke segments are parallel and in-line with each other, and are therefore interpreted to represent a single dyke structure. Azimuth data weighted by length for all interpreted geophysical lineaments display a broad west-northwest to north-northwest trend (285°-340°) within which two peaks at 295°-305° and 340° are dominant. There is also a minor northeast (030°-070°) trend (see inset Figure 8).

Of the total geophysical lineaments, the reproducibility assessment identified coincidence for 619 (43%; RA\_1 = 2) and a lack of coincidence for 810 (57%; RA\_1 = 1). The reproducibility assessment identified coincidence (RA\_1 = 2) for all the 13 dyke lineaments. Of the 1,427 lineaments interpreted, 613 (43 %) were assigned the highest level of certainty (three), while 671 (47 %) were assigned certainty values of two, and 143 (10 %) were assigned certainty values of one.

West-northwest-trending lineaments and north-northwest trending lineaments are interpreted to define a conjugate set in which the west-northwest trending lineaments show evidence of displacement with a sinistral offset by the most prominent north-northwest trending lineaments. Total strike-separation amounts along north-northwest lineaments are locally interpreted to be up to 150 to 300 metres. An example of this sinistral strike-separation can be seen along the north-northwest-trending lineaments shown in Figure A4.

Block (A) includes a total of 254 geophysical lineaments (Figure 8a). Of these, 253 were interpreted as brittle lineaments and 1 was interpreted as a dyke lineament. The lengths of geophysical lineaments within this block range from 0.45 to 20.17 km, with a median length of 2.31 km and a mean length of 3.47 km. Of the 254 lineaments interpreted in Block A, 119 (47%) were assigned the highest level of certainty (three), while 110 (43%) were assigned certainty values of two, and 25 (10%) were assigned certainty values of one. The assessment of reproducibility indicates that 98 (39%; RA\_1 = 2) of the geophysical lineaments in Block (A) are coincident between both interpreters, whereas the remaining 156 (61%; RA\_1 = 1) were identified by one interpreter only. The interpreted dyke lineament was coincident between both interpreters. Azimuth data weighted by length for the geophysical lineaments interpreted in Block (A) exhibit two dominant northwest orientations (330° to 350° and 280° to 295°) and a minor northeast orientation (045° to 065°) (see inset Figure 8a).

Block (B) includes a total of 1,173 geophysical lineaments (Figure 8b). Of the 1,173 lineaments within Block (B) 1,161 were interpreted as brittle lineaments and 12 were interpreted as dykes. These lineaments show a range in length from 0.21 to 36.36 km, with a median of 2.09 km and a mean of 3.53 km. Of the 1,173 lineaments interpreted in Block (B), 494 (42%) were assigned the highest level of certainty (three), while 561 (48%) were assigned certainty values of two, and 118 (10%) were assigned certainty values of one. All 12 interpreted dyke lineaments were assigned a certainty value of three. The assessment of reproducibility indicates that 521 (44%; RA\_1 = 2) of the geophysical lineaments within Block (B) are coincident between both interpreters, whereas the remaining 652 (56%; RA\_1 = 1) were identified by one interpreter. The reproducibility assessment identified coincidence (RA\_1 = 2) for all the interpreted dyke lineaments. Azimuth data weighted by length for the geophysical lineaments interpreted in Block (B) exhibit a broad spread between 270° and 360°, with the greatest frequency in the 295° to 310° bin. The 12 lineaments that were identified as dykes occur along a dominant west-northwest (300° to 310°) orientation (Figure A3 (A)). A broad northeast to east (045°-090°) orientation, with two distinct peaks at ca. 040° and 065°, is also evident (see inset Figure 8b).

## 4.2 Surficial Lineaments

Surficial lineaments include lineaments interpreted from the DEM topography and aerial imagery data sets, and are shown on Figures 9 and 10, respectively. An overview of the lineament interpretation based on these surface-based data sets is provided below.

### 4.2.1 DEM Lineaments

A total of 2,244 lineaments were identified by the two interpreters from the DEM topography data (Figure 9). The length of all DEM lineaments ranges from 0.12 to 15.81 km, with a median of 1.22 km and a mean of 1.72 km. Of the 2,244 interpreted lineaments, 738 (33 %) were assigned the highest level of certainty (three), while 1,261 (56 %) were assigned certainty values of two, and 245 (11 %) were assigned certainty values of one. The reproducibility assessment identified coincidence for 721 (32%; RA\_1 = 2) and a lack of coincidence for 1,523 (68%; RA\_1 = 1) of the total lineaments. Azimuth data weighted by length for all DEM lineaments exhibit two prominent orientations, one to the northeast between 035° and 065° and a second to the northwest between 305° and 330° (see inset Figure 9). Minor north-south and east-west trends are also evident.

Block (A) includes a total of 459 DEM lineaments (Figure 9a). The length of DEM lineaments in Block (A) ranges from 0.18 to 8.99 km, with a median of 1.09 km, and a mean of 1.41 km. Of the 459 lineaments interpreted in Block (A), 200 (44%) were assigned the highest level of certainty (three), while 225 (49%) were assigned certainty values of two, and 34 (7%) were assigned certainty

values of one. The assessment of reproducibility for DEM lineaments identified in Block (A) showed that 127 (28%; RA\_1 = 2) lineaments have coincidence between the two interpreters, and that the remaining 332 (72%; RA\_1 = 1) lineaments were interpreted by a single interpreter only. Azimuth data weighted by length for the DEM lineaments interpreted in Block (A) exhibit a prominent northeast trend (between 035° and 065°; see inset Figure 9a). In addition, there is also a less prominent spread of data between west-northwest and north (280°-360°)

Block (B) includes a total of 1,785 DEM lineaments (Figure 9b). The length of DEM lineaments in Block (B) ranges from 0.25 to 15.58 km, with a median of 1.41 km, and a mean of 2.0 km. Of the 1,785 lineaments interpreted in Block (B), 538 (30%) were assigned the highest level of certainty (three), while 1,036 (58%) were assigned certainty values of two, and 211 (12%) were assigned certainty values of one. The assessment of reproducibility for DEM lineaments identified in Block (B) showed that 594 (33%; RA\_1 = 2) lineaments have coincidence between the two interpreters, and that the remaining 1,191 (67%; RA\_1 = 1) lineaments were interpreted by a single interpreter only. Azimuth data weighted by length for the DEM lineaments exhibit a bimodal population with a prominent northwest trend (between 305° and 320°) and a dominant northeast trend (between 035° and 065°). Minor north-south and east-west trends are also evident (see inset Figure 9b).

#### 4.2.2 Digital Aerial Imagery Lineaments

A total of 2,108 lineaments were identified by the two interpreters from the digital aerial imagery data (Figure 10). The length of all lineaments ranges from 0.03 to 5 km, with a median of 0.40 km and a mean of 0.55 km. Of the 2,108 interpreted lineaments, 741 (35 %) were assigned the highest level of certainty (three), while 908 (43 %) were assigned certainty values of two, and 459 (22 %) were assigned certainty values of one. The reproducibility assessment identified coincidence for 1,071 (51%; RA\_1 = 2) and a lack of coincidence for 1,037 (49%; RA\_1 = 1) of the total lineaments. Azimuth data weighted by length for the digital aerial imagery lineaments exhibit a broad range in trends between west-northwest and east-northeast, with more dominant but still broad peaks to the north-northwest (between 325° and 355°) and northeast (between 025° and 045°) and a third northeast (between 050° and 065°; see inset Figure 10).

Block (A) includes a total of 626 aerial lineaments (Figure 10a). The length of digital aerial lineaments in Block (A) ranges from 0.03 to 2.97 km, with a median of 0.32 km and a mean of 0.37 km. Of the 626 lineaments interpreted in Block (A), 154 (25%) were assigned the highest level of certainty (three), while 244 (39%) were assigned certainty values of two, and 228 (36%) were assigned certainty values of one. The reproducibility assessment identified coincidence between the two interpreters for 250 (40%; RA\_1 = 2) lineaments, with the remaining 376 (60%; RA\_1 = 1) lineaments being identified by a single interpreter only. Azimuth data weighted by length for the digital aerial lineaments interpreted in Block (A) exhibit a dominant north-northeast orientation between 025° and 060° as well as less prominent north-northwest (340° to 355°) and west-northwest (285° to 295°; see inset Figure 10a).

Block (B) includes a total of 1,482 aerial lineaments (Figure 10b). The length of digital aerial lineaments in Block (B) ranges from 0.04 to 5.00 km, with a median of 0.45 km and a mean of 0.62 km. Of the 1,482 lineaments interpreted in Block (B), 587 (40%) were assigned the highest level of certainty (three), while 664 (45%) were assigned certainty values of two, and 231 (16%) were assigned certainty values of one. The reproducibility assessment identified coincidence between the two interpreters for 821 (55%; RA\_1 = 2) lineaments, with the remaining 661 (45%; RA\_1 = 1) lineaments being identified by a single interpreter only. Azimuth data weighted by length for the digital aerial imagery lineaments interpreted in Block (B) exhibit a broad spread with the greatest frequency in the bins between 290° and 055° (see inset Figure 10b).

### 4.3 Integrated Surficial Lineaments (RA\_2)

The lineaments interpreted based on DEM and digital aerial imagery data were integrated to form the surficial lineament data set. This integration resulted in a total of 3,300 surficial lineaments (Figure 11).

The merging of lineaments interpreted based on DEM and aerial imagery resulted in lineaments of new lengths, either shorter or longer, due to merging of original lineaments. In general, lineaments interpreted from the digital aerial image data are significantly shorter than those interpreted from the DEM data (see Sections 4.2.1 and 4.2.2). The length of all integrated surficial lineaments ranges from 0.03 to 15.81 km, with a median of 0.92 km and a mean of 1.37 km.

Of the 3,300 integrated surficial lineaments, 1,063 (32 %) were assigned the highest level of certainty (three), while 1,726 (52 %) were assigned certainty values of two, and 511 (15 %) were assigned certainty values of one. The reproducibility assessment identified coincidence for 1,208 (37 %) lineaments and a lack of coincidence for 2,092 (63 %) of the total integrated surficial lineaments. Azimuth data weighted by length for the integrated surficial lineaments exhibit two dominant orientations: northeast (030° to 060°) and northwest (295° to 325°) and two less prominent orientations of east-west and north-south (see inset Figure 11).

Within Block (A) a total of 824 integrated surficial lineaments were interpreted. Their lengths range from 0.033 to 8.989 km, with a median of 0.59 km and a mean of 0.90 km. Of the 824 lineaments in Block (A), 279 (34%) were assigned the highest level of certainty (three), while 363 (44%) were assigned certainty values of two, and 182 (22%) were assigned certainty values of one. The reproducibility assessment for Block (A) identified coincidence between the two surficial data sets for 264 (32%) lineaments, with the remaining 560 (68%) lineaments being identified in a single data set only. Azimuth data weighted by length for the integrated surficial lineaments interpreted in Block (A) exhibit a prominent northeast trend (between 035° and 065°; see inset Figure 11a). In addition, there is also a less prominent broad spread of data between west-northwest and north (280°-360°)

Within Block (B) a total of 2,476 integrated surficial lineaments were interpreted. Their lengths range from 0.07 to 15.81 km, with a median of 1.01 km and a mean of 1.52 km. Of the 2,476 lineaments carried forward in Block (B), 784 (32%) were assigned the highest level of certainty (three), while 1,363 (55%) were assigned certainty values of two, and 329 (13%) were assigned certainty values of one. The reproducibility assessment for Block (B) identified coincidence between the two surficial data sets for 944 (38%) lineaments, with the remaining 1,532 (62%) lineaments being identified in a single data set only. Azimuth data weighted by length for the surficial lineaments interpreted in Block (B) exhibit two orientations: northeast (035° to 065°) and northwest (310° to 320°). Minor north-south and east-west trends are also evident (see inset Figure 11b)

### 4.4 Integrated Final Lineaments (RA\_2)

The integrated lineament data set produced by merging all lineaments interpreted from the geophysical (Figure 12) and surficial (DEM and aerial imagery, Figure 11) data is presented on Figure 13.

The integrated lineament data set contains a total of 3,477 lineaments (including 3,464 brittle and 13 dyke lineaments). The integrated lineament data ranges in length from 0.07 to 40.26 km. The median length of these lineaments is 1.33 km and the mean length is 2.30 km. Of all integrated lineaments, 320 lineaments are greater than 5 km in length (9 %), 533 lineaments are between 2.5 and 5 km in



length (15 %), 1,296 lineaments are between 1 and 2.5 km in length (37 %), and 1,328 lineaments are less than 1 km in length (38 %).

Of the 3,477 integrated lineaments, 1,265 (36 %) were assigned the highest level of certainty (three), while 1,765 (51 %) were assigned certainty values of two, and 447 (13%) were assigned certainty values of one. The reproducibility assessment identified coincidence in all three data sets (RA\_2 = 3) for 113 (3%) lineaments, and 780 (23%) lineaments were coincident with a lineament from one other data set (RA\_2 = 2). A total of 2,584 (74%) lineaments were not coincident with any other data set (RA\_2 = 1). Furthermore, a total of 493 lineaments observed in magnetic data were coincident with an interpreted surficial lineament (represents 34% of all geophysical lineaments). All interpreted dykes have a reproducibility assessment of 1 (RA\_2 = 1), as they were only recognized in the magnetic data.

Azimuth data weighted by length for the integrated lineaments exhibit a diffuse northwest (285° to 340°) trend with multiple discrete peaks and a broad northeast (025° to 065°;) trend . A weak east-west is also noted in the final lineament data set (Figure 13 inset).

Within Block (A), the integrated lineament data set contains a total of 789 lineaments (Figure 13a). They have a length range of 0.07 to 20.34 km, with a median length of 1.03 km and a mean length of 1.86 km. Of the 789 integrated lineaments identified in Block (A), 297 (38 %) were assigned the highest level of certainty (three), while 350 (44 %) were assigned certainty values of two, and 142 (18 %) were assigned certainty values of one. The reproducibility assessment identified coincidence in all three data sets (RA\_2 = 3) for 19 (2%) lineaments, and 164 (21 %) lineaments were coincident with a lineament from one other data set (RA\_2 = 2). A total of 606 (77 %) lineaments were not coincident with any other data set (RA\_2 = 1). Azimuth data weighted by length for the integrated final lineaments in Block (A) exhibit dominant northwest (275° to 295°), north-northwest (340° to 360°) trends and a broader northeast (030° to 070°) trend (Figure 13a inset).

Within Block (B), the integrated lineament data set contains a total of 2,688 lineaments (Figure 13b). They have a length range of 0.13 to 40.26 km, with a median length of 1.39 km and a mean length of 2.43 km. Of the 2,688 integrated lineaments identified in Block (B), 968 (35 %) were assigned the highest level of certainty (three), while 1,415 (53 %) were assigned certainty values of two, and 305 (11 %) were assigned certainty values of one. The reproducibility assessment identified coincidence in all three data sets (RA\_2 = 3) for 94 (3 %) lineaments, and 616 (23 %) lineaments were coincident with a lineament from one other data set (RA\_2 = 2). A total of 1,978 (74 %) lineaments were not coincident with any other data set (RA\_2 = 1). Azimuth data weighted by length for the integrated final lineaments in Block (B) exhibit a broad northwest (295° to 340°) and a broad northeast (025° to 065°) trend (Figure 13b inset).

## 4.5 Description of Lineaments by Geological Units

As described in Section 2, the general potentially suitable areas identified in the Ignace area in the Phase 1 Geoscientific Desktop Preliminary Assessment (Golder, 2013) are located on the Revell, Indian Lake and Basket Lake batholiths. The following discussion describes the dominant interpreted lineament orientations for each of these three batholiths, as well as the gneissic unit adjacent to the Indian Lake and Basket Lake batholiths to the northeast of the greenstone belts.

### 4.5.1 Revell Batholith

A total of 264 geophysical lineaments were identified over the Revell batholith, including 3 dykes (Figure 15). Azimuth data, weighted by length, for the lineaments from the Revell Batholith exhibit a

dominant north-northwest (315° to 330°) trend, and less prominent northwest (270° to 290°), north-northeast (000° to 010°), and northeast (050° to 065°) trends (Figure A3 (B)).

A total of 1,000 surficial lineaments were identified over the Revell batholith. Azimuth data, weighted by length, for the lineaments from the Revell batholith exhibit a dominant northeast (035° to 060°) trend, as well as a broad spread of data from west to north-south orientations, with subtle north-south, northwest, and east-west dominant trends within the spread (Figure A3 (B)).

A total of 951 lineaments integrated from all three data sets were identified over the Revell batholith. Azimuth data, weighted by length, for the integrated lineaments in the Revell batholith exhibit distinct northeast (025° to 065°), west-northwest, and northeast trends, as well as a minor north and east trends (Figure A3).

#### **4.5.2 Indian Lake Batholith**

A total of 495 geophysical lineaments were interpreted over the Indian Lake batholith, including 236 brittle lineaments and one dyke lineament in Block (A), and 258 lineaments in Block (B). Azimuth data, weighted by length, for geophysical lineaments in the Indian Lake batholith shows two predominantly northwest (290° to 325°) and north-northwest (330° to 355°) trends, as well as more subtle northeast (060° to 070°) and east-west (085° to 095°) trends (Figure A3 (B)).

A total of 1,015 surficial lineaments were interpreted over the Indian Lake batholith, including 761 lineaments in Block (A), and 254 lineaments in Block (B). Azimuth data, weighted by length, for surficial lineaments in the Indian Lake batholith show a dominant northeast (025° to 060°) trend, and a less prominent northwest (285° to 305°) trend (Figure A3 (B)).

A total of 1,166 lineaments integrated from all three data sets were interpreted over the Indian Lake batholith, including 741 lineaments in Block (A) and 425 lineaments in Block (B). Azimuth data, weighted by length, for integrated lineaments in the Indian Lake batholith show two prominent trends to the northwest (285° to 315°) and north-northwest (330° to 350°) (Figure A3 (B)).

#### **4.5.3 Basket Lake Batholith**

A total of 234 geophysical lineaments were identified over the Basket Lake batholith. Azimuth data, weighted by length for the geophysical lineaments in the Basket Lake batholith show a spread of data with subtle north-northwest (330° to 340°), northwest (290° to 305°), and northeast (025° to 045°) trends (Figure A3 (B)).

A total of 342 surficial lineaments were identified over the Basket Lake batholith. Azimuth data, weighted by length for the surficial lineaments in the Basket Lake batholith show a dominant northeast (035° to 055°) trend (Figure A3 (B)).

A total of 437 lineaments integrated from all three data sets were identified over the Basket Lake batholith. Azimuth data, weighted by length for the integrated lineaments in the Basket Lake batholith show northeast (025° to 035°), north-northwest (340° to 355°), and northwest (295° to 310°) trends (Figure A3 (B)).

#### **4.5.4 Gneissic Rocks**

A total of 264 geophysical lineaments were identified in the gneissic rocks. Azimuth data, weighted by length for the geophysical lineaments in the gneissic rocks show a prominent northwest (300° to

325°) trend, and more subtle north-northwest (330° to 340°) and northeast (020° to 055°) trends (Figure A3 (B)).

A total of 408 surficial lineaments were identified in the gneissic rocks. Azimuth data, weighted by length for the surficial lineaments in the gneissic rocks show a prominent northwest (290° to 310°) trend, and a less prominent northeast (030° to 060°) trend (Figure A3 (B)).

A total of 497 lineaments integrated from all three data sets were identified in the gneissic rocks. Azimuth data, weighted by length for the integrated lineaments in the gneissic rocks show northwest (295° to 315° and 320° to 350°) and northeast (030° to 035°) trends (Figure A3 (B)).

## 5 Discussion

Lineament reproducibility and coincidence, lineament trend, lineament length and the density of lineaments and their intersections are discussed below. In addition, the integration of the final lineament data set into the regional structural history, and the relative age of lineament sets in the Ignace area are discussed.

### 5.1 Lineament Reproducibility (RA\_1) and Coincidence (RA\_2)

Lineament reproducibility and coincidence are assessed in several steps during the analysis. First, the two individual interpretations for each data set are integrated to produce single data set specific (RA\_1) interpretations. Secondly, the individual data set interpretations are integrated to produce the final RA\_2 data set. Reproducibility and coincidence values are presented in detail in Section 4.

The RA\_1 data presented in Section 4 indicate that the reproducibility between interpreters for all three data sets is moderate. Aerial imagery lineaments show the highest reproducibility value, with 51% identified by both interpreters. Importantly, longer lineaments with higher certainty values were identified more often by both interpreters in all three data sets. Differences in the individual lineament interpretations from each interpreter for the same data set can be attributed to the judgement and subjectivity of the expert carrying out the interpretation.

Coincidence between features identified in the various data sets was evaluated for the second reproducibility assessment (RA\_2). Reproducibility values determined by coincidence between data sets (RA\_2) may provide a measure of the confidence in the interpretation and may also highlight significant bedrock structures expressed in these different data sets.

As discussed in Section 4.3, 37% of the surficial lineaments were interpreted in both the DEM and the aerial imagery data sets. The coincidence between surficial data sets is in part explained by the fact that lineaments interpreted from the aerial imagery and the digital elevation data represent surficial expressions of the same bedrock feature. For example, a lineament drawn along a stream channel shown on the aerial imagery is expected to be coincident with a lineament that captures the trend of the associated topographic valley expressed in the digital elevation data. Lack of coincidence between the two surficial data sets can be attributed to structures observed in the DEM data that are obscured by vegetation and other surficial elements in the digital aerial imagery data.

The coincidence assessment (RA\_2) revealed that 34% of the interpreted geophysical lineaments were also interpreted in at least one of the two surficial data sets. The lack of coincidence between the geophysical and surficial lineaments may be the result of various factors such as deep structures that are identified in the magnetic data may not have a surface expression; surficial features may not extend to great depth; certain structural features identified in the surficial data may not possess sufficient magnetic susceptibility contrast to be recognized in the magnetic data; and surface expressions of magnetic lineaments may be masked by the presence of overburden. Therefore, it is necessary to objectively analyze the results of the RA\_2 assessment with the understanding that RA\_2 = 1 does not necessarily imply a low degree of confidence that the specified lineament represents a true structural feature.

The assessment of reproducibility values by length indicates that the most reproducible lineaments are typically the longer lineaments, occasionally extending across an entire assessment area, and typically oriented northwest to west-northwest, and north-northeast. In the magnetic data, these

lineaments are typically characterized by continuous magnetic lows. In surficial data, these lineaments are typically characterized by a combination of continuous sharp breaks in topography, vegetation and bedrock, and elongated lakes.

## 5.2 Lineament Trends

Length weighted lineament trends within the Ignace area provide a strong indication of sets of structures with preferred azimuths. In some cases, there are similarities and differences observed between the lineament trends identified in each of the data sets. Figure A3 summarizes the orientation of lineaments for all data sets, and also by geological unit.

Lineament trends observed in the geophysical data set tend to exhibit west-northwest to north-northwest dominant orientations and an east to northeast trend that is locally dominant (e.g., in Block A, Figure 8a) but subdued in the total geophysical data set (Figures 8 and 12). The northeast trending lineaments display a similar orientation to the Finlayson-Marmion fault, which is mapped approximately 30 km to the southeast of Ignace Block (A). Northwest trending lineaments define the boundaries and the internal fabric of the Raleigh Lake and Bending Lake greenstone belts (Figure 12), where they occur as tightly spaced, long lineaments. Northwest trending lineaments also occur within the gneissic domain, and within the Revell, Basket Lake and Indian Lake batholiths, where they display a distinctly bimodal westerly (west-northwest and north-northwest) orientation, larger spacings and generally shorter lengths relative to the greenstone belts.

The west-northwest trending geophysical lineaments parallel the mapped, and interpreted herein, dykes of the Wabigoon suite, while the Kenora-Fort Frances suite of mapped dykes bisects the acute angle between the west-northwest and north-northwest oriented lineaments.

The interpreted surficial lineaments tend to exhibit more distinct trends than the geophysical lineament. Surficial lineaments trend to the northeast, northwest, north-south and east-west (Figure A3). As with geophysical lineaments, the pronounced northeast trend displays a similar orientation to the Finlayson-Marmion Fault. The widespread distribution of the northeast trending surficial lineaments in both blocks, and the spatial coincidence between northeast trending lineaments and glacial features, suggests that the Finlayson-Marmion fault and similarly oriented structures may have formed Quaternary topographic features that posed a significant control over ice flow (Figure 3).

As expected, the final integrated lineament data set exhibits generally similar trends as seen in the geophysical and surficial data sets. These include a diffuse west-northwest to north-northwest trend, a sharper northeast trend, and minor north-south and east-west trends (Figure A3).

### 5.2.1 Relationship between Lineament sets and Regional Stress Field

The principal neotectonic stress orientation in central North America is generally oriented approximately east-northeast ( $63 \text{ degrees} \pm 28 \text{ degrees}$ ; Zoback, 1992) although anomalous stress orientations have also been reported in the mid-continent that include a 90-degree change in azimuth of the maximum compressive stress axis (Brown et al. 1995) and a north-south maximum horizontal compressive stress (Haimson, 1990). Local variations, and other potential complicating factors involved in characterizing crustal stresses, including the effect of shear stress by mantle flow at the base of the lithosphere (Bokelmann, 2002; Bokelmann and Silver, 2002), the degree of coupling between the North American plate and the underlying mantle (Forte et al., 2010), the effects of crustal depression and Holocene rebound, and the influence of the thick lithospheric mantle root

under the Canadian Shield, make it premature to correlate the regional neotectonic stress orientation with the orientation of interpreted lineaments.

However, it is possible to broadly speculate on the potential behavior of the identified lineaments if they were to be reactivated by the regional east-northeast neotectonic stress regime. Four general orientations of lineaments were interpreted based on their existence in the final integrated lineament data set: east-west, north-south, west-northwest to north-northwest and, and north-northeast (Figure A3 (A)). Should the identified lineaments be reactivated under the current stress regime, the: east-west oriented lineaments would likely reactivate as oblique-slip faults, the north-south oriented lineaments would likely reactivate as reverse dip-slip to oblique-slip faults, the west-northwest to north-northwest oriented lineaments would likely reactivate as reverse dip-slip to oblique-slip faults, and the north-northeast oriented lineaments would likely reactivate as normal dip-slip or strike-slip faults. It is also possible that under the current stress regime, several orientations of lineaments could simultaneously react as conjugate sets of structures.

### 5.3 Lineament Length

Interpreted geophysical (RA\_1), surficial (RA\_2) and final integrated (RA\_2) lineaments classified by length are presented in Figures 14 and 15 (geophysical lineaments by length), Figures 16 and 17 (surficial lineaments by length), and Figures 18 and 19 (final integrated lineaments by length). Statistical analyses of the lineament lengths, including box-plots, cumulative log-log plots, and histograms of the geophysical, surficial, and final integrated lineaments graphically display the distribution of lineament length for each data set shown (Figures 14 to 19, and Figure A5). It is important to keep in mind that the reported lengths may not necessarily reflect the full length of the lineament. Lineaments were traced within the assessment areas and could extend beyond its borders.

The histograms and cumulative log-log plots for the lineament data sets show distributions that are generally similar between the different data sets, with a minor skewed distribution of lengths toward shorter lineaments in the surficial lineaments data set. Similarly, a boxplot of data type by logged lineament length for all of the final integrated data (Figures 18 and 19 and Figure A5) shows that the geophysical lineaments have a significantly broader length range, and that the median length of geophysical lineaments is significantly higher than the median length of DEM and digital aerial imagery lineaments.

The difference in lineament length between lineaments interpreted from geophysical and surficial data sets can in part be explained by the nature of the lineaments interpreted from each data set. From the magnetic data, lineaments are typically characterized by long continuous magnetic lows or highs (dykes, for example), or by multiple breaks in the magnetic grain defining a continuous lineament. Conversely, surficial lineaments are typically characterized by a combination of breaks in topography, vegetation and bedrock, and elongated lakes. These surficial features are not as continuous as the magnetic features, often due to their interruption by overburden. This resulted in the interpretation of shorter surficial lineaments relative to the magnetic lineaments.

The coincidence assessment (RA\_2) indicates that the most reproducible lineaments (i.e. RA\_2=3) are typically longer, and often extend throughout an entire block. In general, the west-northwest and north-northwest trending lineaments are consistently longer than other lineament orientations. Block (B) has a larger number of longer lineaments than Block (A) (Figures 18 and 19) due to the presence of numerous north-northwest oriented and west-northwest oriented lineaments in Block (A), but also due to the significantly larger size of Block (B) relative to Block (A).

Examining the final integrated lineaments per bin size reveals that the majority of lineaments have lengths of less than 2.5 km (75 %), with 38 % of the lineaments being less than 1 km long. Only 9 %

of lineaments were greater than 5 km in length and only 15 % of lineaments were between 2.5 and 5 km in length. Amongst the final integrated lineaments that are greater than 2.5 km, 308 lineaments (36%) are lineaments that define the boundaries and internal fabric the Raleigh Lake and Bending Lake greenstone belts, as well as lineaments that are parallel to the greenstone belts but occur within the gneissic units and batholiths.

Although there is no information available on the depth extent of the lineaments interpreted for the Ignace area, the length information described above can be used as a proxy for the depth extent of the identified structures. Therefore, a preliminary assumption may be that the longer interpreted lineaments may extend to greater depths than the shorter interpreted lineaments.

## **5.4 Density**

Analyses of lineament and intersection density were conducted for the Ignace area, as described in Section 3.2.6.

### **5.4.1 Lineament Density**

In order to properly assess the surficial lineament density, it is necessary to take into account the location of lakes and overburden cover, since these may mask DEM and aerial imagery lineaments, resulting in apparently lower densities. This is less of a factor for evaluating the geophysical lineament density, because the magnetic data is not affected by overburden or lake cover. Lineament density is discussed for each data set below. It should also be noted that since interpreted lineaments are only traced to the margins of the Phase 2 assessment areas, there will in many cases be a border of apparent low lineament density around the margins of both Block (A) and Block (B).

The geophysical lineament density in Block (A) is shown in Figure 20. Geophysical lineament density in this part of the Indian Lake batholith is variable. The highest density area is near the northwestern corner of Block (A). The portion of the Indian Lake batholith in Block (B) is characterized primarily by a relatively uniform low geophysical lineament density, with the exception of several small isolated areas of slightly higher density (Figure 21). The highest geophysical lineament density in this portion of the batholiths is found along its southwestern boundary where lineament density is markedly higher adjacent to the greenstone belt. In general, geophysical lineament spacing within the western portion of the Indian Lake batholith (Block (B)) is in the range of 0.3 to 1 km.

The density of geophysical lineaments in the Revell batholith is variable, with areas of lower lineament density, especially in its northern and northwestern portions. Geophysical lineament density is higher further to the south (Figure 21). The lower lineament density in the northwestern portion of the intrusion may potentially reflect the lack of magnetic susceptibility contrast of the intrusive phases in that area rather than an absence of structures. Geophysical lineament density over the megacrystic phase in the central part of the Revell batholith is relatively high. Other areas of increased geophysical lineament density within the Revell batholith are associated with clusters of greenstone-belt parallel lineaments (Figure 21).

The northwestern portion of the Basket Lake batholith within Block (B) shows a relatively higher geophysical lineament density in correspondence to a closely spaced set of curvilinear lineament traces. Over the remainder of the batholith in Block (B) the geophysical lineament density tends to be lower (Figure 21). The surrounding gneissic bedrock units also show variability in the distribution of geophysical lineament density. Approaching the greenstone belt, southwest of the Basket Lake batholith, the geophysical lineament density is relatively high. This increase in lineament density near the greenstone belt units reflects the fact that the margins of the gneissic domain were affected

by penetrative brittle-ductile deformation, whereas the core of the gneissic domain acted as a rigid block at the time of that deformation. Conversely, in the gneissic bedrock units immediately south of the Basket Lake batholith and in the area between, and to the north of the Basket Lake and Indian Lake batholiths, the geophysical lineament density is lower (Figure 21).

The surficial lineament density over the Indian Lake batholith in Block (A), shown in Figure 22, is highly variable. The regions of lowest surficial lineament density are mostly associated with surface water features (e.g. Cecil Lake), suggesting that the surficial lineament density variations in Block (A) most likely reflect the distribution of Quaternary landforms rather than geological features. Similarly, in the western portion of the Indian Lake batholith, within Block (B), the lower surficial lineament densities are mostly observed over the large Mameigwess Lake, and surrounding areas with overburden cover (Figure 22).

The Revell batholith shows a relatively uniform density of surficial lineaments. Areas of lower surficial lineament density are locally observed over certain lakes (e.g. Menning Lake, Revell Lake) and in the northernmost portion of the batholith, where overburden deposits have been mapped. In the remainder of the Revell batholith, the surficial lineament density is higher, likely due in part to good bedrock exposure and lack of large water bodies (Figure 22).

The gneissic units and the Basket Lake batholith generally show a decreasing surficial lineament density moving northeastwards away from the greenstone belt (Figure 22). The lowest surficial lineament density in the gneissic units is observed between the Basket Lake and Indian Lake batholiths. The Basket Lake batholith has a variable surficial lineament density. Areas of lower surficial lineament density in this batholith coincide with large water bodies (e.g. Basket Lake), which suggest that density variations most likely reflect the distribution of lakes rather than geological features in the Basket Lake batholith.

The final integrated lineament density (Figures 24 and 25) shows a generally similar distribution as that of the geophysical and surficial data sets throughout the Ignace assessment areas. Higher density of final integrated lineaments in the Ignace area is observed uniformly through much of the Revell batholith, with the exception of the extreme northwestern portion of the batholith, where both geophysical and surficial lineament density was observed to be lower (Figures 21 and 23). Higher density of integrated lineaments is also observed along the northwestern boundary of Block (B) and in the northwestern part of Block (A). Lower integrated lineament density is observed in the gneissic units between the Basket Lake and Indian Lake batholiths, and in the Basket Lake and Indian Lake batholiths, where these are covered by large water bodies (Figures 24 and 25).

#### **5.4.2 Intersection Density**

SRK analyzed the distribution of lineament intersections within the Ignace area. The geophysical lineament intersection density plots for both Block (A) and Block (B) (Figures 26 and 27) show similar distributions to those of the geophysical lineament density plots, although there are some slight differences throughout.

Within the Indian Lake Batholith in Block (A) geophysical lineament intersection density is variable, with areas of lower density occurring intermittently between larger areas of higher intersection densities (Figure 26). In the portion of the Indian Lake batholith within Block (B), geophysical lineament intersection density is higher in areas southwest of Mameigwess Lake and in the southern portion of the intrusion adjacent to the greenstone belt (Figure 27).



In Block (B), the northwestern portion of the Revell batholith exhibits a lower geophysical lineament intersection density, whereas the central part of the batholith, over the late intrusive phase, shows higher magnetic lineament intersection density (Figure 27). As with the density of geophysical lineaments, the lower intersection density observed in the northwestern portion of the Revell batholiths may potentially reflect the lack of magnetic susceptibility contrast of the bedrock in that area rather than an absence of structures. The northwestern portion of the Basket Lake batholith displays a higher magnetic lineament intersection density, corresponding to the area of curvilinear lineaments, with the remaining portion of the batholith showing lower intersection densities. Within the gneissic bedrock units surrounding both the Indian Lake and Basket Lake batholith the geophysical lineament intersection density is variable (Figure 27).

The distribution of surficial lineament intersection density in the Indian Lake batholith within Block (A) is variable, with localized patches of higher intersection density between larger areas of significantly lower intersection density. The density of surficial lineament intersections in the Indian lake batholith within Block (B) is generally relatively low, with areas of higher intersection density mostly located in the southwestern portion of the intrusion, along the margins adjacent to the greenstone belts. Areas of lowest surficial lineament intersection density generally correspond to regions of large surface water coverage (Figures 28 and 29).

Within Block (B), the surficial lineament intersection density is generally uniform and relatively high throughout most of the Revell batholith (Figure 29). The density of surficial lineament intersections in this batholith is mainly attributed to bedrock in this area being well exposed, and the lack of large water bodies. In the Basket Lake batholith, the surficial intersection density is lower over the large water bodies, which make the interpretation of surficial lineaments in this area difficult.

In general, similar distributions in density are observed in the final integrated lineament intersection density plots (Figures 30 and 31) as were observed in the final integrated lineament density plots. The Revell batholith contains a large area of lower final integrated lineament intersection density in the northwest part of the batholiths, which coincides with an area of low magnetic contrast. Areas of lower intersection density in the the Indian Lake batholith tend to coincide with large lakes, such as Mameigwess Lake and Cecil Lake (Figure 30 and 31). Within the Basket Lake batholith, areas of higher final integrated lineament intersection density coincide with the presence of northeast trending curvilinear lineaments intersecting with a set of long northwest trending lineaments.

## 5.5 Lineament Truncation and Relative Age Relationships

The structural history of the Ignace area, outlined in Section 2.4 provides a framework that may aid in constraining the relative age relationships of the interpreted bedrock lineaments. In summary, six main regionally distinguishable deformation episodes ( $D_1$ - $D_6$ ) are inferred to have affected the bedrock geological units of the Ignace area.

$D_1$ - $D_2$  resulted in the development of a gneissic foliation and isoclinal folding between approximately 2.725 and 2.713 Ga, which only affected the older, gneissic tonalities.  $D_3$ - $D_4$  produced the dominant ductile structures observed within the greenstone belts, including orthogonal folds and steeply dipping foliation, prior to approximately 2.689 Ga.  $D_5$  was a protracted event that is interpreted to span the transition from ductile to brittle deformation and involved the activation and possible re-activation of major regional faults between approximately 2.690 and 2.4 Ga.  $D_6$  represents multiple events beginning with localized brittle re-activation of major regional faults at approximately 1.947 Ga, as well as all younger tectonic events. The most recent period of major fault displacement may be constrained by the approximately 1.9 Ga old Wabigoon dykes that transect the Ignace area with no apparent fault offset.

The 3,477 lineaments identified in the Ignace area represent successive stages of brittle-ductile and brittle deformation and dyke emplacement. These lineaments can be classified into four main stages based on relative age and in accord with the structural history described above in Section 2. From oldest to youngest this includes: 531 D<sub>1</sub>-D<sub>4</sub> (ductile to brittle-ductile) lineaments; 1,662 D<sub>5</sub>-D<sub>6</sub> (early, brittle) lineaments; 1,251 D<sub>5</sub>-D<sub>6</sub> (intermediate brittle) lineaments; 20 D<sub>5</sub>-D<sub>6</sub> (late, brittle) lineaments, and 13 dyke lineaments (Figure 32).

The 531 D<sub>1</sub>-D<sub>4</sub> brittle-ductile lineaments are interpreted in Block (B) exclusively. They define shear zones within the Raleigh Lake and Bending Lake greenstone belts and have a dominantly northwest-southeast trend (295° to 340°). Additionally, they are interpreted to occur along an arcuate zone in the northwestern part of Block (B).

Of the 1,662 D<sub>5</sub>-D<sub>6</sub> early brittle lineaments, 422 are interpreted in Block (A) and 1,240 are interpreted in Block (B). The D<sub>5</sub>-D<sub>6</sub> early, brittle lineaments have a dominantly northeast orientation in Block (A) and dominantly north-northeast orientation in Block (B). This orientation is generally coincident with that of glacial features. They truncate D<sub>1</sub>-D<sub>4</sub> ductile to brittle-ductile lineaments defining the greenstone belts (Figure A6), and are locally observed to be truncated and displaced by the intermediate and late D<sub>5</sub>-D<sub>6</sub> lineaments (Figure A7). In places, a subtle sinistral sense of motion can be inferred, but in general the sense of motion of the early brittle D<sub>5</sub>-D<sub>6</sub> lineaments is uncertain. In the gneissic domain and in the Indian Lake and Basket Lake batholiths D<sub>5</sub>-D<sub>6</sub> early brittle lineaments occur as weak magnetic disruptions within the fault block defined by the later brittle faults.

Of the 1,251 D<sub>5</sub>-D<sub>6</sub> intermediate brittle lineaments, 365 are interpreted in Block (A) and 886 are interpreted in Block (B). The D<sub>5</sub>-D<sub>6</sub> (intermediate brittle) lineaments form a conjugate set of north-northeast trending lineaments with sinistral displacement, and west-northwest trending lineaments with dextral displacement (Figure A8). The most continuous intermediate brittle lineaments have anastomosing geometry, and are defined by pronounced magnetic lows. Their mutual displacements can be observed locally in the eastern part of Block (B).

Of the 20 D<sub>5</sub>-D<sub>6</sub> (late, brittle) lineaments, 1 is in Block (A) and 19 are in Block (B). The late brittle lineaments are interpreted to be a local set of north-northeast trending lineaments that occurs primarily in the northwestern portion of Block (B). They have a similar trend as the early brittle D<sub>5</sub>-D<sub>6</sub> lineaments, but are distinguished on the basis of the strength and continuity of their low magnetic character. They may represent local reactivation of the early D<sub>5</sub>-D<sub>6</sub> structures. In places, these late D<sub>5</sub>-D<sub>6</sub> structures are seen to truncate and to produce minor displacements in all other lineament generations (Figure A9).

### 5.5.1 Mapped Fault, Dyke and Lineament Relationships

As described in Section 4.2, there are no mapped faults within the two assessment areas where the lineament interpretation was conducted (Blocks (A) and (B)). An unnamed northeast oriented fault is mapped to the northwest of Ignace Block (B), and the northeast-trending Finlayson-Marmion fault is located approximately 30 km south of Ignace Block (A), where it intersects the Indian Lake batholith.

Given that there are no mapped faults within Block (A) and Block (B), the relative age relationships described in detail in Section 5.5 above was based on the interpreted mutual displacements of the interpreted lineaments themselves, rather than on mapped faults.

Thirteen dykes are interpreted from the geophysical data for the Ignace area, including one in Block (A) and 12 in Block (B). The majority of these interpreted dykes occur along a dominant west-northwest ( $300^{\circ}$  to  $310^{\circ}$ ) orientation across both blocks, which is consistent with the orientation of the mapped, ca. 1.9 Ga Wabigoon suite of dykes. Another suite of mapped dykes, the ca. 2.12 Ga Kenora-Fort Frances suite, bisects the acute angle between the prominent west-northwest and north-northwest oriented geophysical lineaments in the region where the Basket Lake and Indian Lake batholiths are in closest proximity.

## 6 Summary of Results

This report documents the source data, workflow, and results from a lineament interpretation of geophysical (magnetic) and surficial (digital aerial imagery, DEM topography) data sets acquired as part of Phase 2 Preliminary Assessment for the Ignace area. The lineament analysis provides an interpretation of the location and orientation of possible ductile, brittle and dyke lineaments on the basis of remotely sensed data, and helps to evaluate their relative timing relationships within the context of the regional geological setting. The workflow involves a three step process that was designed to address the issues of subjectivity and reproducibility. The distribution of lineaments in the Ignace area reflects the bedrock structure, resolution of the data sets used, and surficial cover.

Within the Ignace area, a total of 1,427 geophysical lineaments, 2,224 DEM lineaments, and 2,108 digital aerial imagery lineaments were interpreted by the two interpreters (RA\_1) from their respective data sets. Merging the lineaments derived from the DEM and digital aerial data resulted in a total of a 3,300 surficial lineaments (RA\_2). Merging the surficial lineaments with those derived from the geophysical data resulted in a total of 3,477 final integrated lineaments (RA\_2).

The reproducibility assessment (RA\_1) revealed a moderate reproducibility between interpreters for all three data sets (i.e. 43% of the geophysical lineaments, 32% of the DEM lineaments, and 51% of the aerial imagery lineaments were identified by both interpreters). The variability between interpreters could be attributed to the judgement and subjectivity of the expert carrying out the interpretation. In general, longer lineaments were identified more often by both interpreters.

The coincidence assessment (RA\_2) revealed that 34% of the interpreted geophysical lineaments were interpreted in at least one of the two surficial data sets. The lack of coincidence between geophysical and surficial lineaments could be attributed to multiple variables, including deep structures identified in the magnetic data that may not have a surface expression, surficial features that may not extend to depth, features identified in the surficial data that may not possess sufficient magnetic susceptibility contrast to be recognized in the magnetic data, and the masking of surface expressions of magnetic lineaments by the presence of overburden. Evaluating lineament lengths of the final integrated lineaments reveals that longer lineaments were identified more often in the various data sets.

An analysis of lineament orientations reveal an overall moderate consistency between the orientations of lineaments identified in the various different data sets, which suggests that the majority of lineaments interpreted from all three data sets are identifying the same sets of structures. Examination of all data sets revealed dominant west-northwest to east-west, northwest, north to north-northeast, and northeast trends. The west-northwest to east-west oriented lineaments define the structural grain of the Raleigh Lake and Bending Lake greenstone belts, as along with the northwest oriented lineaments they are interpreted as intermediate D<sub>5</sub>-D<sub>6</sub> brittle faults that form the most prominent geophysical features within the Indian Lake batholith and gneissic domain in blocks (A) and (B), and in the Basket Lake batholith in Block (B). The north to north-northeast oriented lineaments are ubiquitous throughout the Ignace area.

Evaluation of lineaments by length revealed relatively few lineaments longer than 2.5 km (i.e. 24 % of lineaments are greater than 2.5 km) and 38% of lineaments are less than 1 km in length. The longer lineaments trend predominantly west-northwest and northwest, and the shorter lineaments exhibit all dominant trends, including the west-northwest to east-west, northwest, north to north-northeast, and northeast trends.

Analysis of lineament density provides insight on the distribution of bedrock structures. Density of geophysical lineaments is variable through the different geological units, but an increased density is observed in the gneissic units and Indian Lake batholith in the areas adjacent to the greenstone belts. A distinct area of low geophysical lineaments is observed in the northern portion of the Revell batholith. The lower lineament density in this portion of the intrusion may potentially reflect the lack of magnetic susceptibility contrast of the bedrock rather than an absence of structures. Higher geophysical lineament density is observed in the megacrystic phase of the Revell batholith.

Surficial lineament density in the Revell, Basket Lake and Indian Lake batholiths in the Ignace area was observed to be largely influenced by the presence of overburden cover and large waterbodies, indicating that surficial lineament density variations most likely reflect the distribution of Quaternary landforms rather than geological features. Surficial lineament density is uniformly higher over the Revell batholith, most likely due to good bedrock exposure and lack of large water bodies.

Based on the six main regionally distinguishable deformation episodes ( $D_1$ - $D_6$ ) recognized in literature in the Ignace area, the final interpreted lineaments can be classified within the structural history into four successive stages of brittle-ductile and brittle deformation, including: 531  $D_1$ - $D_4$  (ductile to brittle-ductile) lineaments; 1,662 early  $D_5$ - $D_6$  (brittle) lineaments; 1,251 intermediate (brittle) lineaments, and 20 late  $D_5$ - $D_6$  (brittle) lineaments.

The  $D_1$ - $D_4$  brittle-ductile lineaments trend northwest-southeast to west-northwest and define the Raleigh Lake and Bending Lake greenstone belts in Block (B). The early  $D_5$ - $D_6$  brittle lineaments trend northeast to north-northeast and are generally parallel to the ice flow direction. The orientation of the Finlayson-Marmion Fault, which occurs to the southeast of the Ignace area is compatible with the orientation of the interpreted early  $D_5$ - $D_6$  brittle lineaments. The intermediate  $D_5$ - $D_6$  brittle lineaments are interpreted to form a conjugate set trending west-northwest and north-northwest. In addition, 13 dykes have been interpreted.

## 7 References

- Berger, B.R., 1988. Geology of the Melgund Lake Area, District of Kenora; Ontario Geological Survey, Open File Report 5680, 184p., 24 figures, 10 tables, 9 photographs and maps P.3068, P.3069, and P.3070 in the back pocket.
- Bethune, K.M., Helmstaedt, H.H., and McNicoll, V.J. 2006. Structural analysis of the Miniss River and related faults, western Superior Province: post-collisional displacement initiated at terrane boundaries. *Canadian Journal of Earth Sciences*, vol. 43, p. 1031-1054.
- Blackburn, C.E., Johns, G.W., Ayer, J.W. and Davis, D.W. 1991. Wabigoon Subprovince; in *Geology of Ontario*, Ontario Geological Survey, Special Volume 4, Part 1, 303-382.
- Blackburn, C.E., and Hinz, P., 1996. Gold and Base Metal Potential of the Northwest Part of the Raleigh Lake Greenstone Belt, Northwestern Ontario-Kenora Resident Geologists's District. *In Summary of Field Work and Other Activities, 1996*, Ontario Geological Survey, Miscellaneous Paper 166, p. 113-115.
- Bokelmann, G.H.R., 2002. Which forces drive North America?, *Geology*, v.30, p.1027-1030.
- Bokelmann, G.H.R. and Silver, P.G. 2002. Shear Stress at the Base of Shield Lithosphere. *Geophysical Research Letters*, v. 29, p.61-64.
- Brown, J.L. 2002. Neoproterozoic evolution of the western-central Wabigoon boundary zone, Brightsand Forest area, Ontario. Unpublished M.Sc. thesis, University of Ottawa, Ottawa.
- Brown, A., Everitt, R.A., Martin C.D. and Davison, C.C. 1995. Past and future fracturing In AECL research areas in the Superior Province of the Canadian Precambrian Shield, with emphasis on the Lac Du Bonnet Batholith; Whiteshell Laboratories, Pinawa, Manitoba.
- Buchan, K.L. and Ernst, R.E. 2004. Diabase dike swarms and related units in Canada and adjacent regions. Geological Survey of Canada, Map 2022A, scale 1:5,000,000.
- Buse, S., Stone, D., Lewis, D., Davis, D., and Hamilton, M. A., 2010. U/Pb geochronology results for the Atikokan Mineral Development Initiative. Ontario Geological Survey, Miscellaneous Release-Data 275.
- Corfu, F., G.M. Stott and F.W. Breaks, 1995. U-Pb geochronology and evolution of the English River Subprovince, an Archean low P – high T metasedimentary belt in the Superior Province; *Tectonics*, v.14, p.1220-1233.
- Davis, D.W., 1989. Final Report for the Ontario Geological Survey on precise U-Pb age constraints on the tectonic evolution of the western Wabigoon subprovince, Superior Province, Ontario. Earth Science Department, Royal Ontario Museum, 30 p.
- Easton, R.M., 2000. Metamorphism of the Canadian Shield, Ontario, Canada. I. The Superior Province: *Canadian Mineralogist*, April 2000, v. 38, p.287-317.
- Everitt, R.A., 1999. Experience gained from the geological characterisation of the Lac du Bonnet batholith, and comparison with other sparsely fractured granite batholiths in the Ontario
-

- portion of the Canadian Shield. OPG Report 06819-REP-01200-0069-R00. OPG. Toronto. Canada.
- Fahrig, W.F. and West, T.D. 1986. Diabase dike swarms of the Canadian Shield; Geological Survey of Canada, Map 1627A.
- Forte, A., Moucha, R., Simmons, N., Grand, S., and Mitrovica, J., 2010. Deep-mantle contributions to the surface dynamics of the North American continent. *Tectonophysics*, v. 481, p. 3–15
- Golder (Golder Associates Ltd.), 2011. Initial screening for siting a deep geological repository for Canada's used nuclear fuel. The Corporation of the Township of Ignace, Ontario. Nuclear Waste Management Organization, March 2011, 31p.
- Golder (Golder Associates Ltd.), 2013. Phase 1 Desktop Geoscientific Preliminary Assessment of Potential Suitability for Siting a Deep Geological Repository for Canada's Used Nuclear Fuel, Township of Ignace, Ontario. Prepared for Nuclear Waste Management Organization (NWMO). NWMO Report Number: APM-REP-06144-0011.
- Golder (Golder Associates Ltd.), 2015. Phase 2 Geoscientific Preliminary Assessment, Findings from Initial Field Studies, Township of Ignace, Ontario. Prepared for the Nuclear Waste Management Organization (NWMO), NWMO Report Number: APM-REP-06145-0001.
- Haimson, B.C. 1990. Scale effects in rock stress measurements. In *Proceedings international workshop on scale effects in rock masses*, Loen, AA Balkema, Rotterdam, p.89-101.
- Hanes, J.A. and D.A. Archibald. 1998. Post-orogenic tectonothermal history of the Archean western Superior Province of the Canadian Shield by conventional and laser Ar-Ar dating. *Abstracts with programs - Geological Society of America*, vol. 30(7), p.110-110.
- JDMA (J. D. Mollard and Associates Ltd.), 2013. Phase 1 Desktop Geoscientific Preliminary Assessment, Terrain and Remote Sensing Study, Township of Ignace, Ontario. Prepared for Nuclear Waste Management Organization (NWMO). NWMO Report Number: APM-REP-06144-0012.
- Kamineni, D.C. and Stone, D. 1983. The ages of fractures in the Eye–Dashwa pluton, Atikokan, Canada; *Contributions to Mineralogy and Petrology*, 83, 237-246.
- Kamineni, D.C., D. Stone and Z. E. Peterman, 1990. Early Proterozoic deformation in the western Superior province, Canadian Shield, *Geological Society of America Bulletin* 1990;102;1623-1634
- Larbi, Y., Stevenson, R., Breaks, F., Machado, N., Gariépy, C. 1998. Age and isotopic composition of Late Archean leucogranites: implications for continental collision in the western Superior Province. *Canadian Journal of Earth Science*, vol. 36, p.495–510.
- MNR (Ministry of Natural Resources), 2010. Forest Resource Inventory (FRI) Digital Aerial Imagery. Accessed through Land Information Ontario (accessed May 2014).
- NWMO (Nuclear Waste Management Organization), 2010. Moving forward together: process for selecting a site for Canada's deep geological repository for used nuclear fuel, Nuclear Waste Management Organization, May 2010. (Available at [www.nwmo.ca](http://www.nwmo.ca)).
-

- NWMO (Nuclear Waste Management Organization), 2013. Preliminary Assessment for a Siting a Deep Geological Repository for Canada's Used Nuclear Fuel – Township of Ignace, Ontario – Findings from Phase One Studies. NWMO Report Number APM-REP-06144-0009.
- OGS (Ontario Geological Survey), 2011. 1:250 000 scale bedrock geology of Ontario, Miscellaneous Release Data 126 - Revision 1.
- Osmani, I.A. 1991. Proterozoic mafic dike swarms in the Superior Province of Ontario; in *Geology of Ontario*, Ontario Geological Survey, Special Volume 4, Part 1, 661-681.
- Percival, J.A., 2004. Insights on Archean continent—ocean assembly, western Superior Province, from new structural, geochemical and geochronological observations: introduction and summary: *Precambrian Research* 132 (2004) 209–212
- Percival, J.A., McNicoll, V.J., Brown, J.L., and Whalen, J.B. 2004. Convergent margin tectonic, central Wabigoon subprovince, Superior Province, Canada. *Precambrian Research*, vol. 132, p. 213-244.
- Percival, J.A., Sanborn-Barrie M., Skulski, T., Stott, G.M., Helmstaedt, H., and White, D.J., 2006. Tectonic Evolution of the Western Superior Province from NATMAO and Lithoprobe Studies; *Canadian Journal of Earth Sciences*, v. 43, p. 1085-1117.
- Percival, J.A. and R.M. Easton, 2007. *Geology of the Canadian Shield in Ontario: an update*. Ontario Power Generation, Report No. 06819-REP-01200-10158-R00.
- Peterman, Z.E. and Day, W. 1989. Early Proterozoic activity on Archean faults in the western Superior Province: Evidence from pseudotachylite. *Geology*, vol. 17, p. 1089-1092.
- PGW (Patterson, Grant and Watson Ltd.), 2013. Phase 1 Geoscientific Desktop Preliminary Assessment, Processing and Interpretation of Geophysical Data, Township of Ignace, Ontario. Prepared for Nuclear Waste Management Organization (NWMO). NWMO Report Number: APM-REP-06144-0013
- Sage, R. P., Breaks, F.W., Stott, G.M., McWilliams, G.M. and Atkinson, S. 1974. Operation Ignace-Armstrong, Ignace-Graham Sheet, Districts of Thunder Bay, Kenora, and Rainy River; Ontario Division of Mines, Preliminary Map P. 964.
- Sanborn-Barrie, M., and Skulski, T. 2006. Sedimentary and structural evidence for 2.7 Ga continental arc-oceanic-arc collision in the Savant-Sturgeon greenstone belt, western Superior Province, Canada. *Canadian Journal of Earth Sciences*, vol. 43, p. 995-1030.
- Schwerdtner, W.M., Stone, D., Osadetz, K., Morgan, J. and Stott, G.M. 1979. Granitoid complexes and the Archean tectonic record of the southern part of northwestern Ontario; *Canadian Journal of Earth Sciences*, vol.16, p.1965-1977.
- SGL (Sander Geophysics Limited), 2015. Phase 2 Geoscientific Preliminary Assessment, Acquisition, Processing and Interpretation of High-Resolution Airborne Geophysical Data, Township of Ignace, Ontario. Prepared for Nuclear Waste Management Organization (NWMO). NWMO Report Number: APM-REP-06145-0002.
-



- Southwick, D.L. and Halls, H. 1987. Compositional characteristics of the Kenora- Kabetogama dike swarm (Early Proterozoic), Minnesota and Ontario; *Canadian Journal of Earth Sciences*, 24, 2197-2205.
- Stone, D., J. Halle, M. Lange, B. Hellebrandt and E. Chaloux, 2007. Precambrian Geology, Ignace Area; Ontario Geological Survey, Preliminary Map P.3360—Revised, scale 1:50 000
- Stone, D., 2009a. The Central Wabigoon Area; Ontario Geological Survey, poster, Northwest Ontario Mines and Minerals Symposium, Thunder Bay, Ontario, April 7-8, 2009.
- Stone, D., 2009b. Geology of the Bending Lake Area, Northwestern Ontario; in Summary of Field Work and Other Activities 2009, Ontario Geological Survey, Open File Report 6240, pp.14-1 to 14-7.
- Stone, D. 2010a. Precambrian geology of the central Wabigoon Subprovince area, northwestern Ontario. Ontario Geological Survey, Open File Report 5422, 130p.
- Stone, D. 2010b. Geology of the Bending Lake area, northwest Ontario, poster paper, Northwestern Ontario Mines and Minerals Symposium.
- Stone, D., J. Halle and E. Chaloux, 1998. Geology of the Ignace and Pekagoning Lake Areas, Central Wabigoon Subprovince; in Summary of Field Work and Other Activities 1998, Ontario Geological Survey, Miscellaneous Paper 169, pp.127-136.
- Stone, D., D.W. Davis, M.A. Hamilton and A. Falcon, 2010. Interpretation of 2009 Geochronology in the Central Wabigoon Subprovince and Bending Lake Areas, Northwestern Ontario, Project Unit 09-003. Summary of Field Work and Other Activities 2010, Ontario Geological Survey, Open File Report 6260, p.14-1 to 14-13.
- Stone, D., B. Hellebrandt and M. Lange, 2011a. Precambrian geology of the Bending Lake area (north sheet); Ontario Geological Survey, Preliminary Map P.3623, scale 1:20 000.
- Stone, D., B. Hellebrandt and M. Lange, 2011b. Precambrian geology of the Bending Lake area (south sheet); Ontario Geological Survey, Preliminary Map P.3624, scale 1:20 000.
- Stott, G.M. 1973. Area III, Operation Ignace-Armstrong. Ontario Division of Mines, Miscellaneous Paper 56, 60-61 (also Preliminary Map, P.964, Geological Survey of Canada).
- Szewczyk, Z.J. and West, G.F. 1976. Gravity study of an Archean granitic area northwest of Ignace, Ontario *Canadian Journal of Earth Sciences* 13, 1119-1130.
- Tomlinson, K.Y., Stott, G.M., Percival, J.A. and Stone, D. 2004. Basement terrane correlations and crustal recycling in the western Superior Province: Nd isotopic character of granitoid and felsic volcanic rocks in the Wabigoon Subprovince, N. Ontario, Canada; *Precambrian Research*, vol.132, p. 245-274.
- Zoback, M.L., 1992. First- and second-order patterns of stress in the lithosphere: the world stress map project; *Journal of Geophysical Research*, 97, p.11, 703-11,728.
-



## 8 APPENDIX

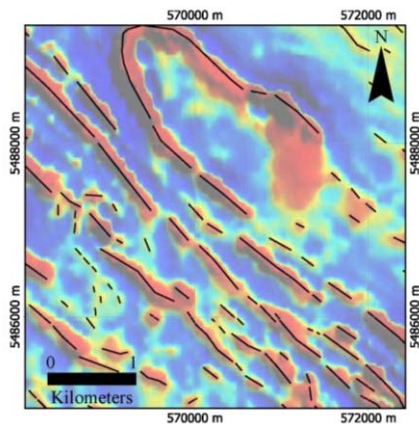


**Figure A1: Example ductile lineaments from the Ignace area defined by curvi-linear magnetic highs.**

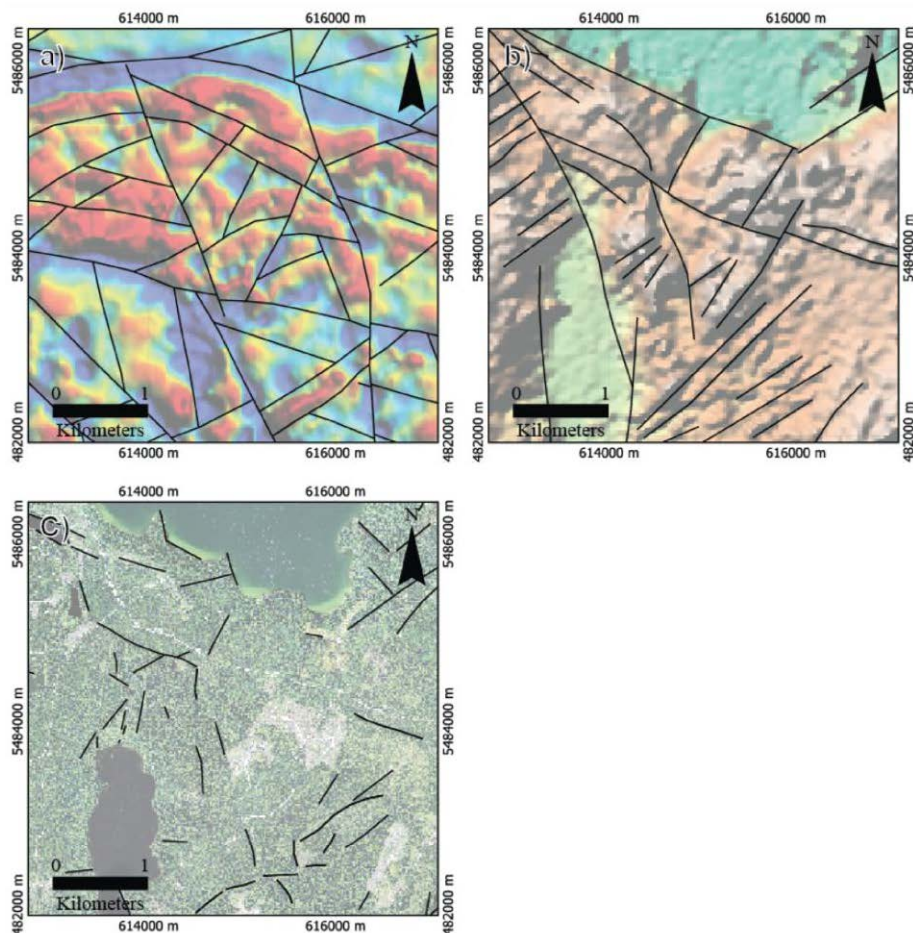


**Figure A2: Example brittle lineaments from the Ignace area, defined by (a) breaks in magnetic highs and curvi-linear magnetic lows in magnetic data, (b) breaks in topography in DEM data, and (c) curvi-linear breaks in exposed bedrock and vegetation in digital aerial imagery data.**

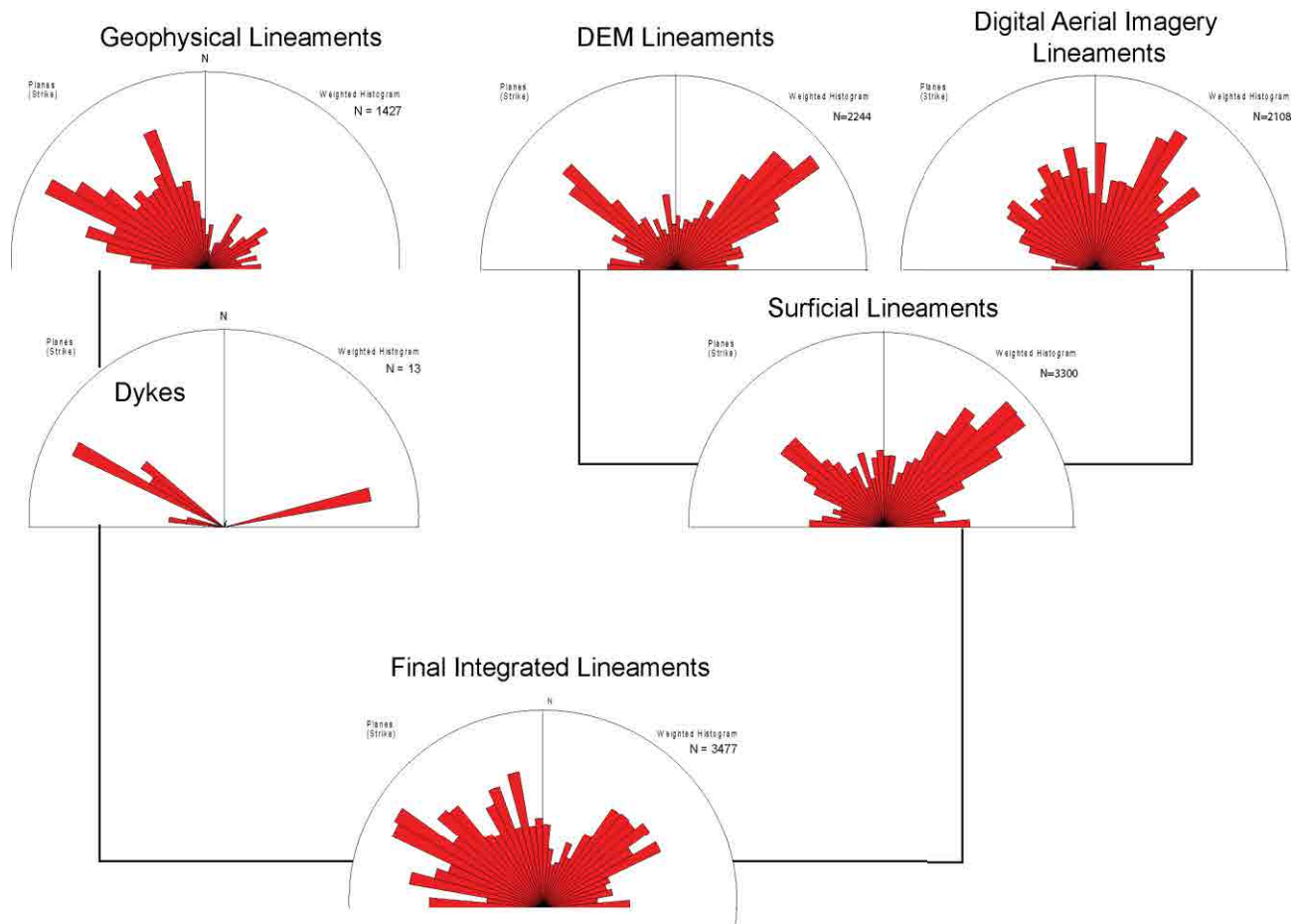


**Figure A3: (A) Summary of lineament orientations in the Ignace area.**

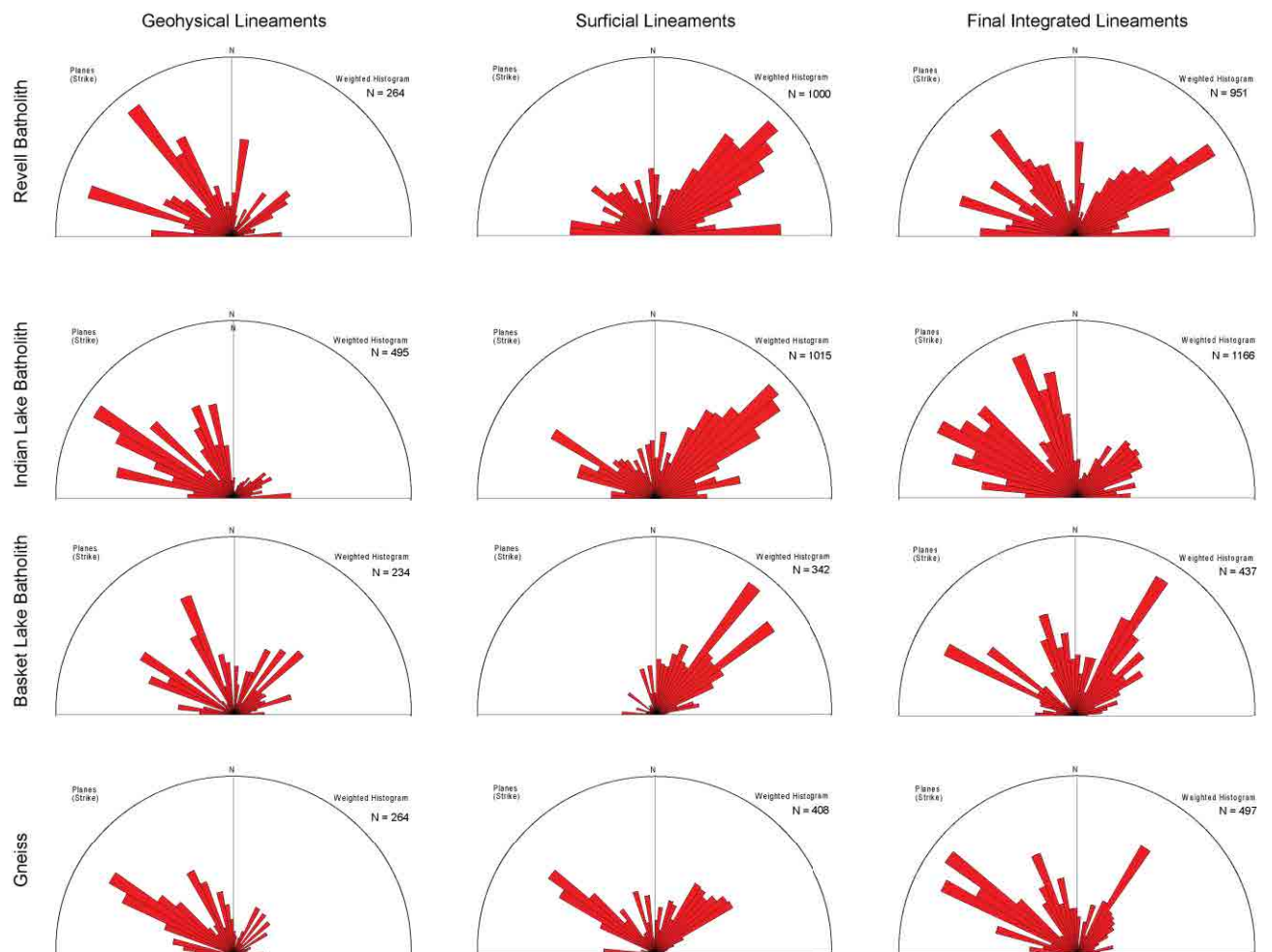
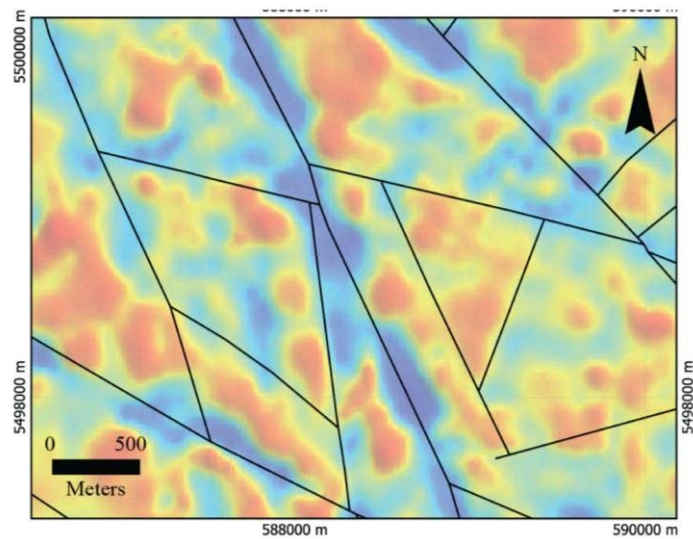


Figure A3: (B) Summary of lineament orientations by geological unit in the Ignace area.



**Figure A4: Example of northwest oriented lineaments producing a sinistral displacement of west-northwest oriented lineaments.**

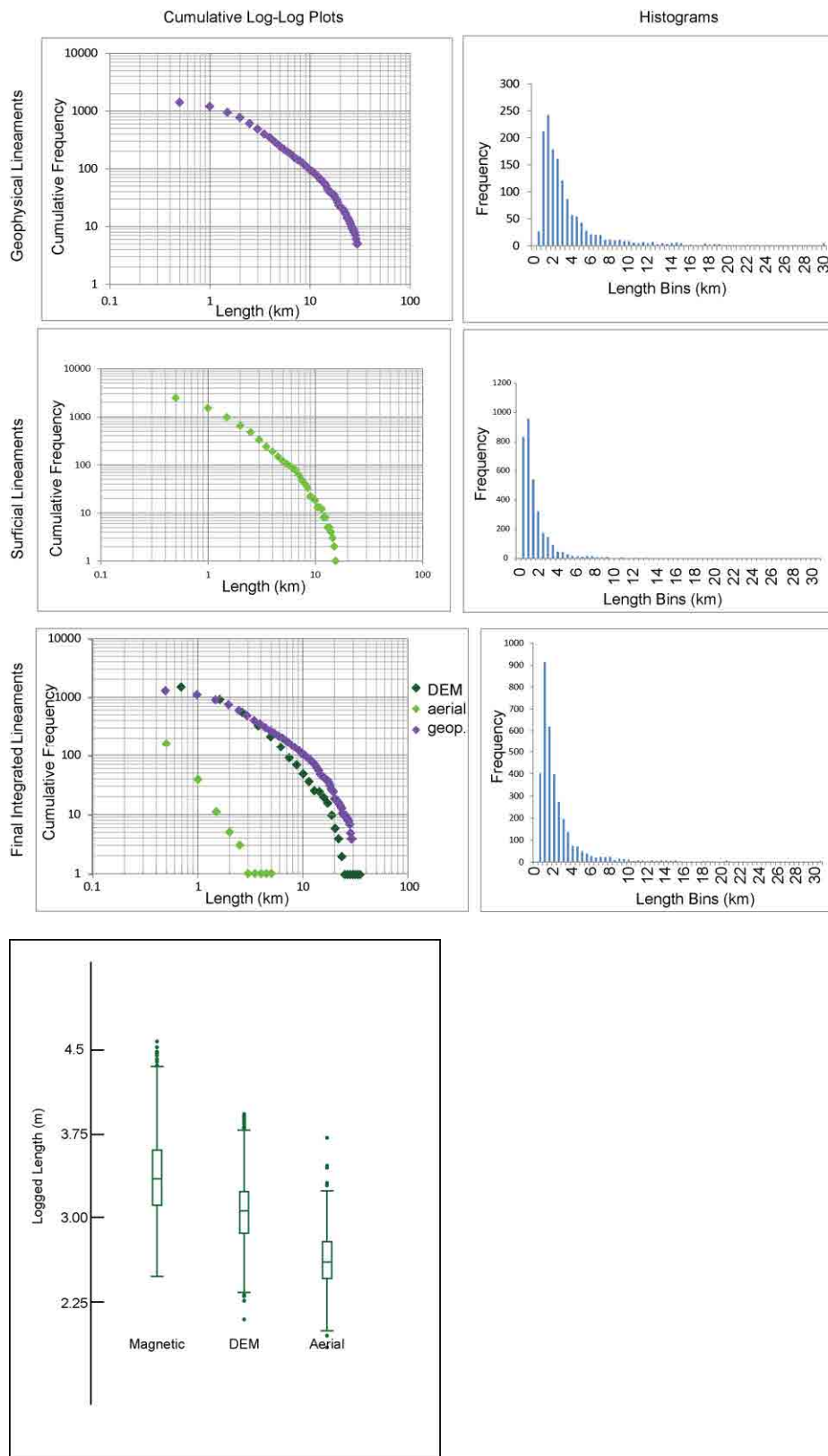
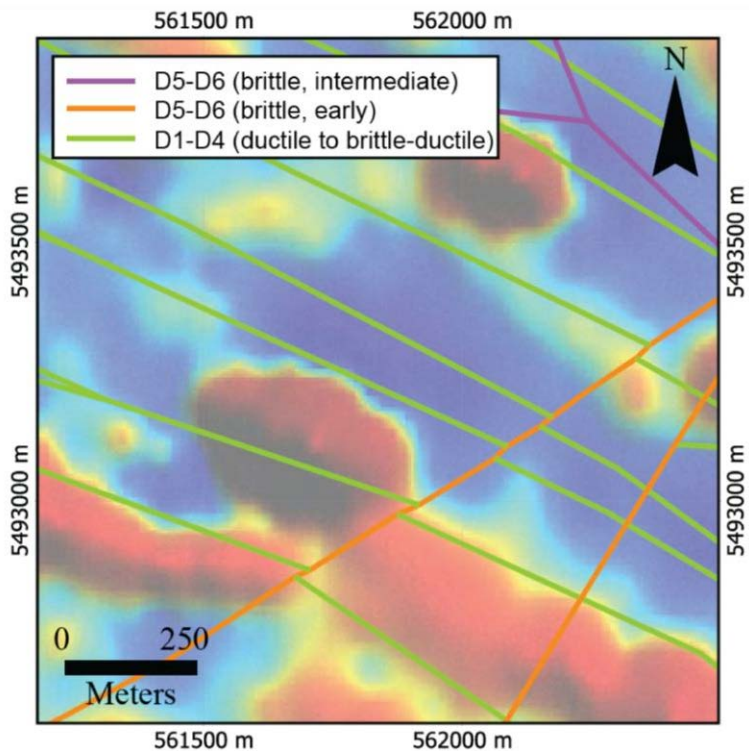
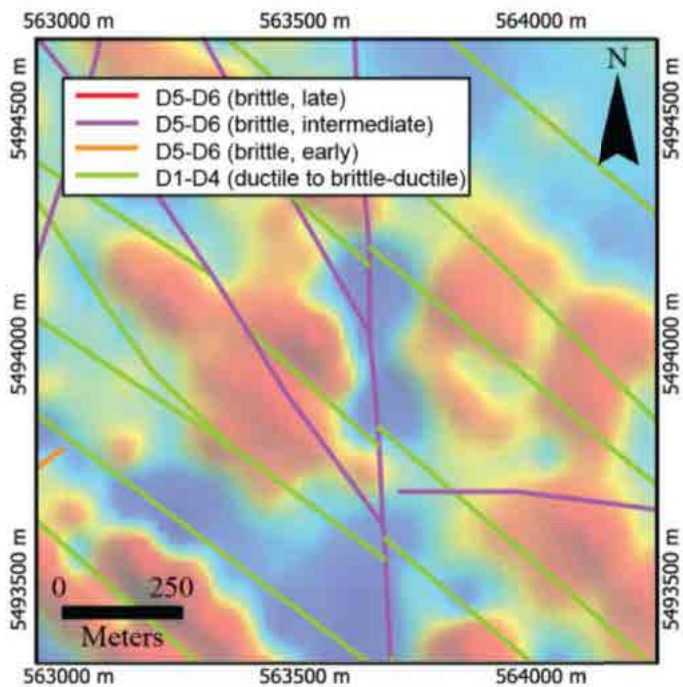


Figure A5: Summary of length statistics of the Ignace area.





**Figure A6: Example of  $D_5$ - $D_6$  early brittle lineament cross-cutting  $D_1$ - $D_4$  ductile to brittle-ductile lineaments**



**Figure A7: Example of  $D_5$ - $D_6$  intermediate brittle lineament cross-cutting  $D_5$ - $D_6$  early brittle lineaments**



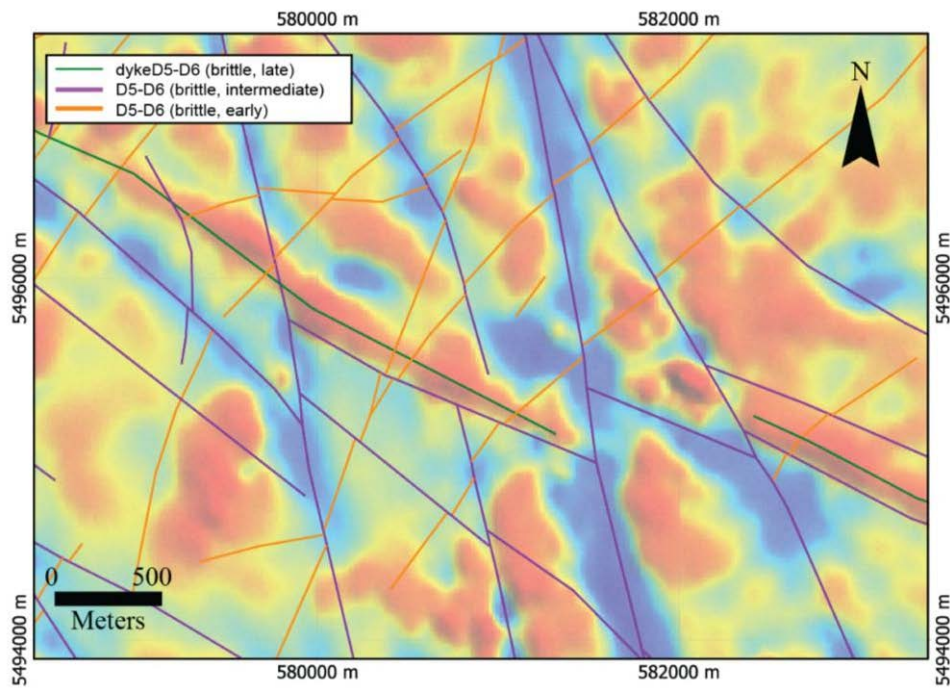


**Figure A8: Example of dextral and sinistral displacements produced by  $D_5$ - $D_6$  intermediate brittle lineaments**

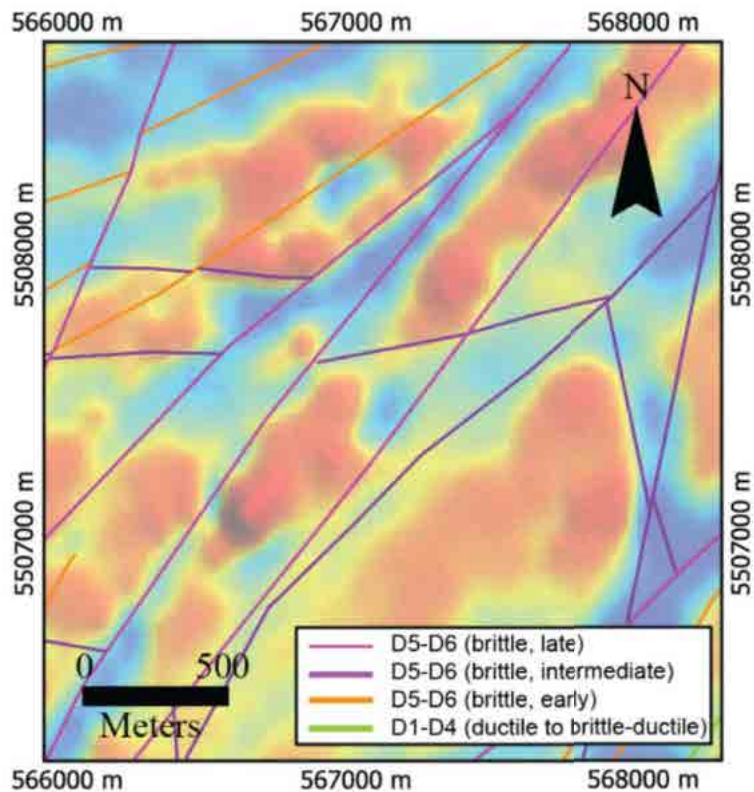
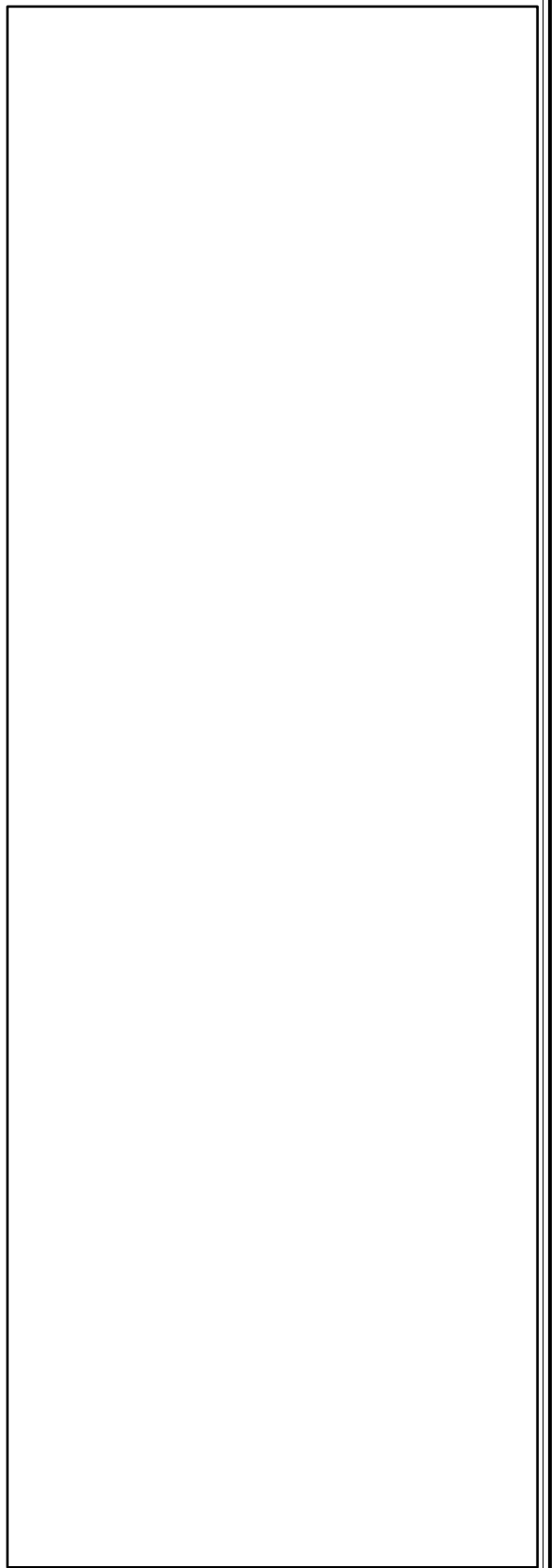
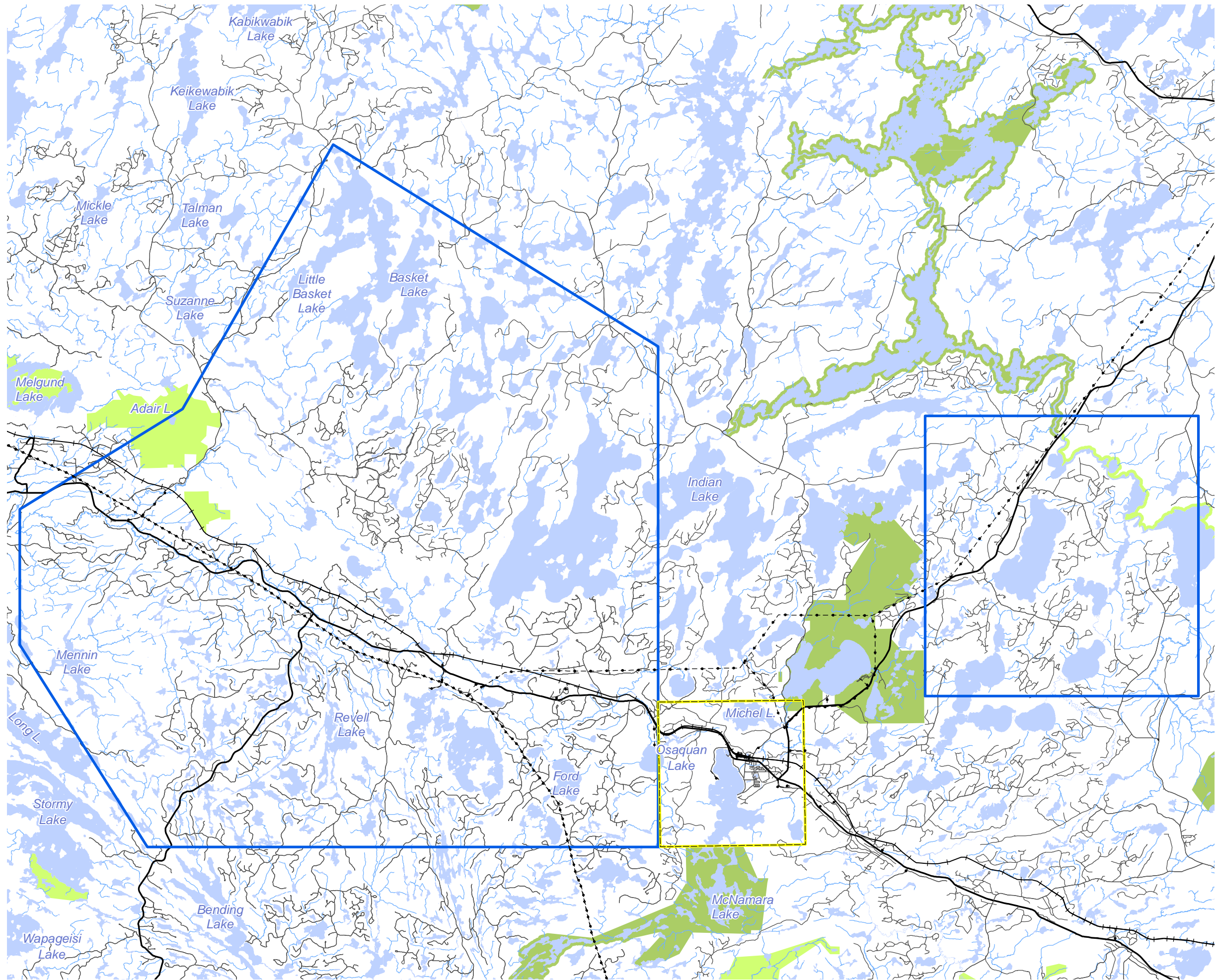


**Figure A9: Example of  $D_5$ - $D_6$  late brittle lineament cross-cutting  $D_5$ - $D_6$  intermediate brittle lineaments**

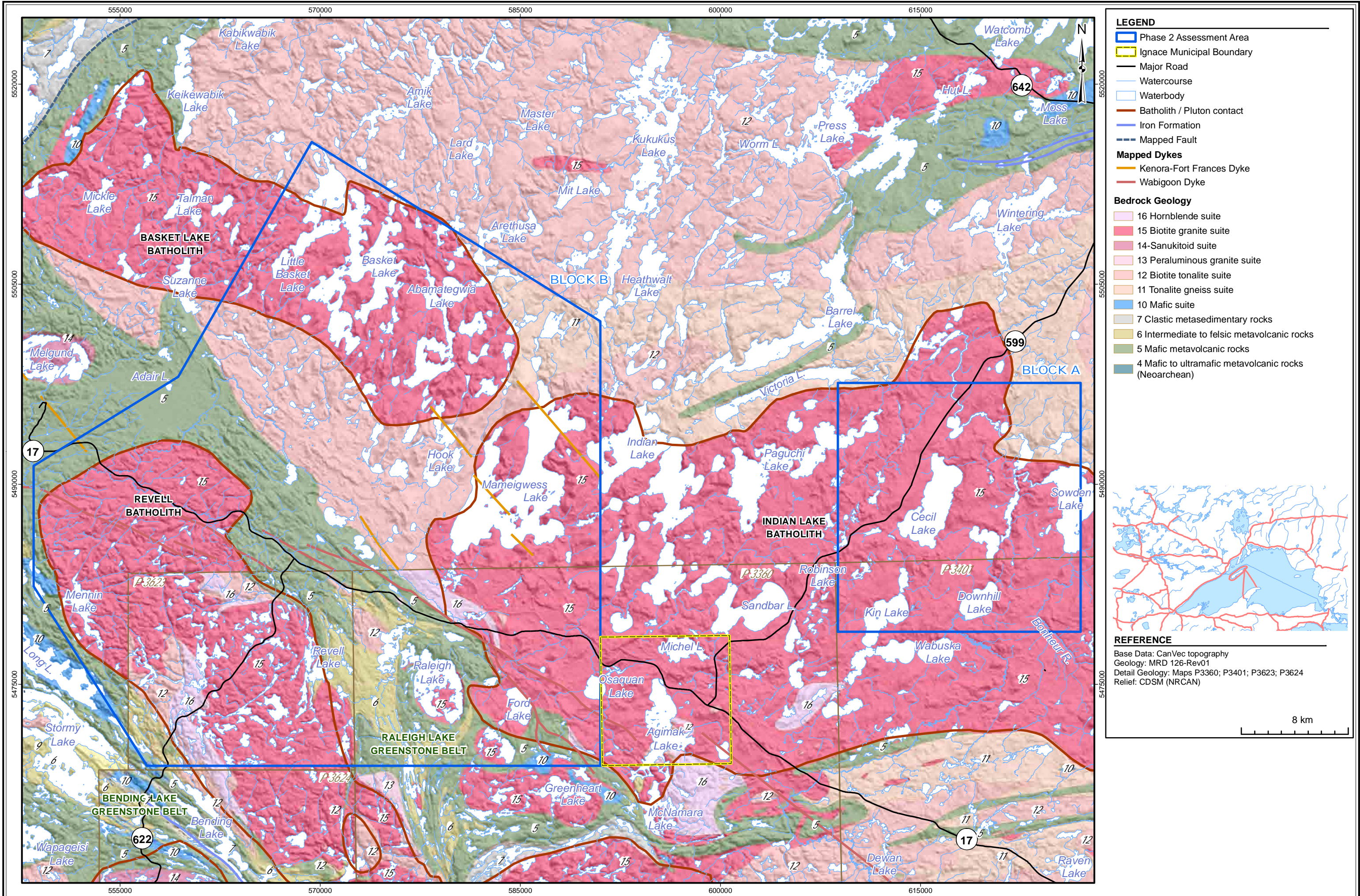
## **FIGURES**



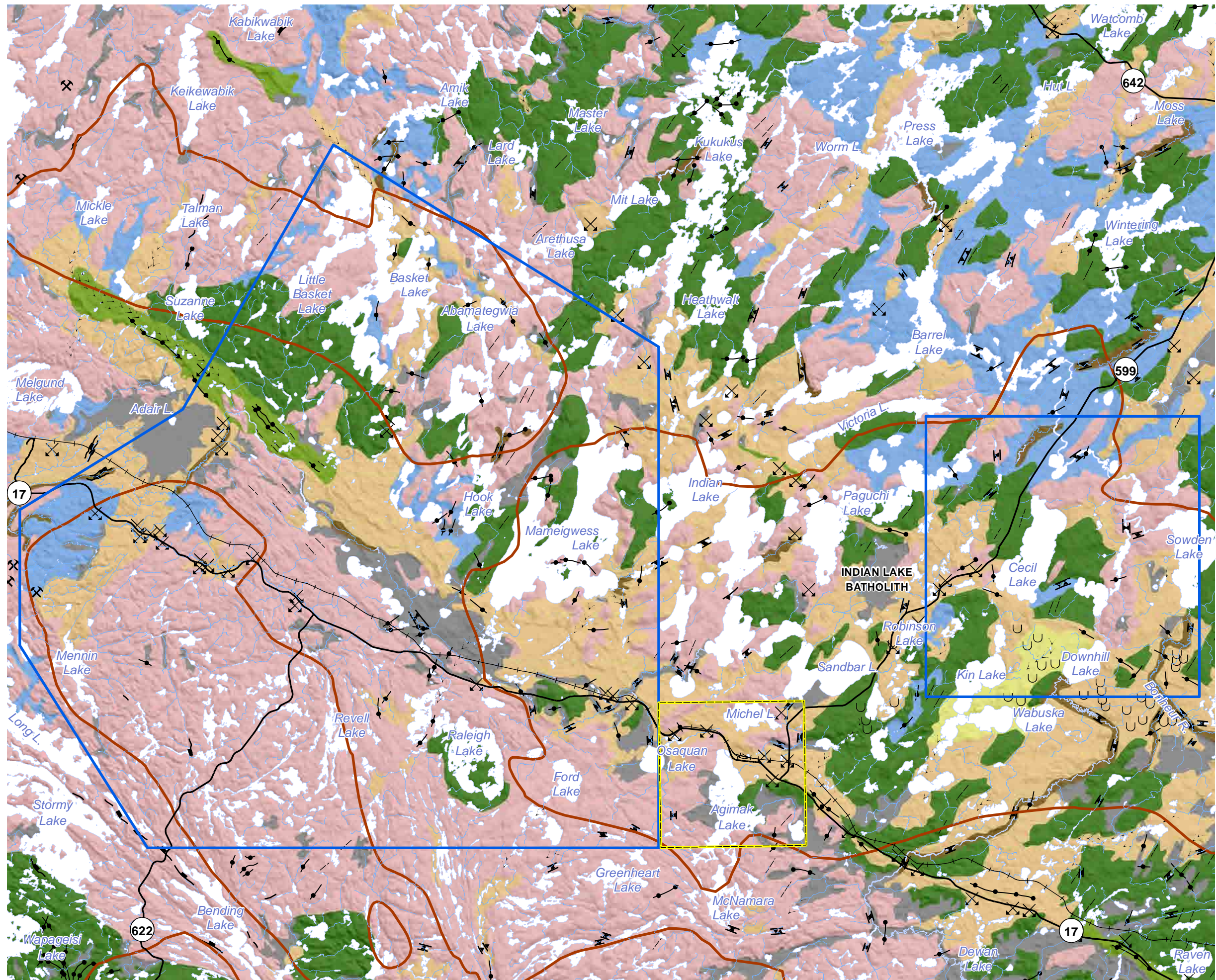




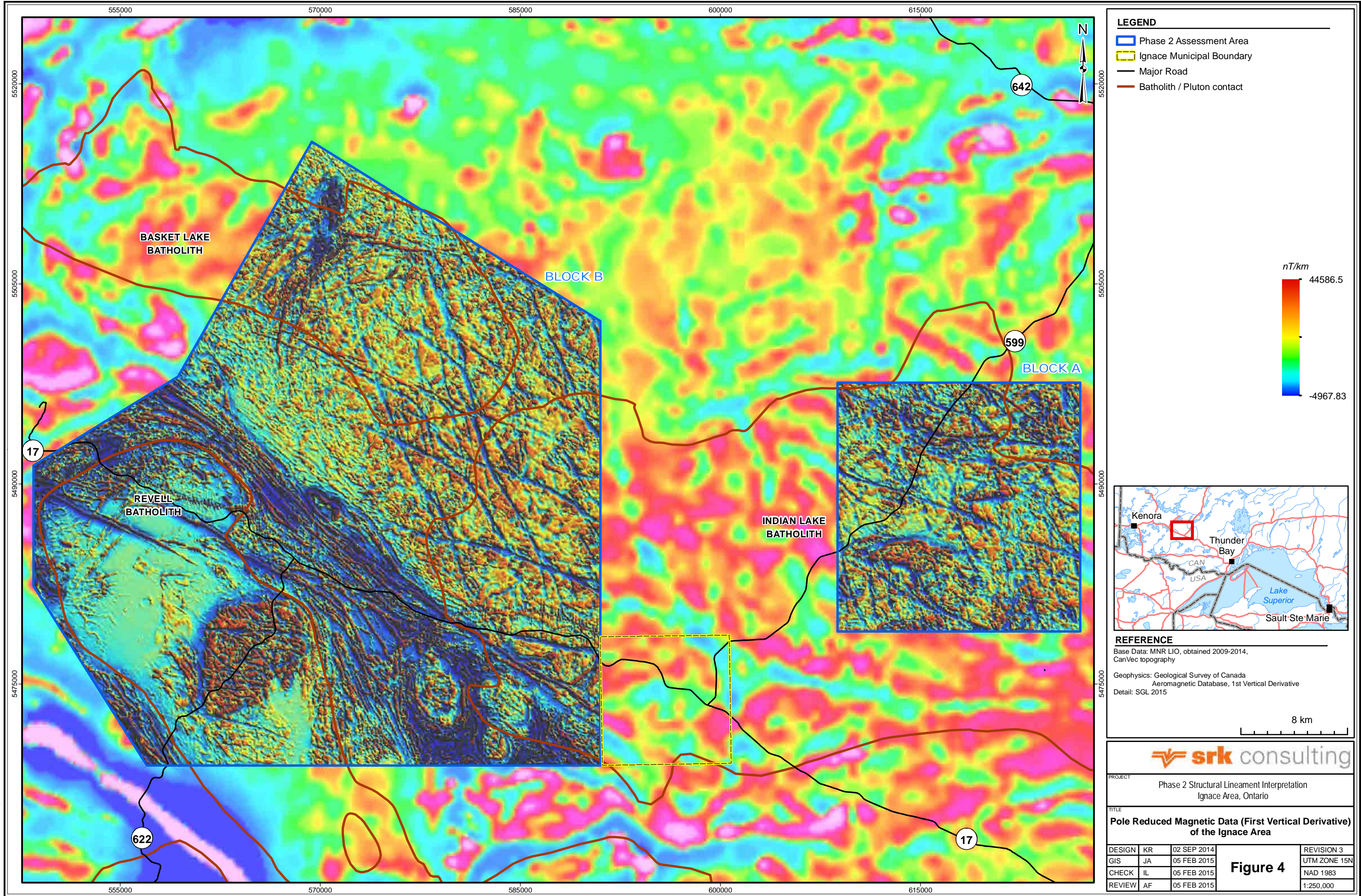




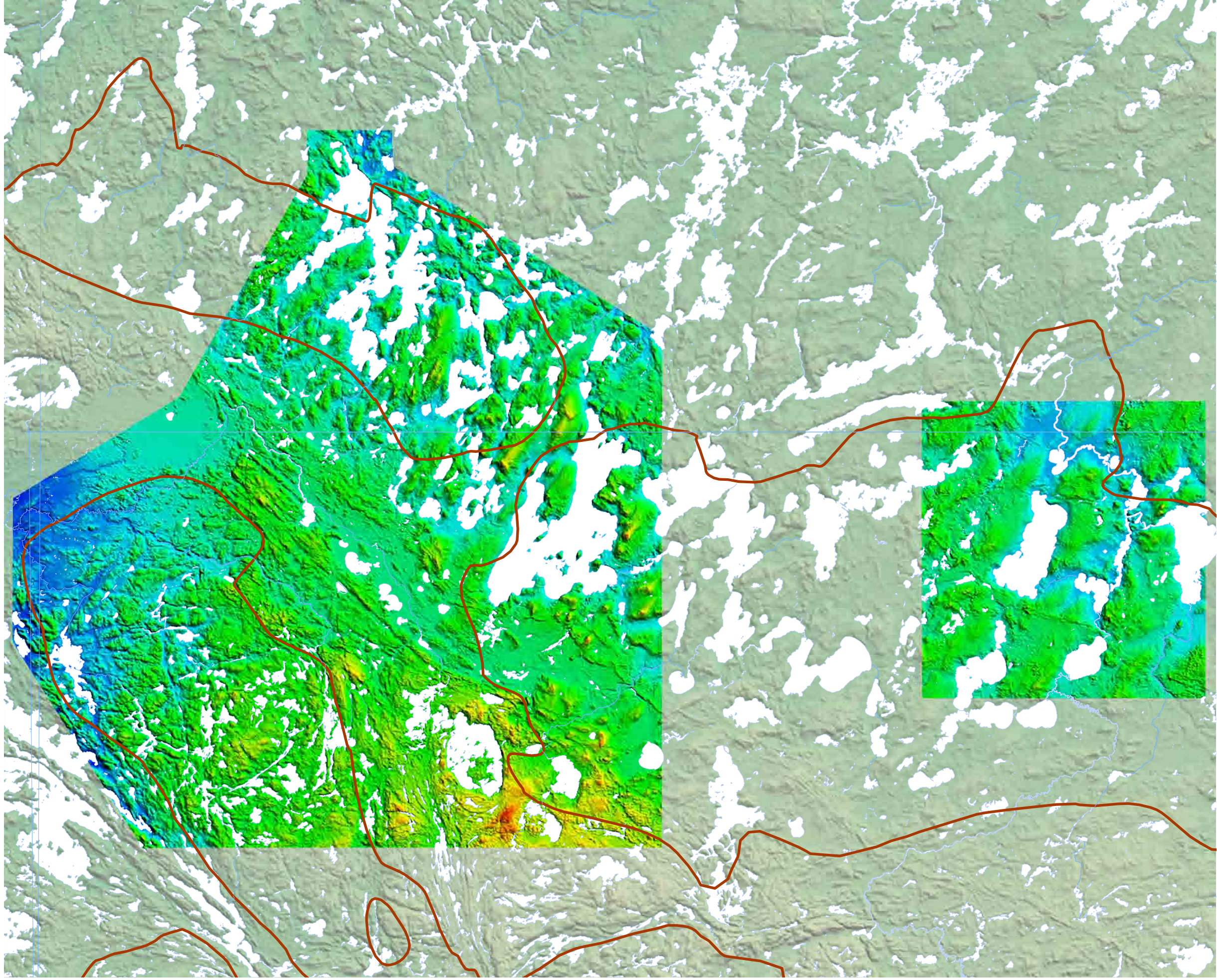




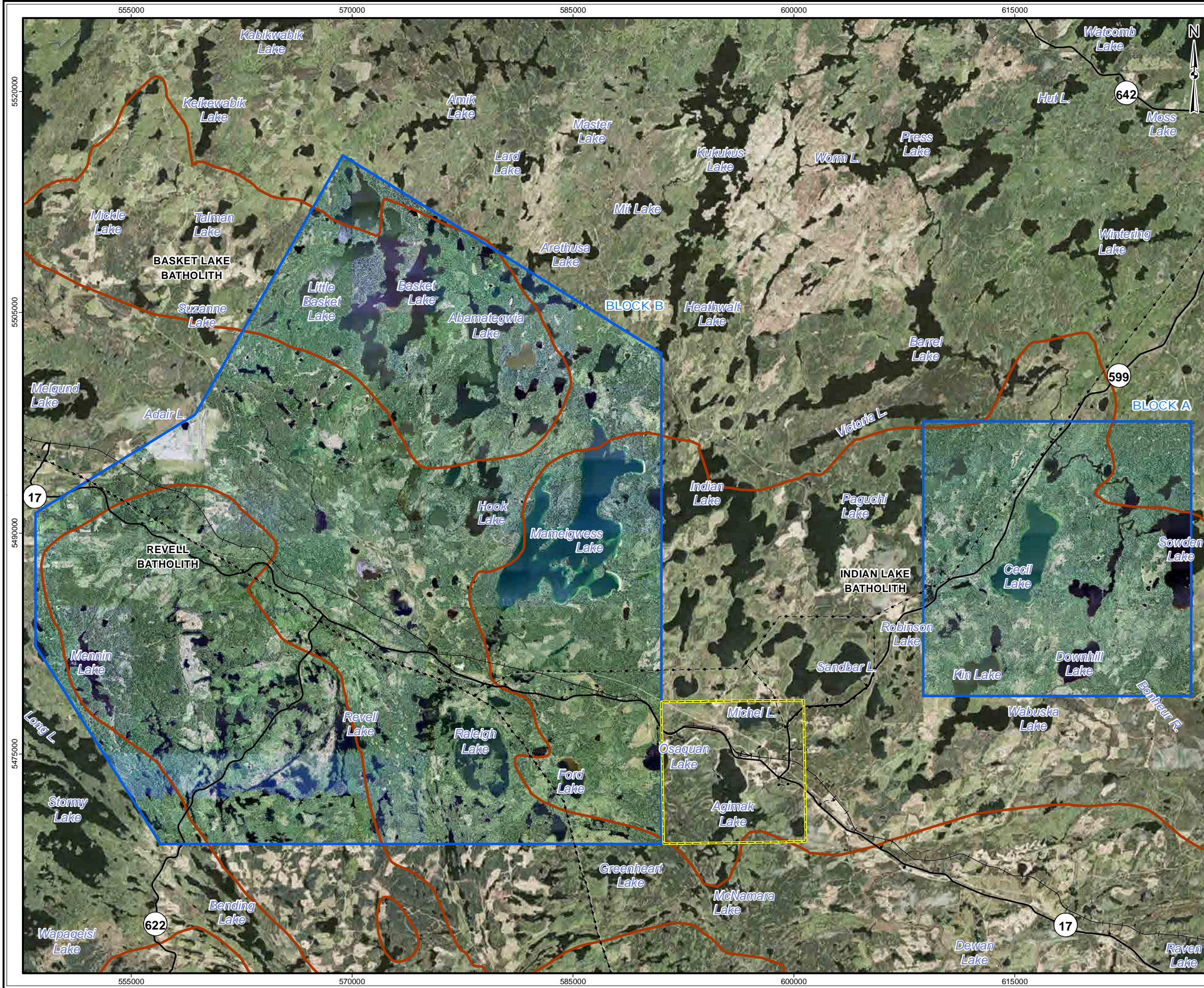












**LEGEND**

- Ignace Municipal Boundary
- Phase 2 Assessment Area
- Major Road
- Powerline
- Railway
- Batholith / Pluton contact

**REFERENCE**

Base Data: CanVec topography  
Image backdrop: TerraMetrics 2014  
Detail: Ontario Forest Resource Inventory

8 km

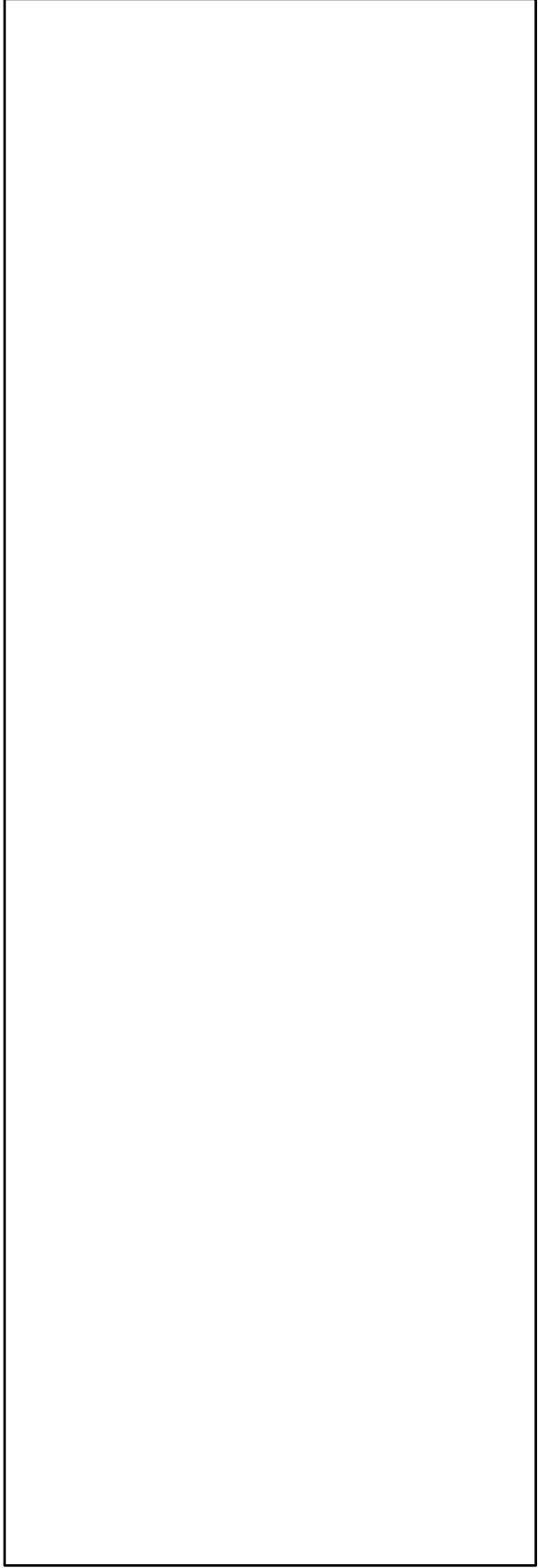
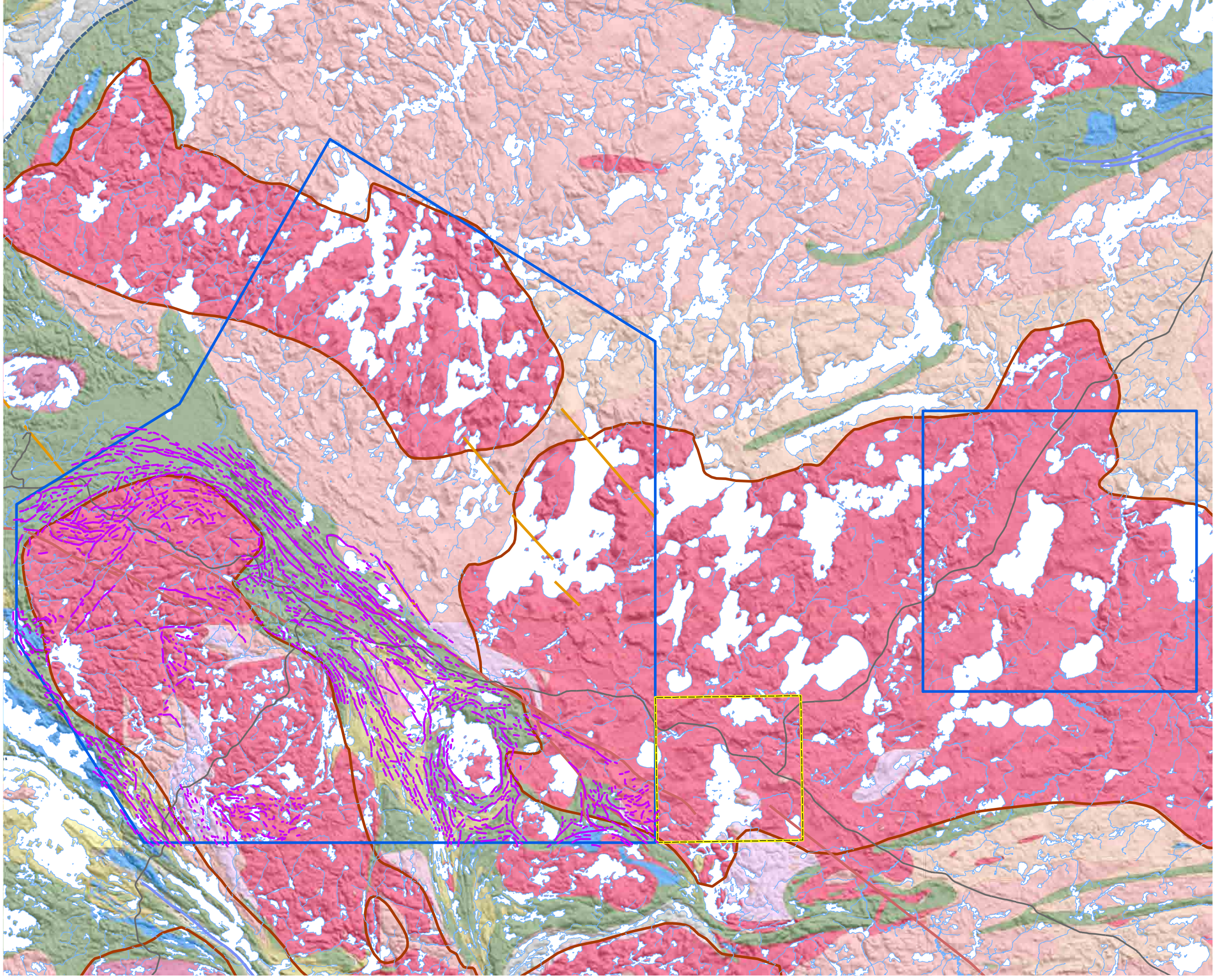
**srk consulting**

PROJECT: Phase 2 Structural Lineament Interpretation  
Ignace Area, Ontario

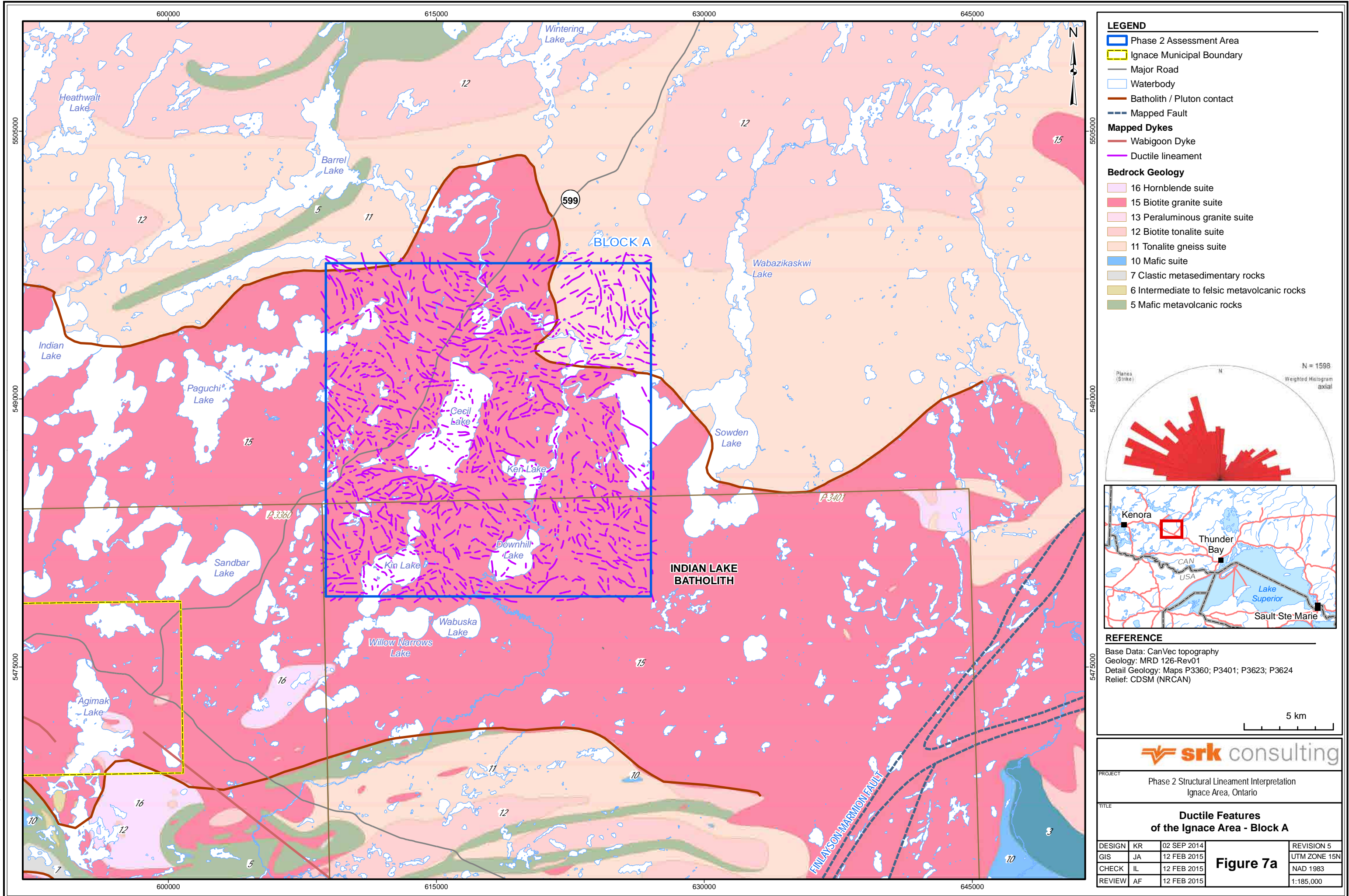
TITLE: **Aerial Imagery Data  
of the Ignace Area**

DESIGN	KR	02 SEP 2014	<b>Figure 6</b>	REVISION 3
GIS	JA	05 FEB 2015		UTM ZONE 15N
CHECK	IL	05 FEB 2015		NAD 1983
REVIEW	AF	05 FEB 2015		1:250,000

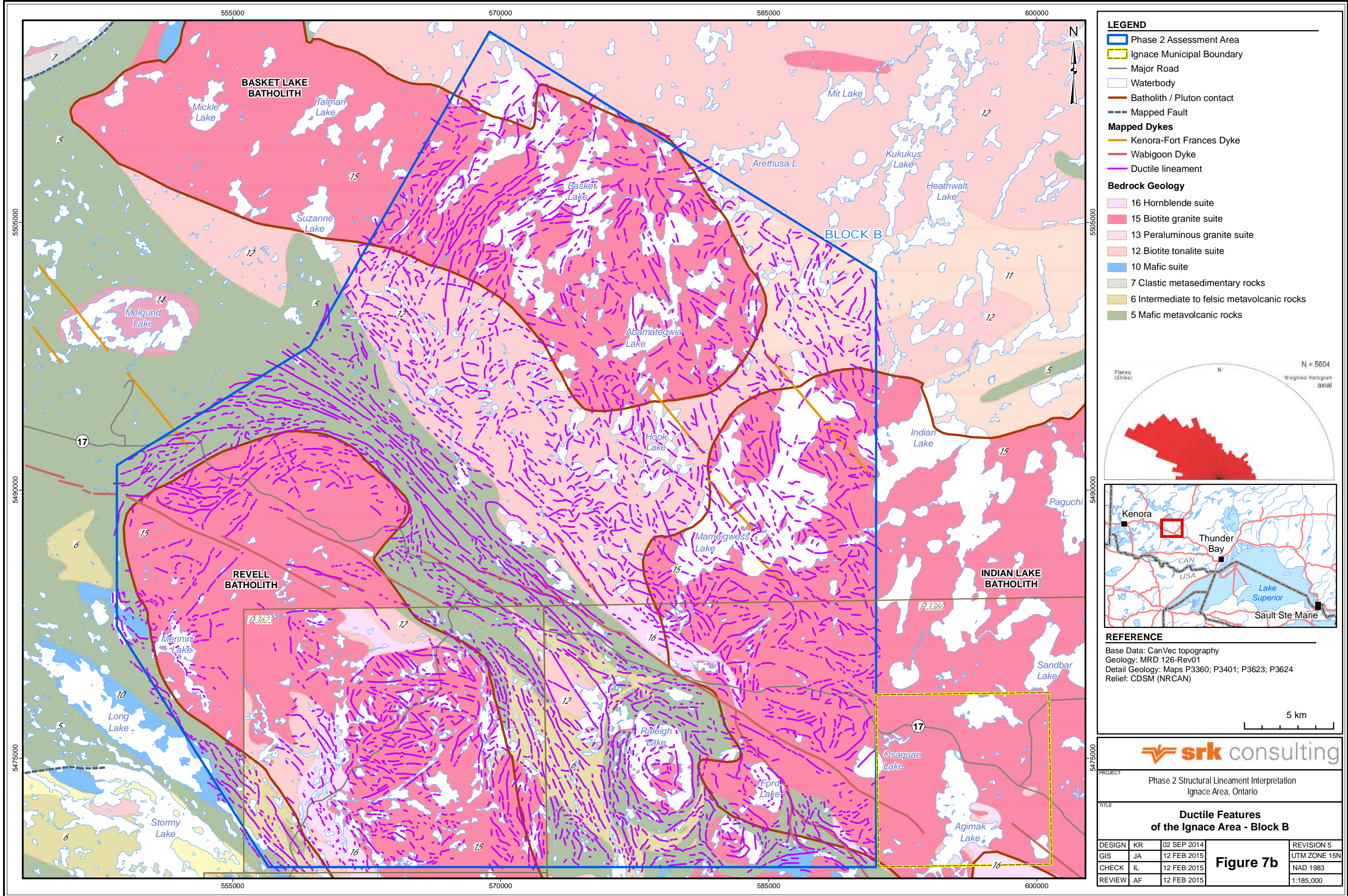




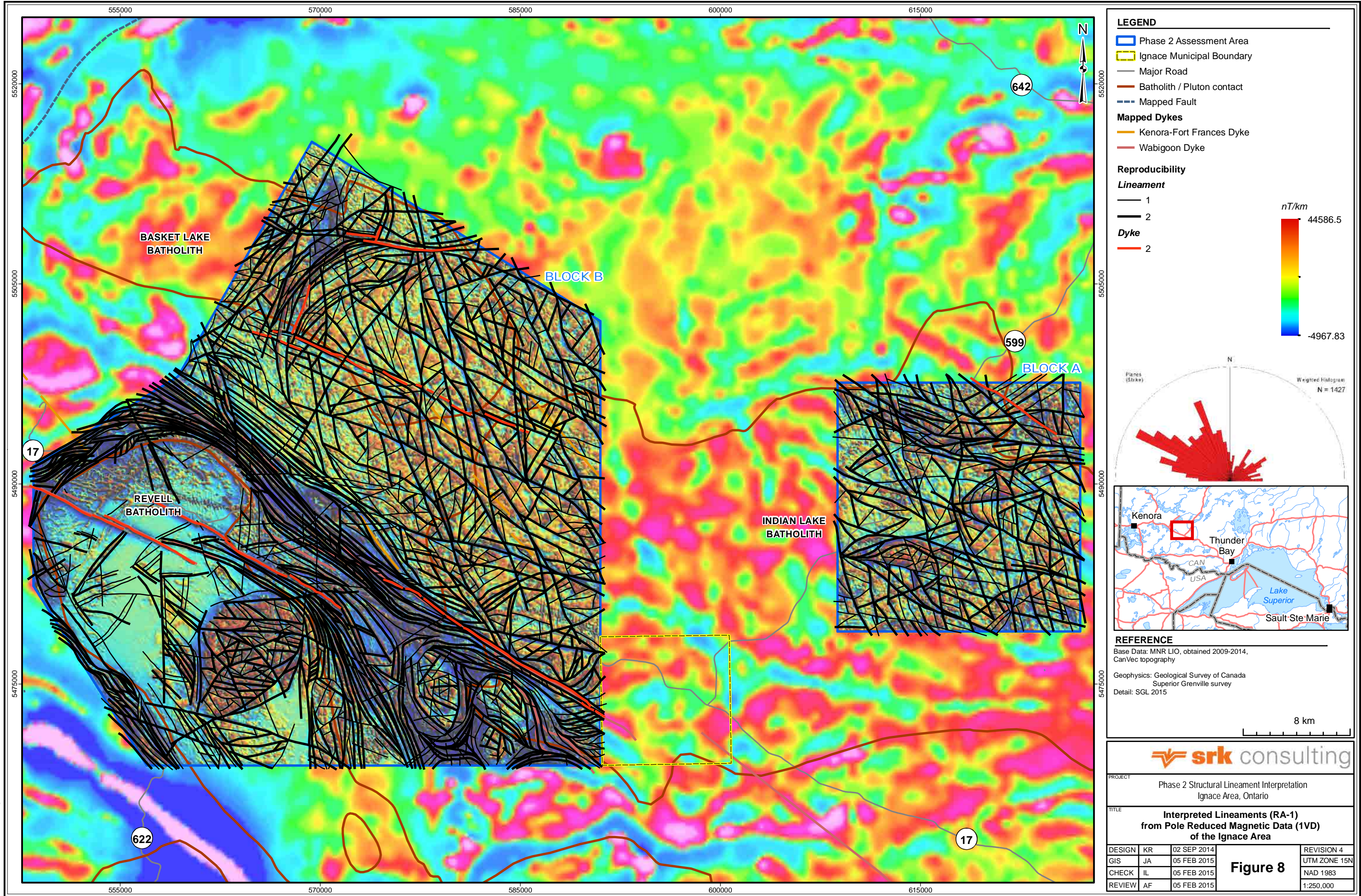




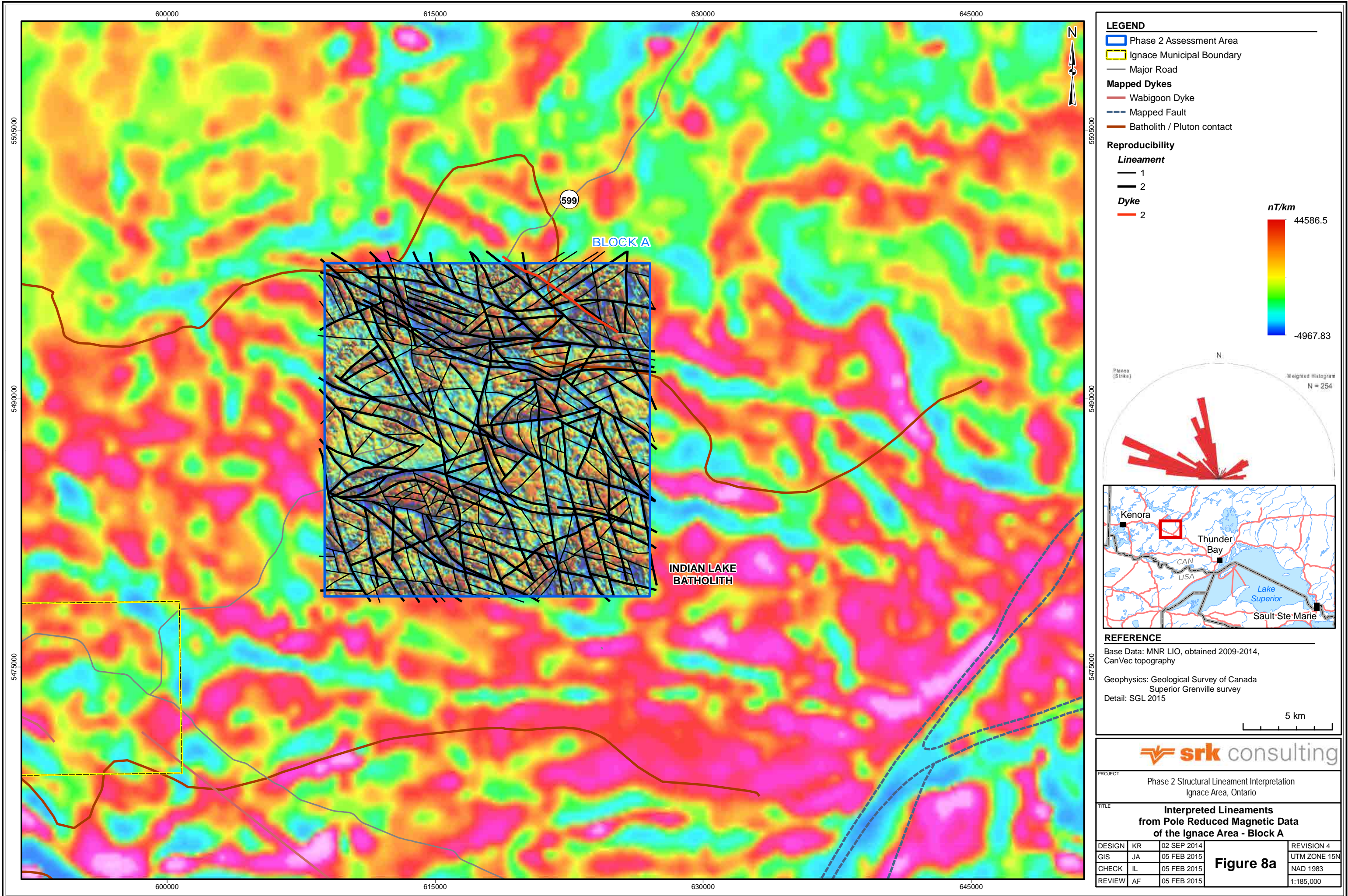












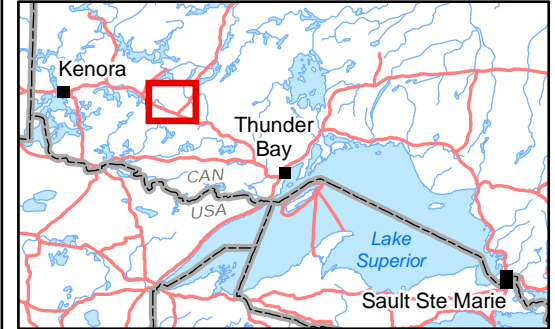
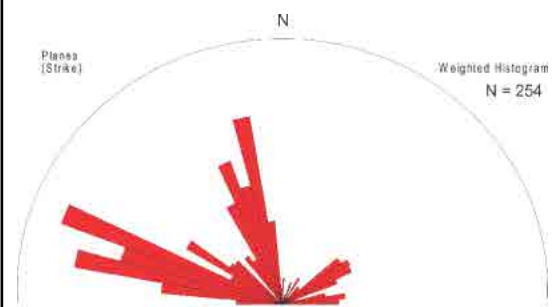
**LEGEND**

- Phase 2 Assessment Area
- Ignace Municipal Boundary
- Major Road
- Mapped Dykes**
  - Wabigoon Dyke
  - Mapped Fault
  - Batholith / Pluton contact
- Reproducibility**
  - Lineament**
    - 1
    - 2
  - Dyke**
    - 2

**nT/km**

44586.5

-4967.83



**REFERENCE**

Base Data: MNR LIO, obtained 2009-2014, CanVec topography

Geophysics: Geological Survey of Canada  
Superior Grenville survey  
Detail: SGL 2015

5 km

**srk consulting**

PROJECT: Phase 2 Structural Lineament Interpretation  
Ignace Area, Ontario

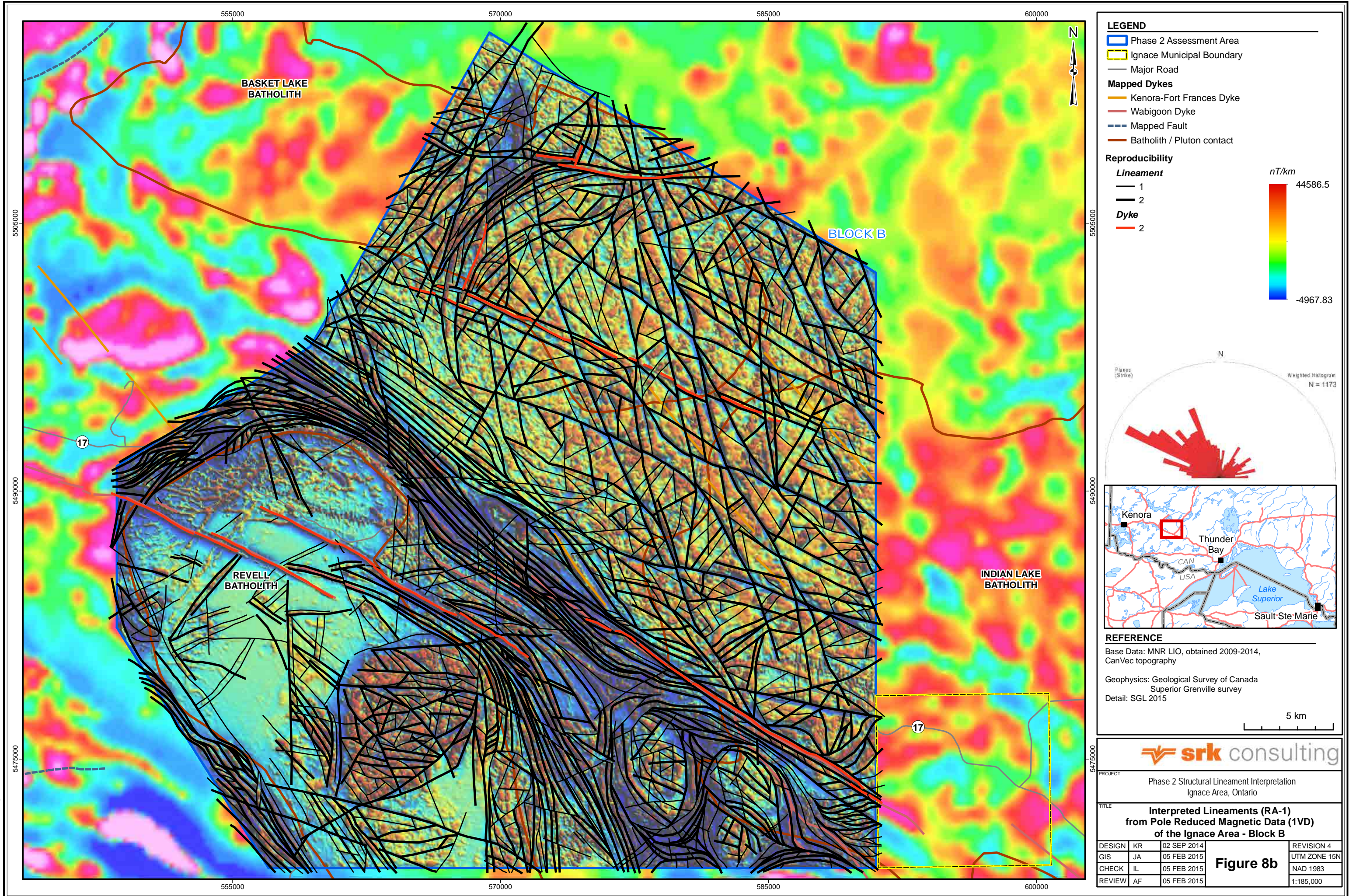
TITLE: **Interpreted Lineaments  
from Pole Reduced Magnetic Data  
of the Ignace Area - Block A**

DESIGN	KR	02 SEP 2014
GIS	JA	05 FEB 2015
CHECK	IL	05 FEB 2015
REVIEW	AF	05 FEB 2015

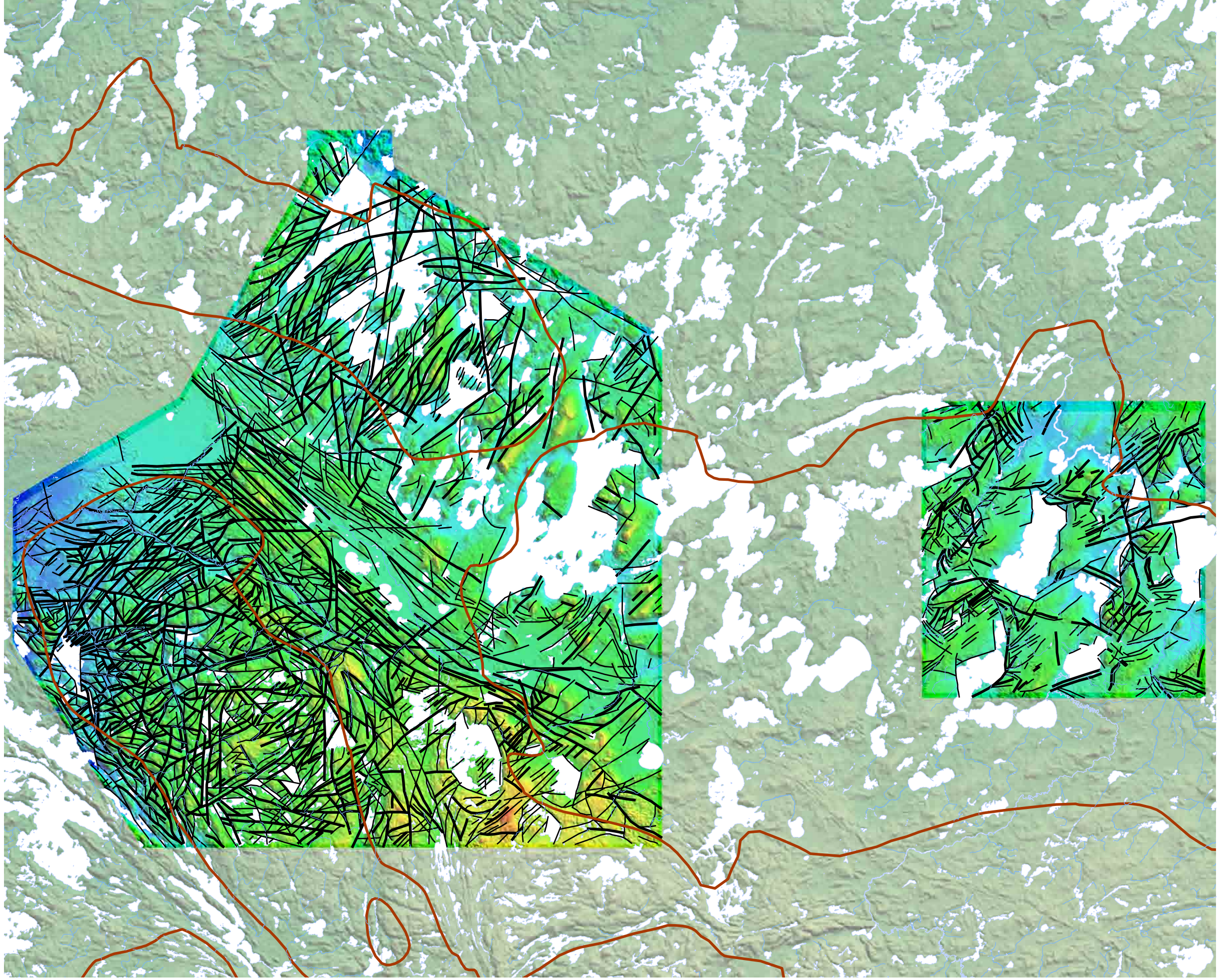
**Figure 8a**

REVISION 4  
UTM ZONE 15N  
NAD 1983  
1:185,000

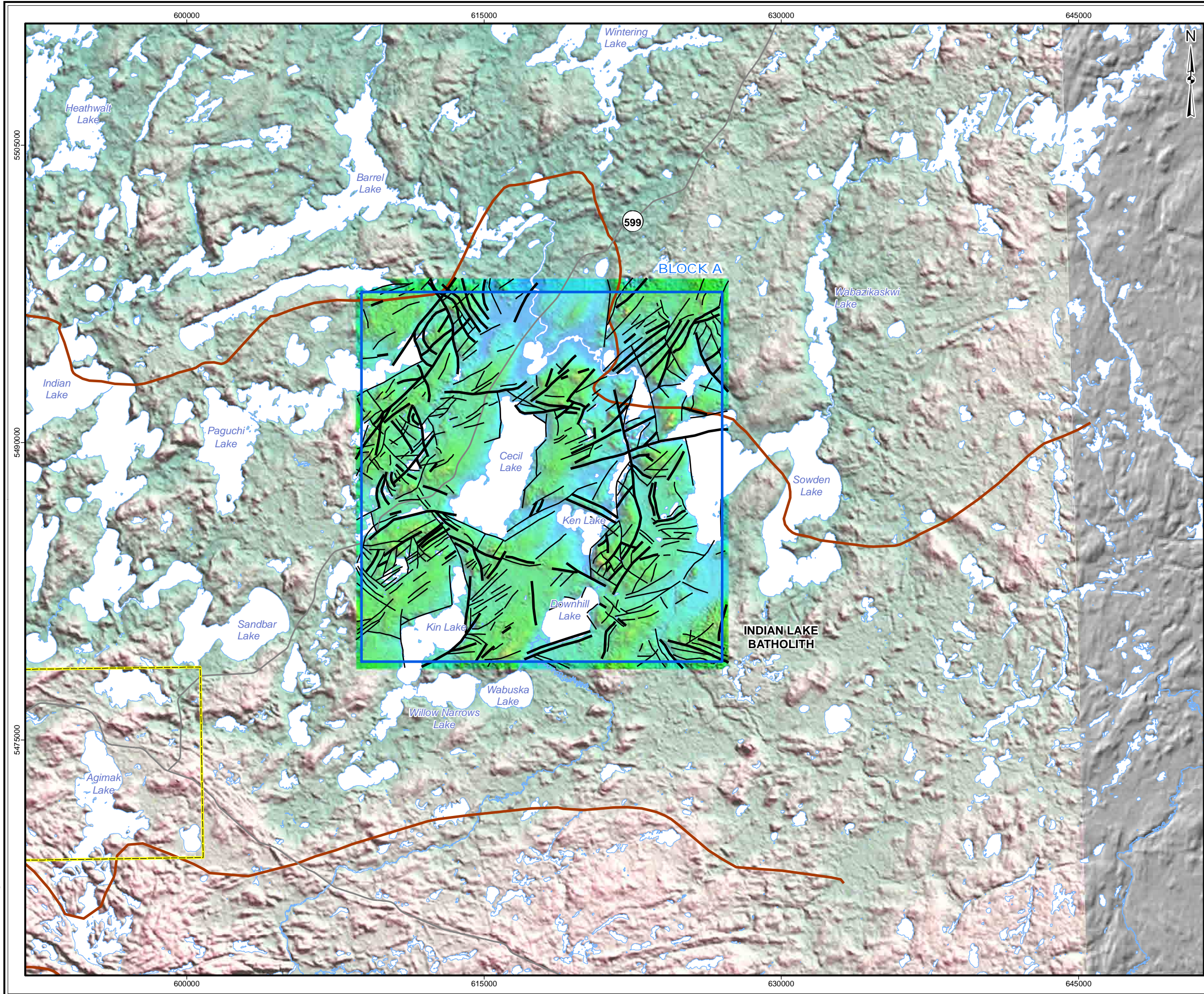












**LEGEND**

- Phase 2 Assessment Area
- Ignace Municipal Boundary
- Major Road
- Waterbody
- Batholith / Pluton contact

**Reproducibility (RA\_1)**

- 1
- 2

**Elevation (masl)**

534m

500

450

400

365

Planes (Strike)

N

Weighted Histogram axial

N = 459

**REFERENCE**

Base Data: CanVec topography  
Relief backdrop: CDSM (NRCAN)  
DEM: SGL 2015

5 km

PROJECT

Phase 2 Structural Lineament Interpretation  
Ignace Area, Ontario

TITLE

**Interpreted Lineaments  
from Digital Elevation Data  
of the Ignace Area - Block A**

DESIGN	KR	02 SEP 2014
GIS	JA	05 FEB 2015
CHECK	IL	05 FEB 2015
REVIEW	AF	05 FEB 2015

REVISION 4

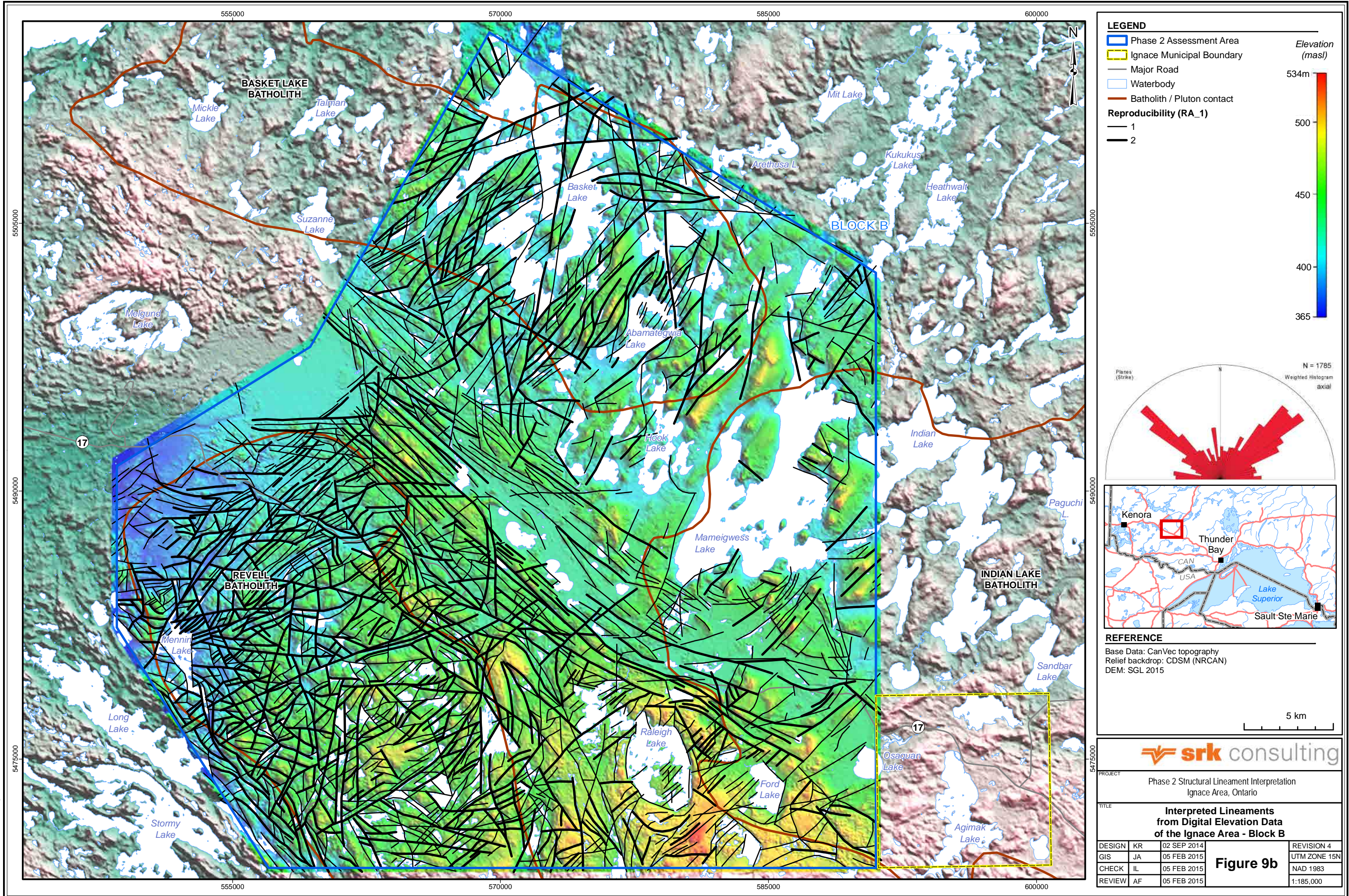
UTM ZONE 15N

NAD 1983

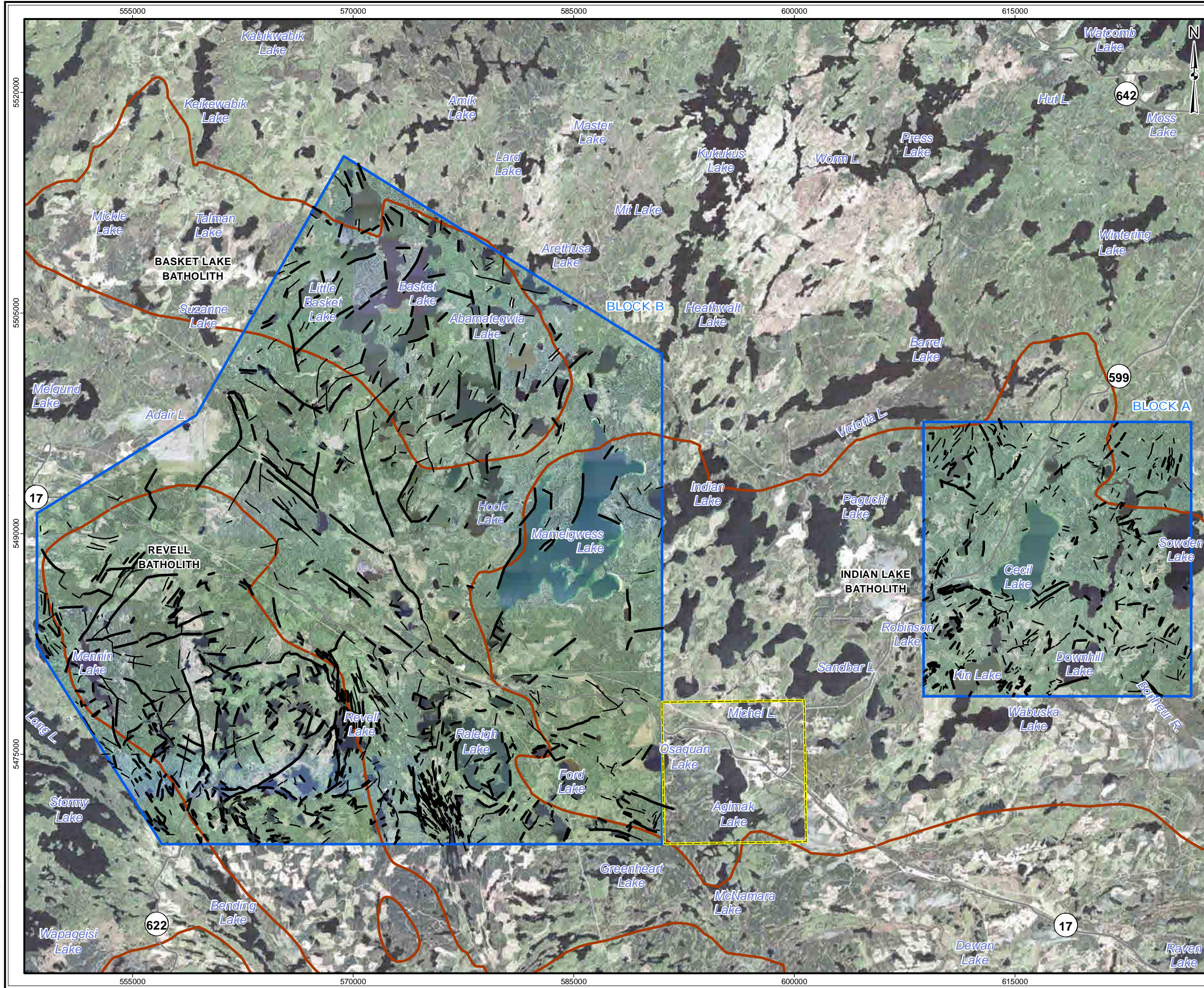
1:185,000

**Figure 9a**









**LEGEND**

- Ignace Municipal Boundary
- Phase 2 Assessment Area
- Major Road
- Batholith / Pluton contact

**Reproducibility (RA\_1)**

- 1
- 2

Planes (Strike)

N = 2108

axial

**REFERENCE**

Base Data: CanVec topography  
Image backdrop: TerraMetrics 2014  
Detail: Ontario Forest Resource Inventory

8 km

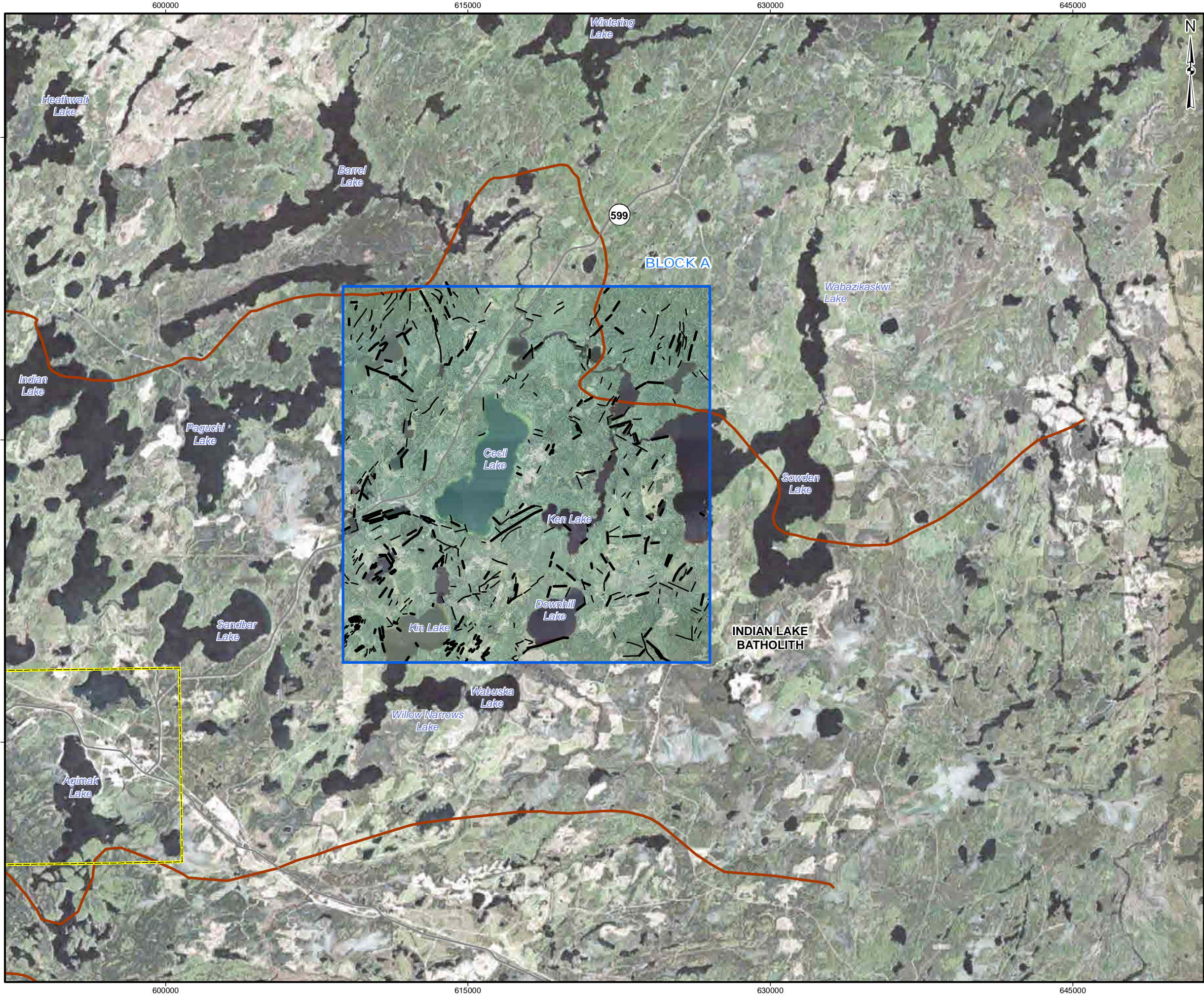
**srk consulting**

PROJECT: Phase 2 Structural Lineament Interpretation  
Ignace Area, Ontario

TITLE: **Interpreted Lineaments from Aerial Imagery Data of the Ignace Area**

DESIGN	KR	02 SEP 2014	<b>Figure 10</b>	REVISION 4
GIS	JA	05 FEB 2015		UTM ZONE 15N
CHECK	IL	05 FEB 2015		NAD 1983
REVIEW	AF	05 FEB 2015		1:250,000





**LEGEND**

- Phase 2 Assessment Area
- Ignace Municipal Boundary
- Major Road
- Batholith / Pluton contact

**Reproducibility (RA\_1)**

- 1
- 2

**REFERENCE**

Base Data: CanVec topography  
Image backdrop: TerraMetrics 2014  
Detail: Ontario Forest Resource Inventory

5 km

**srk consulting**

PROJECT: Phase 2 Structural Lineament Interpretation  
Ignace Area, Ontario

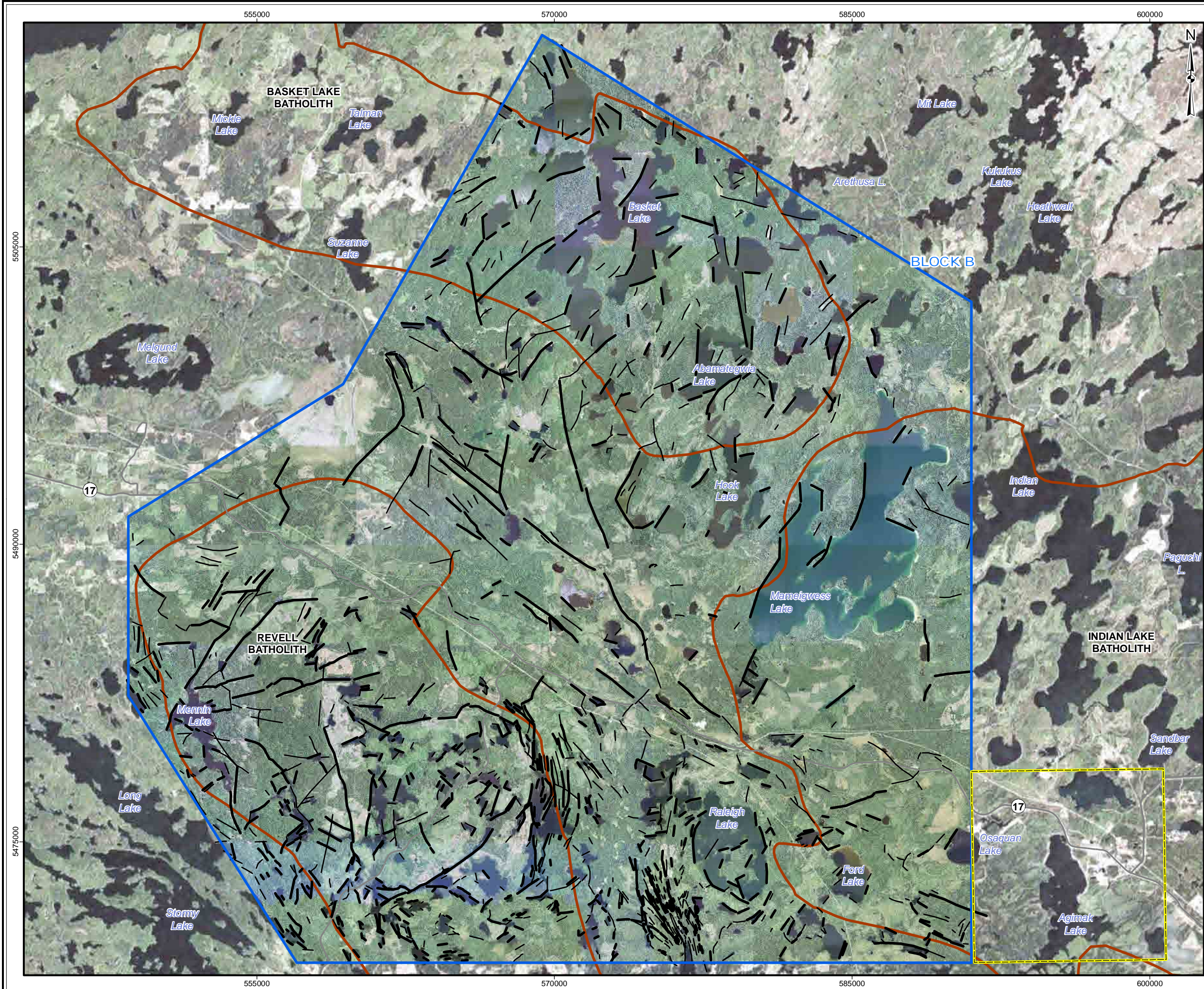
TITLE: **Interpreted Lineaments  
from Aerial Imagery Data  
of the Ignace Area - Block A**

DESIGN	KR	02 SEP 2014
GIS	JA	05 FEB 2015
CHECK	IL	05 FEB 2015
REVIEW	AF	05 FEB 2015

**Figure 10a**

REVISION 4
UTM ZONE 15N
NAD 1983
1:185,000





**LEGEND**  

Phase 2 Assessment Area

Ignace Municipal Boundary

Major Road

Batholith / Pluton contact

**Reproducibility (RA\_1)**  

1

2

Planes (Strike)

N = 1482

Weighted Histogram axial

Kenora

Thunder Bay

Sault Ste Marie

Lake Superior

CAN

USA

**REFERENCE**  
Base Data: CanVec topography  
Image backdrop: TerraMetrics 2014  
Detail: Ontario Forest Resource Inventory

srk consulting

PROJECT

Phase 2 Structural Lineament Interpretation  
Ignace Area, Ontario

TITLE

**Interpreted Lineaments  
from Aerial Imagery Data  
of the Ignace Area - Block B**

DESIGN	KR	02 SEP 2014	<b>Figure 10b</b>	REVISION 4
GIS	JA	05 FEB 2015		UTM ZONE 15N
CHECK	IL	05 FEB 2015		NAD 1983
REVIEW	AF	05 FEB 2015		1:185,000



